DETECTION OF CASCADIA SLOW SLIP IN BOREHOLE PORE PRESSURE DATA

A Thesis

by

JOSHUA RICHARD EDGINGTON

Submitted to the Office of Graduate and Professional Studies of
Texas A&M University
in partial fulfillment of the requirements for the degree of

MASTER OF SCIENCE

Chair of Committee,	Patrick Fulton
Committee Members,	Peter Knappett
	Stephanie Paal
Head of Department,	Michael Pope

May 2019

Major Subject: Geophysics

ABSTRACT

The Cascadia subduction zone hosts quasi-periodic, large-scale slow slip events which have been shown to be precursors to large, tsunamigenic earthquakes at other active subduction zone margins. Detection of these events in Cascadia utilizes continuous GPS measurements and high-resolution seismic stations to capture geodetic reversals and spatially correlated tremor, respectively, associated with slow slip. Borehole pore pressure data have been shown to record signals related to slow slip and may provide an alternate means of detection for these events, potentially in near real-time. We evaluate this hypothesis by developing and testing anomalous signal detection methods for these data, specifically using evaluations of STA/LTA and a Holt-Winter's predictive model. We also perform Bayesian statistical analysis on these detections to determine the posterior probability of a slow slip event given an anomalous pore pressure detection. Our results show that a Holt-Winter's model readily detects strongly correlated anomalous activity across multiple boreholes at known times of slow-slip, and the posterior probability of slow slip given a detection ranges from 50-100%. We conclude that borehole pore pressure data do record anomalous signals associated with slow slip, and we speculate that groups of multiple, closely located boreholes may perform as a real-time detection network for slow slip events.

ACKNOWLEDGEMENTS

I would like to thank my faculty advisor and committee chair, Dr. Fulton, for pouring immense amounts of guidance, patience, and humor (when needed) during the course of this research. This work would have been impossible without his counsel and support.

Thanks goes to my department, its faculty, and its students, for making my seven years at Texas A&M University productive, insightful, and overall well spent.

Thanks to my family, whose love and encouragement supported me through my time at Texas A&M University.

I would especially like to thank my close friend, Charles A. Lozano Jr., who coded the first version of a data downloader script in BASH that acted as the first workhorse for this research. This script prevented weeks of painstakingly downloading, organizing, and unzipping data files.

Thanks to my God, who calmed me during the rough times and blessed me and surrounded me with supportive and friendly faces.

CONTRIBUTORS AND FUNDING SOURCES

Contributors

This work was primarily supervised by Dr. Patrick Fulton, of the Department of Geology and Geophysics [advisor and committee chair].

The data analyzed for this research was collected by NSF Earthscope's Plate Boundary Observatory Network, available publicly online by UNAVCO.
[http://www.unavco.org/data/data.html]

Progress of this work was also reviewed Dr. Peter Knappett of the Department of Geology and Geophysics [committee member], and Dr. Stephanie Paal of the Department of Civil Engineering [committee member].

All other work conducted for the thesis was completed by the student independently.

Funding Sources

This project was supported in part by NSF Award #1829492 to P. M. Fulton. I also wish to acknowledge support from the US Science Support Program for IODP, for my participation in borehole observatory installation during IODP Expedition 380.

NOMENCLATURE

HPa	Hectopascals
Hz	Hertz
LTA	Long-term average
Pa	Pascals
PBO	Plate Boundary Observatory
p(Pd)	Probability of a pressure detection
p(Pd|SS)	Probability of a pressure detection during slow-slip
p(SS)	Probability of slow-slip
p(SS|Pd)	Probability of slow-slip during a pressure detection
SSE	Slow-slip event
STA	Short-term average

TABLE OF CONTENTS

LIST OF FIGURES

LIST OF TABLES

1. INTRODUCTION

The Cascadia subduction zone along the coast of the Pacific Northwest of the United States and Vancouver Island exhibits a range of earthquake activity including large-scale slow-slip events (SSEs). SSEs are nearly silent, large-scale earthquakes with very slow durations compared to that of regular earthquakes. SSEs have been observed at multiple subduction zone margins at depths ranging from above to below regular earthquake nucleation [e.g. Dragert et al. 2001; Obara et al. 2004; Davis et al. 2011]. Cascadia SSEs have magnitudes of M_w = ~6 – 7, last anywhere from a few days to upwards of 2 months, and occur regularly every 12-16 months. Previous studies have shown that SSEs can be precursors to large tsunamigenic earthquakes [Kato et al. 2012; Bouchon et al. 2013; Ito et al. 2013(1), Ito et al. 2013 (2)]. Thus, it is important to develop methods to efficiently recognize the occurrence of SSEs in near-real-time.

SSEs are commonly recognized by geodetic signals from continuous GPS monitoring stations that suggest large-scale transient slip on the subduction zone plate boundary fault [e.g. Rogers and Dragert, 2003; Wallace et al. 2010; Crowell et al. 2016]. Eight-day to two-month long episodes of very low amplitude, spatially correlated seismic signals, otherwise known as tremor, are sometimes observed on high-resolution seismograms during SSEs and are often used as a proxy indicator of ongoing slow-slip [Wech and Bartlow 2014]. In Cascadia, the spatio-temporal nature of SSEs is commonly identified by tremor observations first and then later confirmed and clarified with GPS observations [Schwartz and Rokosky, 2007; Peng and Gomberg, 2010]. These geodetic transients occur as 8-20 day westward reversals in the otherwise easting component of continuous GPS station data [Dragert et al. 2001].

As a means of SSE detection, GPS data are noisy, and it can be difficult to resolve or recognize SSEs within these data until considerable time has elapsed during an event. Alternatively, tremor has better temporal resolution, but is not always present during SSEs

[Schwartz and Rokosky, 2007; Wech and Bartlow, 2014]. Here, we investigate the potential for detecting on-going SSEs through the use of borehole pore pressure data and their response to volumetric strains associated with fault slip during SSEs.

We hypothesize that existing and ongoing onshore measurements of borehole pore pressure in Cascadia may respond to SSEs such that it can help detect SSEs in near real-time. Volumetric strains caused by static stress changes from fault slip have long been recognized to influence pore pressure and well water levels [e.g. Roeloffs 1996; Segall 2010; Wang and Manga 2010]. Poroelastic responses from slow slip have also been previously been recognized within pore pressure observatories offshore the Nankai and Costa Rican subduction zones and onshore along the San Andreas Fault [e.g. Roeloffs 1989; Davis et al. 2015; Araki et al., 2017].

More recently, the offshore observatories' pore pressure data have been shown to respond to SSEs at the Nankai subduction zone in Japan, both as precursors to large earthquakes and as statically triggered events [Araki et al. 2017]. These observations from offshore observatory wells reveal signatures of slow slip, sometimes several days before they are otherwise recognized seismically, and in some scenarios when they were otherwise missed by seismic detection methods. With a possibility of similar pore pressure responses to SSEs in Cascadia, we develop and assess a variety of detection methods to capture variations in pore pressure that are potentially related to SSEs in onshore measurements.

This study aims to detect anomalous behavior potentially associated with SSEs by implementing a variety of signal processing techniques, including filtering, short-term averages divided by long-term averages (STA/LTA), and predictive modeling / machine learning. To assess each method's detection ability, we compare detections drawn from existing data to known instances of slow slip constrained by tremor, GPS transients, strainmeter responses, and SSE catalogs. We apply Bayesian statistical analysis to determine the efficacy of each method in

detecting SSEs by assessing the probability that an observed anomaly within pore pressure data is related to an SSE.

2. THE DATA AND PRELIMINARY ANALYSIS

To evaluate whether or not pore pressure can be used to detect SSEs in Cascadia, we analyze pore pressure data from nine borehole observatories that comprise a portion of the Pacific Northwest Borehole Array component of NSF Earthscope's Plate Boundary Observatory (PBO) network. These observatories are specifically designed to be sensitive to strains associated with both seismic and aseismic tectonic activity [Roeloffs 2010]. Each borehole station actively records pore pressure, strain, and atmospheric data. For each station, continuous GPS stations are either co-located or close by. Each station has been operating and recording data for ~11 years, and all datasets analyzed start in April 2007 and end in July 2018. Pore pressure recorded from 2007 to mid-November 2009 is sampled at 1/300 Hz. Sampling rates shift to 1 Hz from mid-November 2009 to July 2018. Strainmeter, atmospheric, and GPS data are recorded at 1/300 Hz, 1/86400 Hz, and 1/86400 Hz respectively. Before analysis, all data are processed to account for shifts in sampling rate and for data gaps.

Figure 1 shows the locations of the observatories in the Cascadia region and their position relative to some known occurrences of SSE-related tremor. Figures 2 shows examples of raw pore pressure and GPS time series. Pore pressure responds to various natural phenomena, including tidal loading, short term meteorological events, and seasonal changes. Even in the raw data, anomalous pore pressure signals are apparent at the time of some SSEs, which provides some initial indication for the potential validity of our hypothesis. The behavior of these anomalies varies, with some occurring as dilatational or contractional steps, contractional spikes, or dilatational spikes lasting anywhere 8 to 15 days.

We apply a 2^{nd} order 6-60 day causal bandpass filter on the data to remove most tidal signals, signals from short-term meteorological events, and long-term seasonal trends. This bandpass however, should preserve signals with periods comparable to the commonly observed

duration of Cascadia SSEs. The pore pressure anomalies observed in the raw data are still clearly visible in the filtered data and coincide with GPS and strainmeter transients at known times of SSEs. Visual inspection of both filtered and raw data at the time of known SSEs finds anomalous pore pressure signals in at least one observatory borehole for about 60% of cataloged SSEs. The durations of these anomalies in filtered data ranges between 8 and 15 days. Figures 2a and 2b show examples of these anomalies within pore pressure data for a few borehole sites at two different time periods, 2013 and 2015-2016. Note that these anomalies do not persist through the entire SSE, marked in orange. These anomalies primarily coincide with tremor swarms as they migrate into the area near the PBO borehole site.

3. DETECTION METHODS

To develop an objective and effective means of detecting potential signatures of slow slip, we implement a variety of techniques, including STA/LTA and a Holt-Winter's predictive model, and test their effectiveness through Bayesian analysis. Each technique returns detections from input data as a function of time and each can potentially be updated in a machine-learning sense as new data are recorded at the PBO boreholes observatories.

3.1 STA/LTA

We first evaluate the ratio of short-term over long-term averages (STA/LTA), a common detection method used in seismology for detecting earthquakes in seismograms [Murdock and Hutt, 1983; Allen, 1978]. For the pore pressure data here, the short-term average (STA) is a measure of the average behavior of high-frequency signals similar in duration to the STA, such as earth tides and short-term meteorological events. The long-term average (LTA) is a measure of the average behavior for low-frequency signals within the data, such as those related to seasonal weather patterns or other background behaviors. An STA/LTA ratio that surpasses a set trigger threshold indicates that anomalous high-frequency signals are being recorded.

We are interested in detecting anomalous signals with durations similar to that of SSEs. As such, we use an 8-day STA over an 80-data LTA, which will encompass signals with lengths comparable to the typical durations of SSEs in Cascadia. The averages are calculated using causal moving windows. Detections are defined as when the ratio STA/LTA exceeds an arbitrary threshold. We evaluate detections from four different variants of processed input data: 1) the absolute value of raw, demeaned data, 2) the square of raw, demeaned data, 3) the absolute value of bandpass filtered data, and 4) the square of bandpass filtered data. Figure 3 shows examples of these processed data. Taking the square or absolute value of the data takes only the amplitude of the signal into account when searching for anomalous transients, with the former amplifying larger

signals and dampening weaker signals. The applied bandpass filter of 6-60 days removes high frequency signals related to earth tides, short-term meteorological effects, and long-term seasonal changes.

We apply a range of ratio thresholds for each borehole site and determine the thresholds that best detect anomalous behavior compared to a catalog of known SSEs. The range is set to include thresholds that constantly detect anomalous activity to thresholds that detect very few anomalies. The ideal threshold is one that detects anomalous activity caused by SSEs. As such, we chose the best threshold as the one that detects anomalous activity during known times of SSEs and little anomalous activity at other times (see Table 1 for a list of applied STA/LTA parameters and tested thresholds). Figure 4 shows an example of this detection method, with anomaly detections marked within the STA/LTA plot. Detections, or STA/LTA ratios that surpass the threshold, are converted into a time series plot where a value of "1" is assigned to data point of anomalous activity and a value of "0" indicates no anomalous activity, shown by the stem plot in Figure 4.

3.2 Predictive Model Anomaly Detection

As another means of detection, we use anomaly detection via a Holt-Winter's forecasting model. This forecasting algorithm is designed to model short-term trends and long-term seasonality within data and is often used to detect outliers from otherwise cyclic data [Holt, 1957; Winters, 1960; e.g. Barford et al., 2002; Szmit and Adamus, 2012].

Holt-Winter's forecasting, also known as triple-exponential smoothing, allows for forecasting of future data based on input data's cyclicity (or seasonality), trends, and point-to-point behavior, without the need for removal of components by filtering. Triple exponential smoothing follows [from Szmit and Adamus, 2012]:

$$\hat{y}_{x+m} = \mathrm{I}_x + \mathrm{mB}_x + \mathrm{S}_{x-\mathrm{L}+1+(\mathrm{m}-1)\mathrm{modL}}$$

with

$$\hat{y}_{x+m} = expected\ value\ at\ x+m, with\ m\ an\ integer$$

$$\mathrm{I}_x = \ intercept, or\ linear\ component$$

$$\mathrm{B}_x = \ trend\ component$$

$$\mathrm{S}_{x-\mathrm{L}+1+(\mathrm{m}-1)\mathrm{modL}} = cyclicity\ (seasonal)\ component$$

Each component is defined by:

$$\mathrm{I}_x = \alpha(\mathrm{y}_x - \mathrm{S}_{x-L}) + (1-\alpha)(\mathrm{I}_{x-1} + \mathrm{B}_{x-1})$$

$$\mathrm{B}_x = \beta(\mathrm{I}_x - \mathrm{I}_{x-1}) + (1-\beta)\mathrm{B}_{x-1}$$

$$\mathrm{S}_x = \gamma(\mathrm{y}_x - \mathrm{I}_x) + (1-\gamma)\mathrm{S}_{x-L}$$

where α, β, and γ are smoothing parameters for their respective components, L is the number of measurements associated with one season, m is the number of predicted data points beyond data point x, and (m-1)modL being the modulus after division of (m-1) and L. These smoothing parameters, also known as "forgetting factors," weight the influence of previous seasonal, trend, and data point components on the current value of the model. Generally, the smoothing factors are taken as those that minimize the sum of squared errors of prediction. Note each component requires initial values, each of which are calculated from the time series from a "training period" of desired length for the algorithm.

The Holt-Winter's model acts as a smoothing function that requires initial values to calculate the seasonality, trend, and data variation. These initial values are calculated from a set amount of data that "trains" the model. The more data included in the calculation of these initial values, the more sensitive the model becomes to deviations from "normal" behavior. The output is an exponentially smoothed version of the input data plus a set amount of predicted data points for a forecast of desired length.

Here, data that deviate from the forecast model are marked as anomalous transients. These transients are data that exceed Brutlag confidence bands calculated from the model, which define the upper and lower thresholds of expected behavior [Brutlag, 2000]. The algorithm takes high-frequency changes, short-term trends, and seasonality into account when calculating the model, but the input pore pressure data are demeaned for optional filtering. We iteratively train the model with additional seasonal cycles and trends by adding a year's worth of data for each iteration, beginning with two years and ending at eleven years.

The three smoothing parameters are chosen by iteratively running the Holt-Winter's model until the values minimize the sum of squared errors of prediction. Initial values must be chosen before the iterative error reduction. This is done qualitatively by determining, by eye, the sensitivity of a PBO site's entire pore pressure dataset to seasonal and short-term influences. The more readily seasonal activity, trends, or high frequency signals are observed to stand out, the lower the initial forgetting factors for each are set. After the error reduction returns updated smoothing parameters, manual minor adjustments refine the final parameters, so the model is more sensitive to anomalous activity during SSEs. This is done through trial and error, in which the smoothing parameters are varied slightly until the model consistently detects anomalous activity during SSEs with few detections outside of these events. We then select the most effective training period and smoothing parameters for detecting SSEs by analyzing the marked data. Should data marked as anomalous primarily fall during times of SSEs, the selected parameters are likely effective. We test the model on the final three years of data, from 2014 to 2017, to find detections.

4. BAYESIAN ANALYSIS

Once detections are returned by each method, we utilize Bayesian statistical analysis to assess each method's efficacy in detecting SSEs. Bayesian statistics determines the probability of an event or phenomenon, A, given the occurrence of a different, related event or phenomenon, B. We are interested if anomalous pore pressure detections can be used to detect SSEs without a priori knowledge of their occurrence. We know the probability of a pore pressure detection given the occurrence of slow-slip, aforementioned at roughly 60%, but we want to calculate the probability of slow-slip given the detection of a pore pressure anomaly so as to not rely on any more a priori information than what is already catalogued.

This quantity, formally known as the posterior probability, can be calculated using Bayes' theorem, which in terms applicable here follows [Stone 2013]:

$$p(SS|Pd) = p(Pd|SS) * \frac{p(SS)}{p(Pd)}$$

where p(SS|Pd) is the posterior probability of an SSE (SS) given the detection of pore pressure anomalies (Pd). p(Pd|SS) is the known prior probability of a detected pore-pressure anomaly occurring during known times of SSEs. p(SS) is the known likelihood of an SSE within the data, and p(Pd) is the probability of a pore pressure detection occurring within the data, regardless of cause, from a specific detection method.

Qualitatively, p(SS) is the ratio of a priori known slow slip duration within the region to the total duration of a particular pore pressure time series. p(Pd) is the ratio of total anomalous pressure activity from an applied detection method to the total duration of the pore pressure time series. p(Pd|SS) is the ratio of anomalous pressure detections during slow slip to the total number of measurements taken during slow slip. If a data gap occurs in the pore pressure time series, the amount of missing time is accounted for in the total duration when calculating p(Pd) by removing it from the total slow slip duration used when calculating p(SS) and p(Pd|SS).

We calculate a suite of posterior probabilities: for each of the nine PBO stations, for each applied detection method (STA/LTA and the Holt-Winter's model), for each threshold or training period used for each method, respectively. Each of these single-station probabilities are used to ascertain each method's ability to detect Cascadia SSEs.

5. JOINT PROBABILITY

To potentially improve the efficiency of detections, we calculate posterior probabilities that take multiple stations' detections into account. Large-scale regional phenomena, such as SSEs, are expected to induce observable pore pressure anomalies, at multiple locations, within a short temporal window. By computing joint probabilities, we preserve and enhance those detections that are spatiotemporally correlated and minimize detections related to local, site-specific disturbances. These joint-posterior probabilities are more robust than their site-specific counterparts given that SSEs are spatially large scale in nature, and it is expected that multiple borehole observatories should detect the same event.

To account for the spatiotemporal variation of SSEs, and thus potential delays in response between stations, we use one to four-day causal moving windows when temporally-correlating multiple stations' detections. If a detection is found within the window, the data within that window are marked as anomalous and a single detection is set at the end of the temporal window. Figure 5 shows an example of this procedure.

We calculate the joint-posterior probabilities for each pair of borehole sites for the most effective STA/LTA method and for the Holt-Winter's model. p(Pd) is now calculated by taking the ratio of the total number of detections and the total number of temporal windows. p(Pd|SS) is now calculated using the total number of detections divided by the total number of time windows that fall during SSEs. Time windows that partially fall during known SSEs are included within the calculations. From these values, we then determine the best groups of wells for joint-detections: well groups that have high amounts of temporally correlated detections are more likely to be used in tandem in the form of an SSE detection network. We then calculate the joint-posterior probabilities for these well groups and for all nine stations together, for each detection method, to determine if a full network-wide application is possible.

6. RESULTS

6.1 STA/LTA, Unfiltered Data

Figure 4 shows examples of the processed pore pressure data, STA over LTA, and detections found with the applied threshold for the unfiltered data. The detections are shown in the lowermost stem plots within Figure 4. The processed data, either the absolute value (Figure 4a) or the square of the data (Figure 4b), appear noisy and return fairly similar STA/LTA values for all datasets. The unvarying STA/LTA ratio leads to a widely spread, large number of detections for lower STA/LTA thresholds (3rd plots in Figures 4a/4b) or very few detections at higher STA/LTA thresholds (4th plots in figures 4a/4b). This is consistent across all wells for this application. Lower thresholds return a wide spread of detections throughout the dataset, with many occurring during and outside times of known SSEs. Higher thresholds return significantly fewer detections, but very few occur during more than one SSE.

Examples of the resultant posterior probabilities for the two variants of unfiltered data are shown in Table 2. The probabilities are low, ranging from 9-18% when the detection thresholds are set low (STA/LTA=1.25 or 1.75 for the absolute value and square data, respectively). These probabilities either drop to 0%, or increase to 22-52%, when the detection thresholds are increased slightly (to above STA/LTA=1.5 or 2, for the absolute value and square data, respectively). The increase in posterior probability corresponds with a decrease in the number of detections overall rather than an increase in the number of detections during slow slip. See Supplemental Materials for all calculated probabilities for this application of STA/LTA.

6.2 STA/LTA, Filtered Data

Figure 4 also shows examples of the filtered pore pressure data, STA over LTA, and detections found with the applied threshold for the absolute value of the filtered data. The absolute value of these filtered data (Figure 4c) appear noisy and return fairly constant STA/LTA

values for all datasets, similar to that of the unfiltered data. The occurrence of detections for the absolute value of the filtered data are also similar to that of the unfiltered data. The square of the data (Figure 4d), has a more variable STA/LTA ratio for all datasets and returns significantly fewer detections at both low and high thresholds (lowermost two plots in Figure 4d). At lower thresholds (STA/LTA=1.75-2), multiple detections occur both during and outside of times of known slow-slip. At higher thresholds (STA/LTA>2.75) the number of detections both in and outside of known times of SSEs drops, with few retained during times of SSEs. Detections that are retained during SSEs are done so only during one or two events. This method does not readily detect anomalous behavior for all SSEs.

Table 3 shows examples of the posterior probabilities from the absolute value and square value of the filtered data. The probabilities for the absolute value of the filtered data are similar to that of the unfiltered data- consistently low for lower thresholds which rapidly increase or drop to 0% with increasing threshold. At lower thresholds (STA/LTA=1.75, the posterior probabilities ranges from 8-16%. A slightly higher threshold (STA/LTA=2) increases this range to 9-21%. Higher thresholds still (STA/LTA=2.5) increase this range further to 0-30%. This is again due to a low number of detections made at higher thresholds, with few, if any, occurring during one or two SSEs. The posterior probabilities from the square of the filtered data are less sensitive to changes in STA/LTA threshold. At lower thresholds (STA/LTA=1.75), the probabilities range from 9-16%. At the highest threshold (STA/LTA=3.5), these probabilities range from 9-22%. These values correspond with the fairly constant number of detections beyond a threshold of STA/LTA=2.5. Some detections for the squared data coincide with 4 or more SSEs at higher thresholds (between 2.75 and 3.25) rather than 1 or 2 like the other processed datasets. Very few of the detections from these processed data are temporally correlated.

6.3 Joint Detections- STA/LTA, Filtered Data

Table 4 shows the posterior probabilities for the joint station detections. We omit results for the unfiltered data and the absolute value of the filtered data, as few to no detections are temporally correlated and return values for the joint-detection probabilities. The joint-probabilities for sites located near each other retained values near or above the single-station probabilities (such as sites B001 and B011). Some sites that are not located near each other also shared detections, such as sites B004 and B022. The northernmost wells, B010, B011, and B012, had the most correlated detections during SSEs. Sites B001, B003, B004, and B005 formed another group of wells with multiple temporally correlated detections during SSEs, though detections from these sites often coincided with those from the northern group. Sites B022 and B028, both being located far away from each other and all other sites, had variable correlation between other sites and to each other. In general for STA/LTA, the joint probabilities retained low values similar to that of the single-station probabilities, typically ranging from 13-30%. The strongly correlated groups contained the highest of these probabilities, and often retained detections during 3 or more SSEs. However, many other temporally correlated detections occurred outside of known times of SSEs for these groups. Network-wide probabilities remained below 10%, as very few temporally correlated detections were made across all wells during known SSEs.

6.4 The Holt-Winter's Model and Resultant Probabilities

Figure 6 shows the raw pore pressure data, Holt-Winter's model confidence bands, and resultant detections for a single borehole, Site B010. The detections are show in the lowermost stem plot of Figure 6. The model's detections primarily fall within times of known SSEs, with few detections occurring outside of these events. The model, across all wells, appears to reliably detect anomalous activity primarily during times of known SSEs, here shown in Figure 7. Some

detections occur outside of known times of SSEs, primarily for Site B012. When correlated, however, many of these outside detections are not retained. Group 1 comprised of sites B001, B004, and B005, Group 2 comprised of sites B010, B011, and B012, and Group 3 comprised of sites B022 and B028 had the strongest correlation amongst each other in that each group retained high numbers of detections during times of SSEs and very few elsewhere, shown in Figure 8. The final stem plot in Figure 8 shows the correlated detections across the full borehole network, which further affirms the increasing strength of correlated detections found during SSEs. Some detections across multiple wells are preserved but do not fall during times of known slow slip, such as the event in the Fall of 2016.

The posterior probabilities support the model's ability to detect SSEs. Table 5 lists the single-station posterior probabilities for the Holt-Winter's predictive model, which vary from a minimum of 35% to a maximum of 99% for sites B005 and B011, respectively. Table 6 lists the joint probabilities from each group of wells from the model using a four-day average window. The probabilities found using detections found across all stations within a particular group are greater than single-station values, ranging from 50% to 100%. Table 7 lists the joint probabilities for the entire network of eight wells from the model using a four-day window, which remain at 100% when at detections found across at least four stations are used. See Supplemental Materials for plots of all applications of the model for all nine borehole sites. A single application of the model is used, one for each site, resulting in nine sets of smoothing parameters and their respective detections. See Table 8 for the smoothing parameters applied for each site.

The Holt-Winter's model starts detecting anomalous activity after about eight years of training, and the most effective training period for the model is the entire dataset of 11 years. For most borehole sites, very few detections are made before this eight-year limit. Generally, a majority of detections fall during known times of slow slip. The model consistently detects

anomalous activity during the 2015-2016 and 2017 SSEs for all 8 borehole sites used. Site B003 is omitted for large data gaps, leading to insufficient data. For a few other borehole sites, the model detects anomalous activity for the 2014 event (see Figure 7). A lack of detections during SSEs from 2014 to 2017 is primarily caused by data gaps. When the data is intact, the model reliably picks out anomalous behavior for SSEs in 2014 and beyond.

Some detections do fall outside of known times of slow-slip but very few are uncorrelated between multiple well locations. Most of the correlated detections between the sites occur during SSEs. Some joint detections for the Holt-Winter's model suffer from the same drawback as the STA/LTA method in that only one or two detections are preserved, returning some anomalously high posterior probabilities for some well pairs. The model performs the best, in terms of detecting anomalous activity during SSEs, when a temporal window of four-days is used to find joint detections.

7. DISCUSSION

To assess the effectiveness of an SSE detection method using pore pressure data, we analyze the single-station and joint-station posterior probabilities and the detections they are based on. An effective method returns a higher the posterior probability, while an ineffective method returns lower posterior probabilities. The values of the probabilities alone, however, are not enough to determine a method's efficacy, so we also consider where and how many detections are made. If detections are scattered, or if their positions change with slight changes in the applied method, or if they are not well correlated between borehole sites, it is likely that the method is not effective even if the final posterior probability is relatively high.

In general, STA/LTA proves ineffective in detecting SSEs within these data. The unfiltered pore pressure retains all recorded signals, and the absolute value of the filtered pore pressure retains many signals within the bandwidth of the filter. The resultant unvarying STA/LTA ratio from these processed data makes it difficult to resolve signals that are similar in duration to that of SSEs, including those potentially related to SSEs. The fairly unvarying STA/LTA ratios also suggests that this application of STA/LTA is insensitive to anomalous transients in these three variants of processed data we evaluated. Figures 3 and Figure 4 exemplify these characteristics, in which many signals of similar magnitude persist within the processed data, resulting in an unvarying STA/LTA. This inability to detect SSEs is supported by fairly low posterior probabilities, ranging from 0-20%. Higher STA/LTA thresholds return probabilities greater than 50% for the absolute value of the unfiltered data, however these values are erroneously high due to the overall low number of pore pressure detections. Any detections that fall during an SSE do so for only one or two events, with very few others outside of known times of SSEs. This ultimately results in a low p(Pd) and a much higher p(Pd|SS). The events

that contain signals also change from site to site, resulting in very low joint-probabilities for these processed data, about less than 10%.

For the square value of the filtered data at higher STA/LTA thresholds, some of the resultant single-station posterior probabilities are higher, over 30%. However, the coincidence of the few detections made from these processed data again only lies with one or two SSEs from the group of 10 possible events. This can be easily labeled as happenstance rather than causal, as many other detections still persist outside of known times of slow-slip (see Figure 4d). This is supported by the very low probability of a pore pressure detection occurring during an SSE (p(Pd|SS)) and an overall low probability of a pressure detection occurring at any time (p(Pd)) for all wells (see Tables 2 and 3). The joint-station probabilities for these data are nearly identical to that of the single-station probabilities for lower STA/LTA thresholds, as the large number of widely spread detections persists (Table 4). Higher STA/LTA threshold ratios return fewer correlated detections, however few occur during an SSE, and those that do only do so for a single event and again return misleadingly high posterior probabilities as a result.

Any signals potentially related to SSEs are likely masked and irresolvable utilizing filtering and STA/LTA applications. The anomalies found from the initial by-eye analysis of the raw data occur as relatively low-amplitude decreases or increases in pore pressure over a long-term period, and STA/LTA appears more sensitive to the short-term, high amplitude changes within these data. The deviation of these observed anomalies from background behaviors during SSEs cannot be detected by STA/LTA. Any detections made from STA/LTA applications are either too large in number and widely spread throughout the dataset or are too few in number such that any detections made during an SSE appear coincidental. This results in either very low or erroneously high posterior probabilities, respectively. As such, we deem STA/LTA as ineffective for reliably detecting SSEs in these pore pressure data.

The Holt-Winter's model proves much more promising. Anomaly detections made at each station consistently fall during times of known SSEs, with fewer detections occurring outside of these times in comparison to the STA/LTA. Single station posterior probabilities are consistently high for all wells, typically above 35% (Table 5). In terms of detecting SSEs, the most effective method appears to involve the correlation of multiple wells' detections from the Holt-Winter's model, specifically the wells that comprise Groups 1 through 3. These return high joint-station posterior probabilities, ranging from 50-100%, as multiple detections across 2 or 3 SSEs are retained with even fewer detections remaining outside of the SSEs (See Figure 8, Table 6). Specifically, detections that are found during SSEs that are correlated amongst all of the wells within an individual group return the highest probabilities. For network-wide correlations, detections that are found on at least four stations return the highest posterior probabilities, again confirming that the use of multiple stations detections prove the most effective in detecting SSEs (see Table 7).

Longer temporal windows perform better when finding joint-station SSE detections, specifically a four-day window, as it adjusts for different response times to the same event. Given the migratory nature of slow-slip throughout a single SSE, this result was expected. The model is mostly sensitive to low-frequency, high amplitude signals in the data that deviate from the defined seasonality, such as the step-like or spike phenomena that are observed in both the raw and filtered data at known times of slow slip (see Figure 2). The model readily detects these and other long-term signals that coincide with SSEs. Given that the correlated detections occur for all recorded SSEs beyond the training period limit, and that very few occur outside of known times of SSEs, the Holt-Winter's model appears to reliably detect SSE related signals in these pore pressure data.

We find that the model readily detects all three SSEs beyond the minimum eight-year training period: the 2014, 2015-2016, and 2017 events. To determine if the observed detections coincide with the initially observed anomalous transients in the raw pore pressure data, and if the event in the Fall of 2016 coincides with an undetected SSE, we compare the network detections found across at least 4 or more wells to the raw and filtered pore pressure data, raw strainmeter data, and GPS data at a few borehole sites. Figures 9, 10, and 11 show examples of this. We find that the detections made from the model coincide with the strong anomalous signals from the initial analysis, as well as the strainmeter and GPS transients related to SSEs (Figures 9 and 10). For some locations, an anomaly is not readily recognizable by eye within the raw or filtered pore pressure data (Figure 11), but detections are still made and are correlated with other locations. However, some strongly correlated detections do fall outside of known times of slow slip. Specifically, a group of strongly correlated detections occurs in the Fall of 2016 (Figure 8-lowermost plot), which we believe to be related to an uncatalogued SSE. Hawthorne and Bartlow [2018] note the occurrence of smaller slow-slip subevents that may comprise larger SSEs, of which this detection may be related.

To investigate further, we plot all raw pore pressure data during each SSE and for the event of Fall 2016 and compare the data with the single-station detections, joint station detections, and GPS data (Figures 12 through 15). Figure 13 exemplifies how the model detects step-like anomalies within the data, specifically for sites B004, B005, and B010 for the event of 2015-2016. Other detections, such as those during the 2014 and 2017 SSEs, are found during long-term, non-step like decreases in pore-pressure (Figures 12 and 14). A similar signal is found with the other detections made for the uncatalogued event in the winter of 2016 (Figure 15). For the three catalogued SSEs, the detections coincide with the GPS transients associated with SSEs (see Figures 12 through 14 for examples). We speculate that these types of responses within pore

pressure data may be specific indicators of slow-slip, examples of which are shown in Figure 16. These signals generally occur as long-term dilatations followed by brief recovery to normal pore-pressure levels, however some of these signals occur as contractional steps (for example, site B010 in Figure 13). These dilatation-contraction differences are likely related to the position of the borehole sites relative to the portions of the slipping plate boundary, a behavior shown in pore pressure data from Araki et al. [2017]. For the uncatalogued event, no noticeable transient within GPS data appears, however a when plotted against strainmeter data, a strong transient occurs alongside the anomalous pore pressure detections (see Figure 15). This indicates that some phenomenon is occurring, and it may be related to the aforementioned slow-slip subevents. In general, the Holt-Winter's model readily detects SSEs within these pore pressure data alongside a few other events that require further investigation.

As more data become available, the efficacy of the Holt-Winter's model can be further improved, and the applications further refined to detect SSEs. Given the archive of previous data, this model can potentially update in real-time with new data. Expansion of the catalogue of meteorological phenomena may omit some strongly correlated detections: training the model to ignore weather related signals based on their behavior and temporal occurrence could refine future SSE detections. The model may also be improved by considering the non-stationarity of the data, for which other acceptable statistical approaches can be implemented, such as SARIMA (Seasonal Autoregression Moving Average) models.

8. CONCLUSIONS

Our analysis of borehole pore pressure data from NSF Earthscope's PBO Network in Cascadia supports our hypothesis in that these data can record detectable signals potentially related to SSEs. Our results find that a Holt-Winter's predictive model trained with at least eight years of these pore pressure data readily detects anomalous pore pressure behavior at known times of SSEs. These anomalous detections coincide with GPS and strainmeter transients associated with Cascadia SSEs. Cross correlation of these detections between borehole sites found that multiple locations record anomalous pore pressure activity at similar times during SSEs. We performed Bayesian statistical analysis on these correlated detections and found that the probability of slow-slip given a joint-station detection ranges from 50-100%, and we determine that groups of multiple, closely located sites may readily perform as a real-time detection network for Cascadia SSEs. Some strongly correlated detections outside of known times of slow-slip are also found, and we speculate that they may be related to uncatalogued slow-slip subevents.

Analysis of pore pressure data by-eye revealed anomalous activity during times of known slow-slip, and many are detected by the Holt-Winter's model. We find a specific signal that may be a common type of response to SSEs within pore pressure data. Slight contractional or dilatational variations of this common signal may be explained by the position of borehole stations relative to the contractional or dilatational portions of the slipping plate boundary. A common signal occurs as a strong deviation from seasonal behavior within pore pressure data, typically as a long period of dilatation followed by a brief contraction back to normal levels. Filtering of data reveals some of these anomalous signals, however many remain masked by other recorded signals within the data. Further refinement of analysis techniques, and the use of other predictive models that account for more complex dataset behaviors, may improve the detection of this potentially SSE related activity with borehole pore pressure data.

REFERENCES

Allen, R. V. (1978). Automatic earthquake recognition and timing from single trace, *Bulletin of the Seismological Society of America., 68*, 1521-1532.

Araki, E., Saffer, M. S., Kopf, J. A., Wallace, L. M., Kimura, T., Machida, Y., Ide, S., Davis, E., & IODP Expedition 365 shipboard scientists. (2017). Recurring and triggered slow-slip events near the trench at the Nankai Trough subduction megathrust. *Science, 356*(6343), 1157-1160. https://doi.org/10.1126/science.aan3120.

Barford, P., Kline, J., Plonk, D., & Ron, A. (2002). A signal analysis of network traffic anomalies, *Paper presented at Proceedings of the 2nd ACM SIGCOMM Workshop on Internet measurement*, *Marseille, France 2002.*

Bouchon, M., Durand, V., Marsan, D., Karabulut, H., & Schmittbuhl, J. (2013). The long precursory phase of most large interpolate earthquakes*, Nature Geoscience, 6*, 299-302. https://doi.org/10.1038/NGEO1770.

Brutlag, J. D. (2000). Aberrant behavior detection in time Series for network monitoring, *14th System Administration Conference Proceedings, New Orleans 2000*, pp. 139-146.

Crowell, B. W., Bock, Y., & Liu Z., (2016). Single-station automated detection of transient deformation in GPS time series with the relative strength index: A case study of Cascadian slow slip, *J. Geophys. Res. Solid Earth, 121*, 9077–9094. https://doi.org/10.1002/2016JB013542.

Davis, E., H. Villinger, & Sun, T. (2015). Slow and delayed deformation and uplift of the outermost subduction prism following ETS and seismogenic slip events beneath Nicoya Peninsula, Costa Rica, *Earth Planet. Sci. Lett., 410*, 117–127.

Davis, E., Heesemann, M., & Wang, K. (2011). Evidence for episodic aseismic slip across the subduction seismogenic zone off Costa Rica: CORK borehole pressure observations at the subduction prism toe, *Earth. Planet. Sci. Lett., 306*, 299-305.

Dragert, H., Wang, K., & James, T. S. (2001). A silent slip event on the deeper Cascadia subduction interface, *Science, 292*(5521), 1525-1528. https://doi.org/10.1126/science.1060152.

Hawthorne, J. C., & Bartlow, N. M. (2018). Observing and Modeling the spectrum of a slow slip event, *Journal of Geophysical Research, 123,* 4243-4265. https://doi.org/10.1029/2017JB015124.

Holt, C. E. (1957). Forecasting seasonals and trends by exponentially weighted averages (*O.N.R. Memorandum No. 52)*. Carnegie Institute of Technology, Pittsburgh USA. https://doi.org/10.1016/j.ijforecast.2003.09.015

Ito, Y., Hino, R., Kido, M., Fujimoto, H., Osada, Y., Inazu, D., Ohta, Y., Iiunuma, T., Ohzono, M., Miura, S., Mishina, M., Suzuki, K., Tsuji, T., & Ashi, J. (2013) Episodic slow slip events in the Japan subduction zone before the 2011 Tohoku-Oki Earthquake, *Tectonophysics, 600,* 14-26. https://doi.org/10.1016/j.tecto.2012.08.022.

Ito, Y., Hino, R., Suzuki, S., & Kaneda, Y. (2013). Episodic tremor and slip near the Japan Trench prior to the 2011 Tohoku-oki earthquake, *Geophysical Research Letters, 42*, 1725-1731. https://doi.org/10.1002/2014GL062986.

Kato, A., Obara, K., Igarashi, T., Tsuruoka, H., Nakagawa, S., & Hirata, N. (2012). Propagation of slow slip leading up to the 2011 M_w 9.0 Tohoku-Oki earthquake, *Science, 335*(6069), 705-708. https://doi.org/10.1126/science.1215141.

Murdock, J. N., & Hutt, C. R. (1983). A new event detector designed for the seismic research observatories, *USGS*, Open File Report 83-7851.

Obara, K., H. Hirose, F. Yamamizu, & K. Kasahara (2004), Episodic slow slip events accompanied by non-volcanic tremors in southwest Japan subduction zone, *Geophysical Research Letters, 31*(L23602). https://doi.org/10.1029/2004GL020848.

Peng, Z., & Gomberg, J. (2010). An integrated perspective of the continuum between earthquakes and slow-slip phenomena, *Nature Geoscience, 3*. 599-607. https://doi.org/10.1038/ngeo940.

Scientists operating the Pacific Northwest Seismic Network (PNSN) (2018). Tremor locations by week for last several ETS, https://assets.pnsn.org/oldets/compare_maps/.

Roeloffs, E. (2010). Tidal calibration of Plate Boundary Observatory borehole strainmeters: Roles of vertical and shear coupling, *Journal of Geophysical Research, 115*(B06405). https://doi.org/10.1029/2009JB006407.

Roeloffs, E. (1996). Poroelastic techniques in the study of earthquake-related hydrologic phenomena, *Advances in Geophysics, 37*, 135-195.

Roeloffs, E. A., Burford, S. S., Riley, F. S., and Records A. W. (1989). Hydrologic effects on water level changes associated with episodic fault creep near Parkfield, California, *Journal of Geophysical Research, 94*(B9) 12,387-12,402.

Rogers, G., & Dragert, H. (2003). Episodic tremor and slip on the Cascadia subduction zone: the chatter of silent slip, *Science, 300*(5627). https://doi.org/10.1126/science.1084783.

Ryan, W.B.F., Carbotte, S. M., Coplan, J. O., O'Hara, S., Melkonian, A., Arko, R., Weissel, R. A., Ferrini, V., Goodwillie, A., Nitsche, F., Bonczkowski, J., & Zemsky, R. (2009). Global multi-resolution topography synthesis, *Geochemistry Geophysics Geosystems*, *10*(Q03014). https://doi.org/10.1029/2008GC002332.

Schwartz, S. Y., & Rokosky, J. M. (2007). Slow slip events and seismic tremor at circum-Pacific subduction zones, *Reviews of Geophysics, 45*(RG3004). https://doi.org/10.1029/2006RG000208.

Segall, P. (2010). Earthquake and volcano deformation, 424 pp., Princeton Univ. Press, Princeton, N. J.

Stone, J. V. (2013). Bayes' Rule: A Tutorial Introduction to Bayesian Analysis. Sebtel Press.

Szmit, M., Szmit, A., Adamus, S., and Bugala, S. (2012). *Implementation of Brutlag's algorithm in anomaly detection 3.0,* Paper presented at Proceedings of the Federated Conference on Computer Science and Information Systems, Szczecin, Poland.

Wallace, L. M., Webb, S., C., Ito, Y., Mochizuki, K., Hino, R., Henrys, S., Schwartz, S. Y., & Sheehan, A. F. (2010). Slow slip near the trench at the Hikurangi subduction zone, New Zealand, *Science, 352*(6286), 701-704. https://doi.org/10.1126/science.aaf2349.

Wang, C., & Manga, M. (2010). Hydrologic responses to earthquakes and a general metric, *Geofluids, 10*, 206-216. https://doi.org/10.1111/j.1468-8123.2009.00270.x.

Wech, A. G., & Bartlow, N. M. (2014). Slip rate and tremor genesis in Cascadia, *Geophysical Research Letters, 41*, 392-398. https://doi.org/10.1002/2013GL058607.

Winters, P. R. (1960). Forecasting sales by exponentially weighted moving averages. *Management Science*, *6*, 324–342. https://doi.org/10.1287/mnsc.6.3.324

APPENDIX A

FIGURES AND TABLES

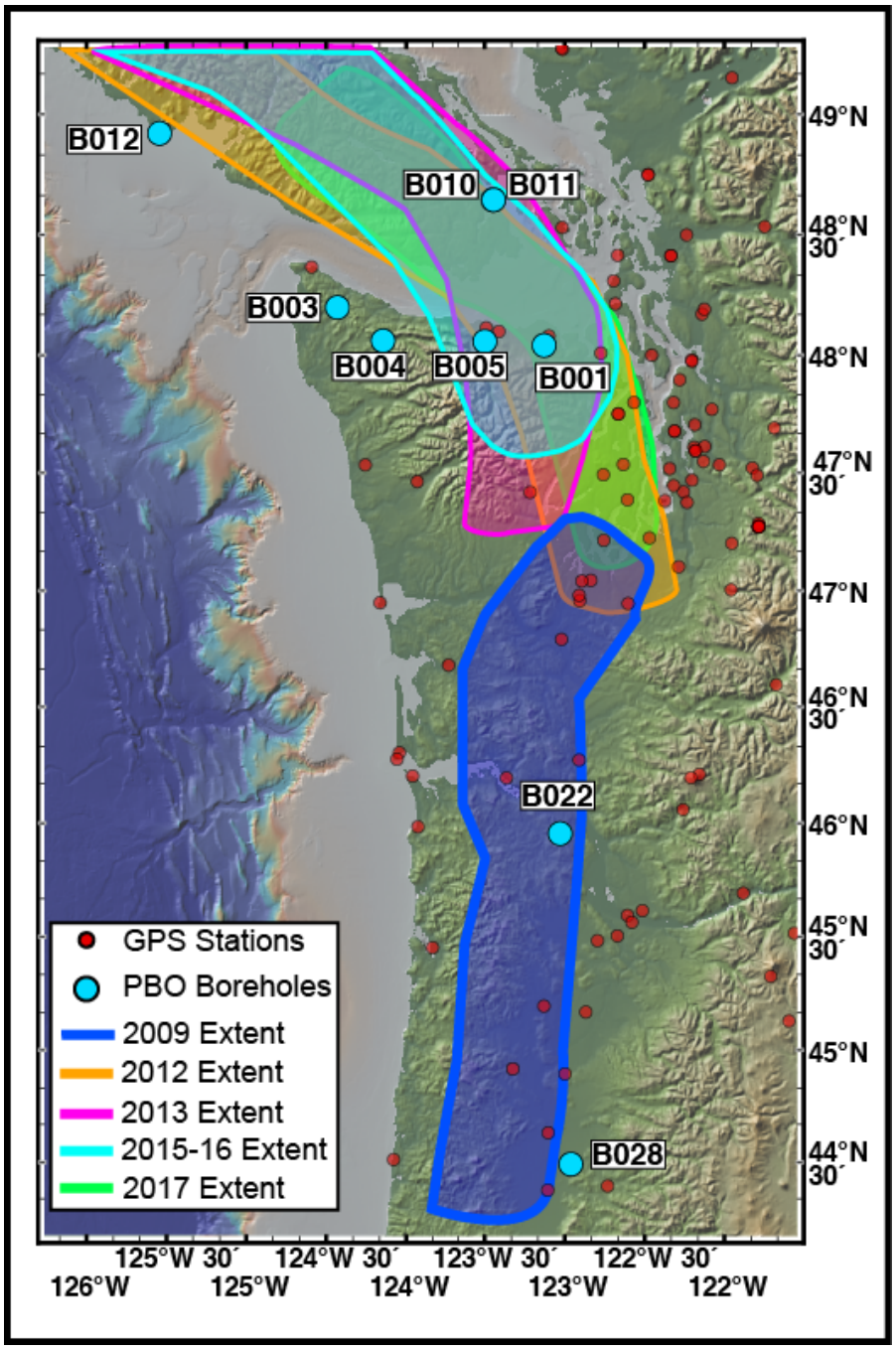

Figure 1. Spatial Extent of Several Cascadia SSEs- Different SSEs are marked by the colored patches. The locations of continuous GPS stations and PBO boreholes are marked by the red and blue dots, respectively. SSEs are primarily constrained to the northwest portion of the region, however some events, like the 2009 event, propagate further south within the Southern Washington-Oregon area [Bathymetry reprinted from Ryan et al. 2009]

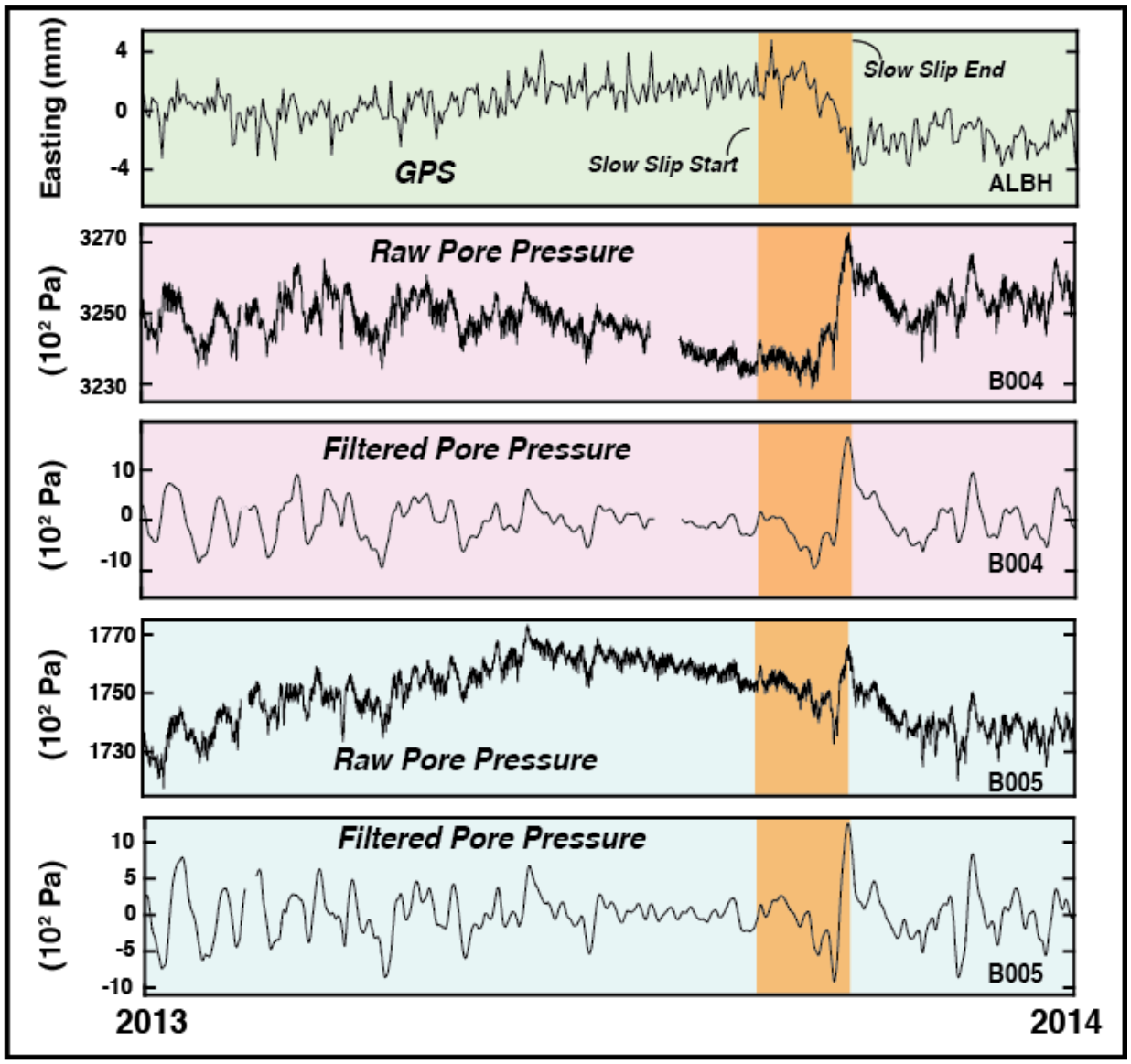

Figure 2A. Pore Pressure Anomalies at Sites B004 and B005, 2013- The top plot shows the easting GPS data for the concurrent GPS site ALBH near borehole B004. The second two plots show the raw and filtered pore pressure data for Site B004 for the year of 2013. The lowermost two plots show the same data for site B005. The SSE that occurred during 2013 is marked in orange. Note the strong step-like transient in both the raw and filtered data that coincides with the GPS transient associated with the SSE for 2013.

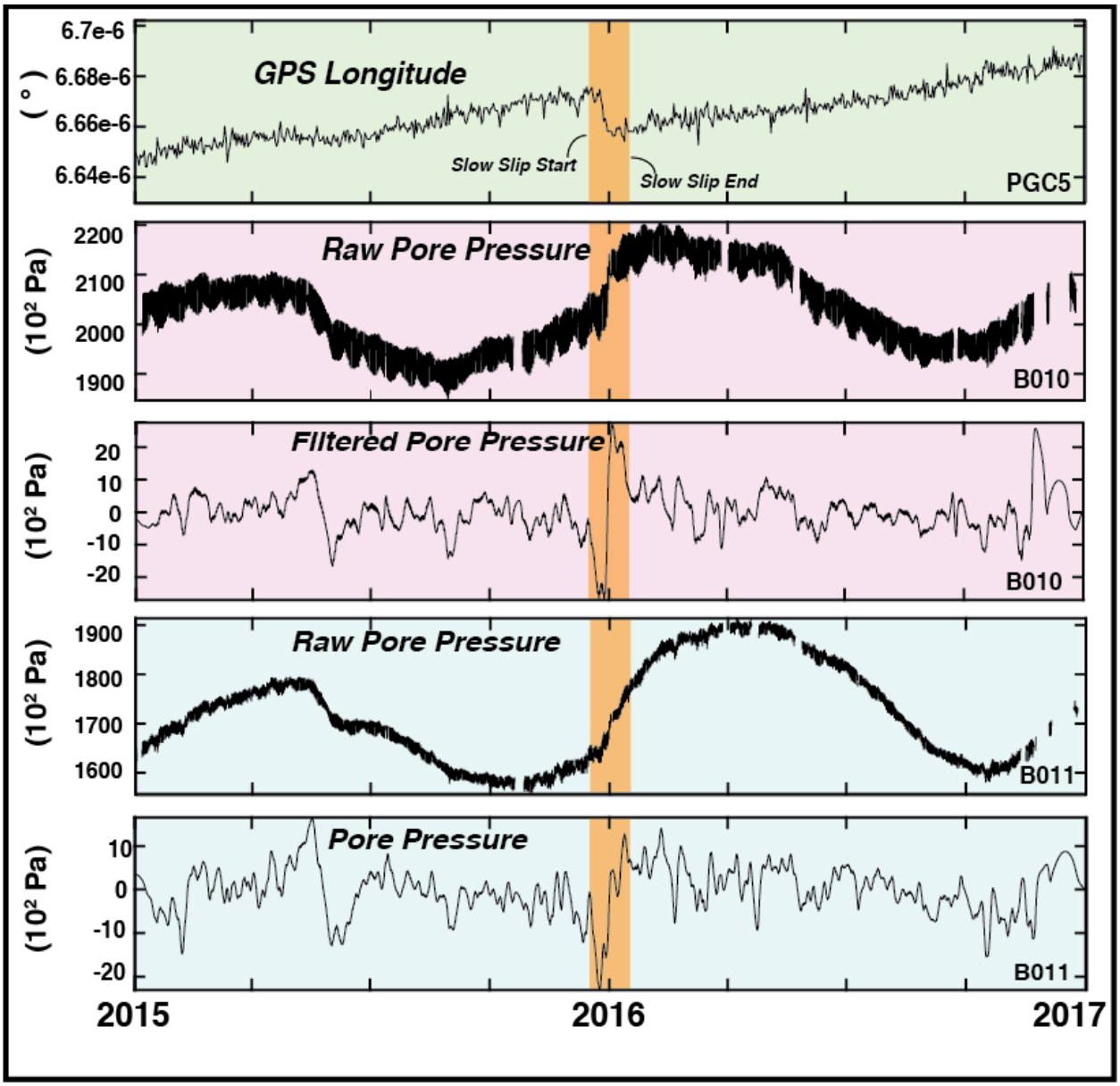

Figure 2B. Pore Pressure Anomalies at Sites B010 and B011, 2015-2016- The top plot displays the GPS data for the concurrent GPS station PGC5 for borehole sites B010 and B011. The second and third plots show the raw and filtered pore pressure data for Site B010. The lower two plots show the same data for site B011. The SSE for 2015-2016 is marked by the orange rectangle. Note the step-like transients that are resolved by the filtered data that coincide with the GPS transient associated with the SSE for 2015-2016.

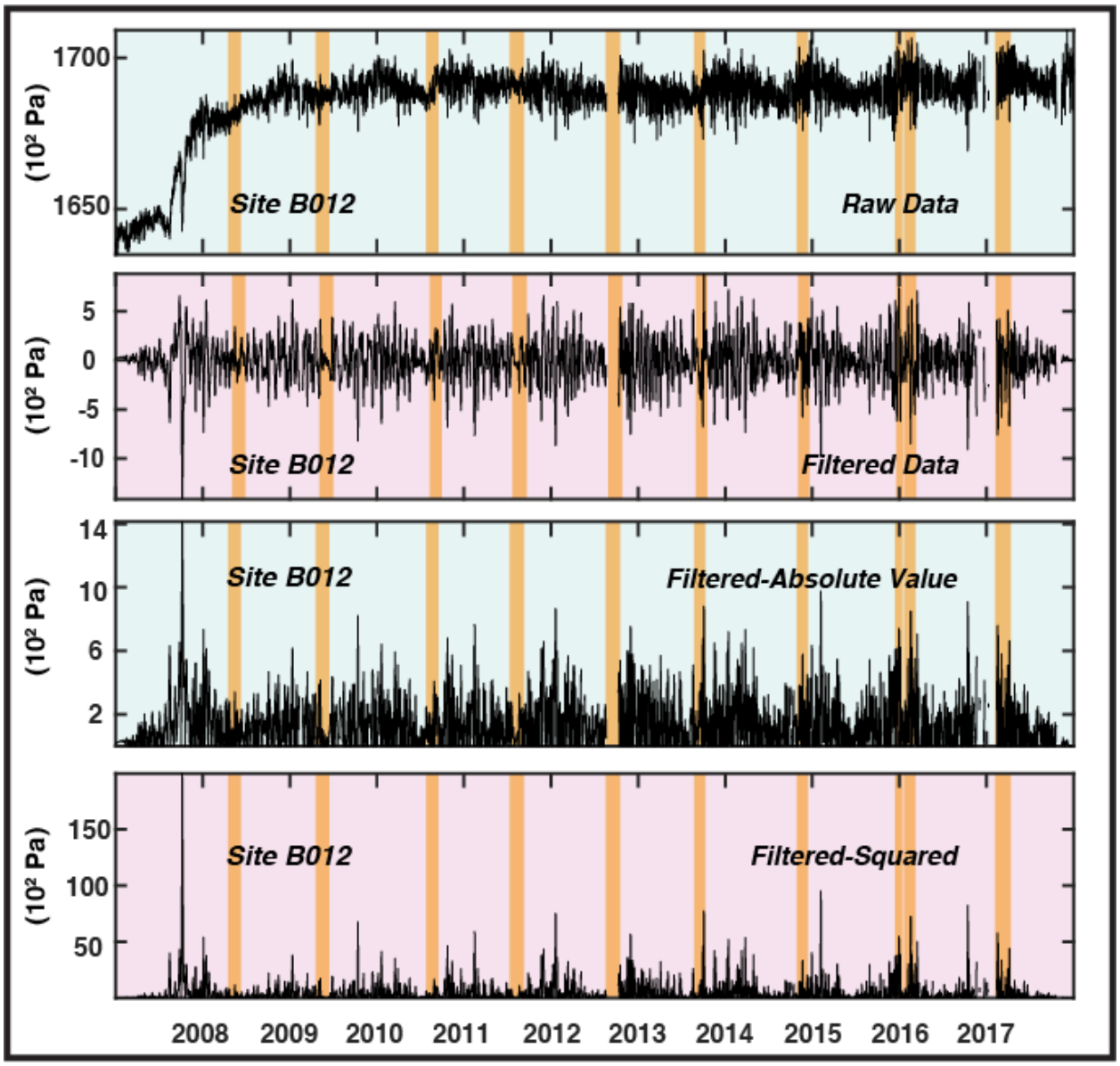

Figure 3. Processed Pore Pressure Data, Site B012- The top plot shows the raw data. The second plot shows the filtered data. The third plot shows the absolute value of the filtered data. The fourth plot shows the square value of the filtered data. Filtering parameters are a 2nd order bandpass, 6-60 day band. Orange rectangles mark known occurrences of slow slip. Interpolation from data gaps is removed.

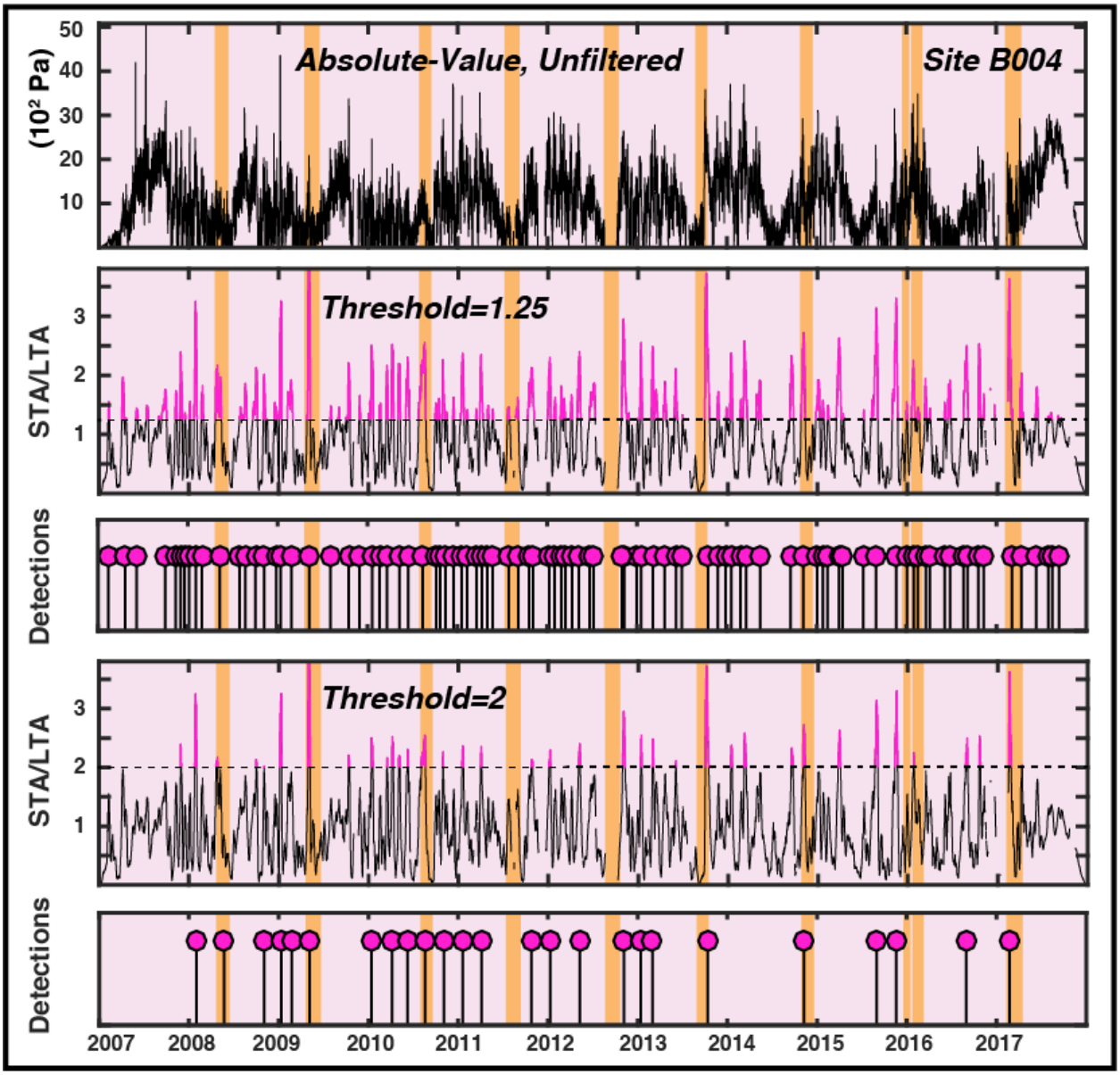

Figure 4A. STA/LTA Results, Site B004, Absolute Value of Unfiltered Data- The top plot shows the absolute value of the unfiltered pore pressure data. The second and fourth plots shows the STA/LTA for the data at two different thresholds, denoted in the figured. Data that surpasses the threshold, marked by the dashed lines, are marked in purple. The stem plot shows the marked data as detections beneath their respective STA/LTA plots. Note that detections occur, for this site, during 5 events, with other detections occurring outside of these events.

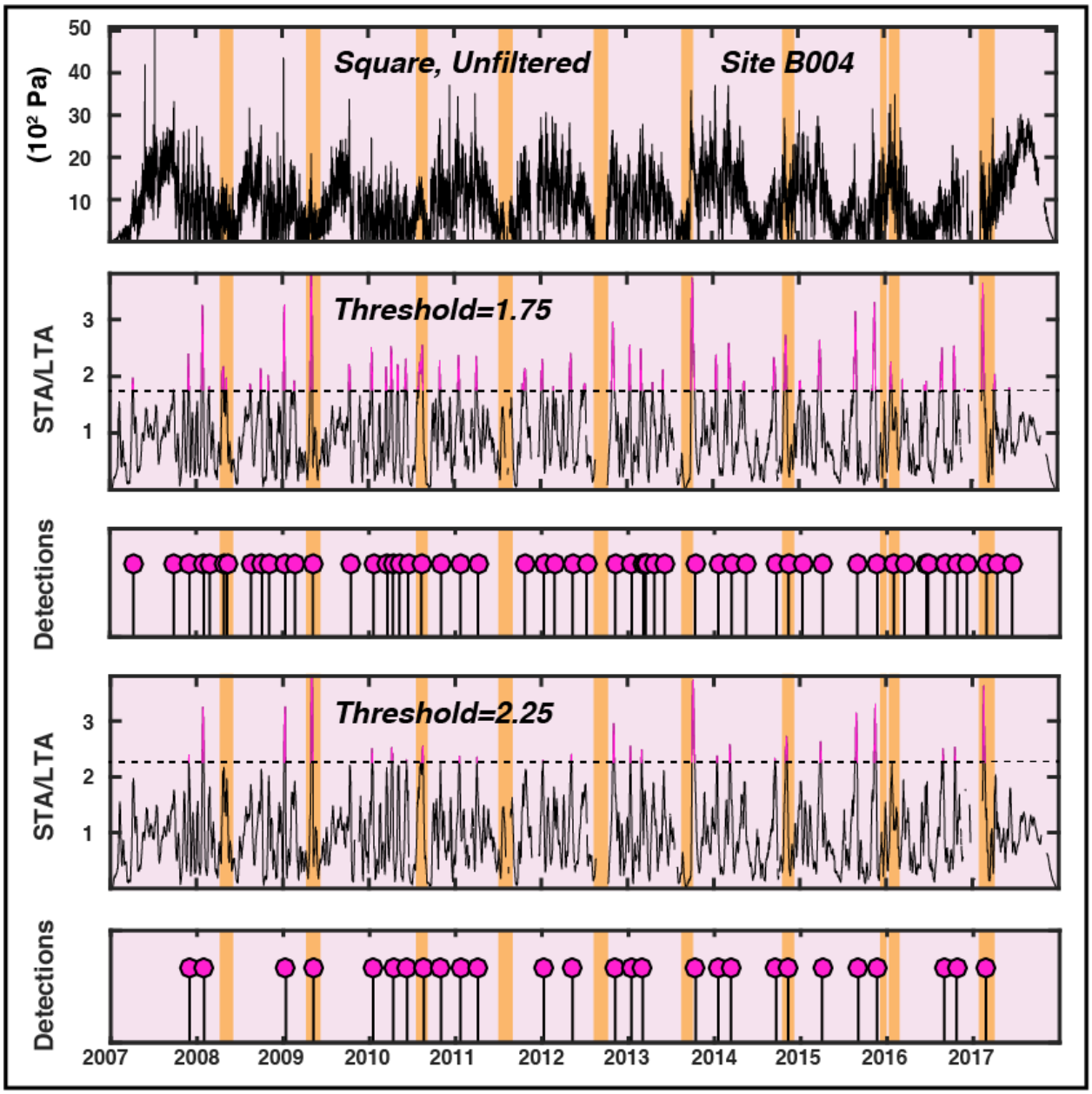

Figure 4B. STA/LTA Results, Site B004, Square Value of Unfiltered Data- This figure is identical to figure 4a, except the processed data in the top plot are now the square value of the unfiltered data. The number and spread of detections are similar to that of the absolute value of the filtered data, in that many detections are made both during at outside of known times of slow slip.

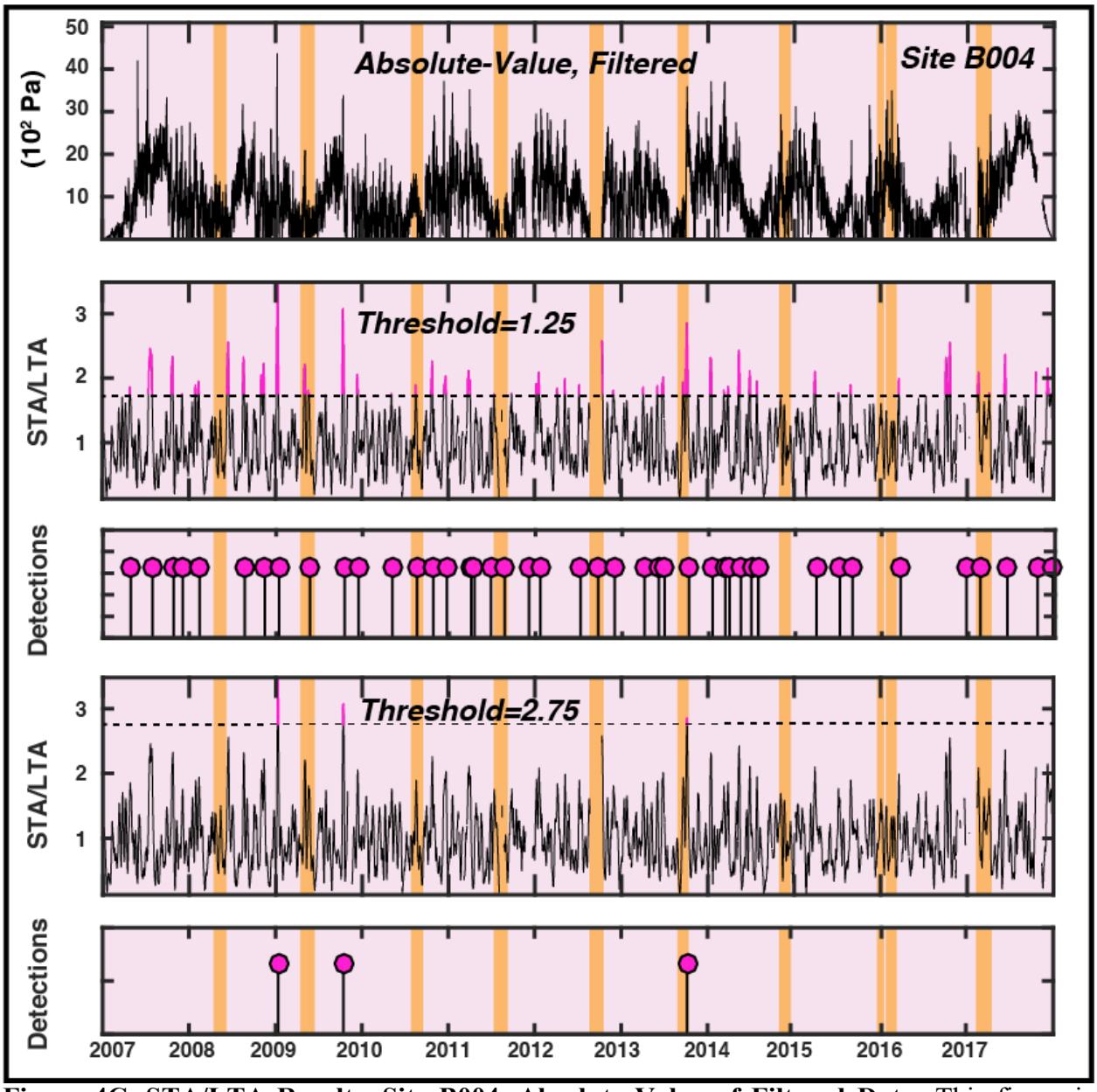

Figure 4C. STA/LTA Results, Site B004, Absolute Value of Filtered Data- This figure is identical to figure 4b, except the processed data in the top plot are now the absolute value of the filtered data. Note that detections occur, for this site, during only one event for the higher threshold, with few others occurring outside of the SSEs.

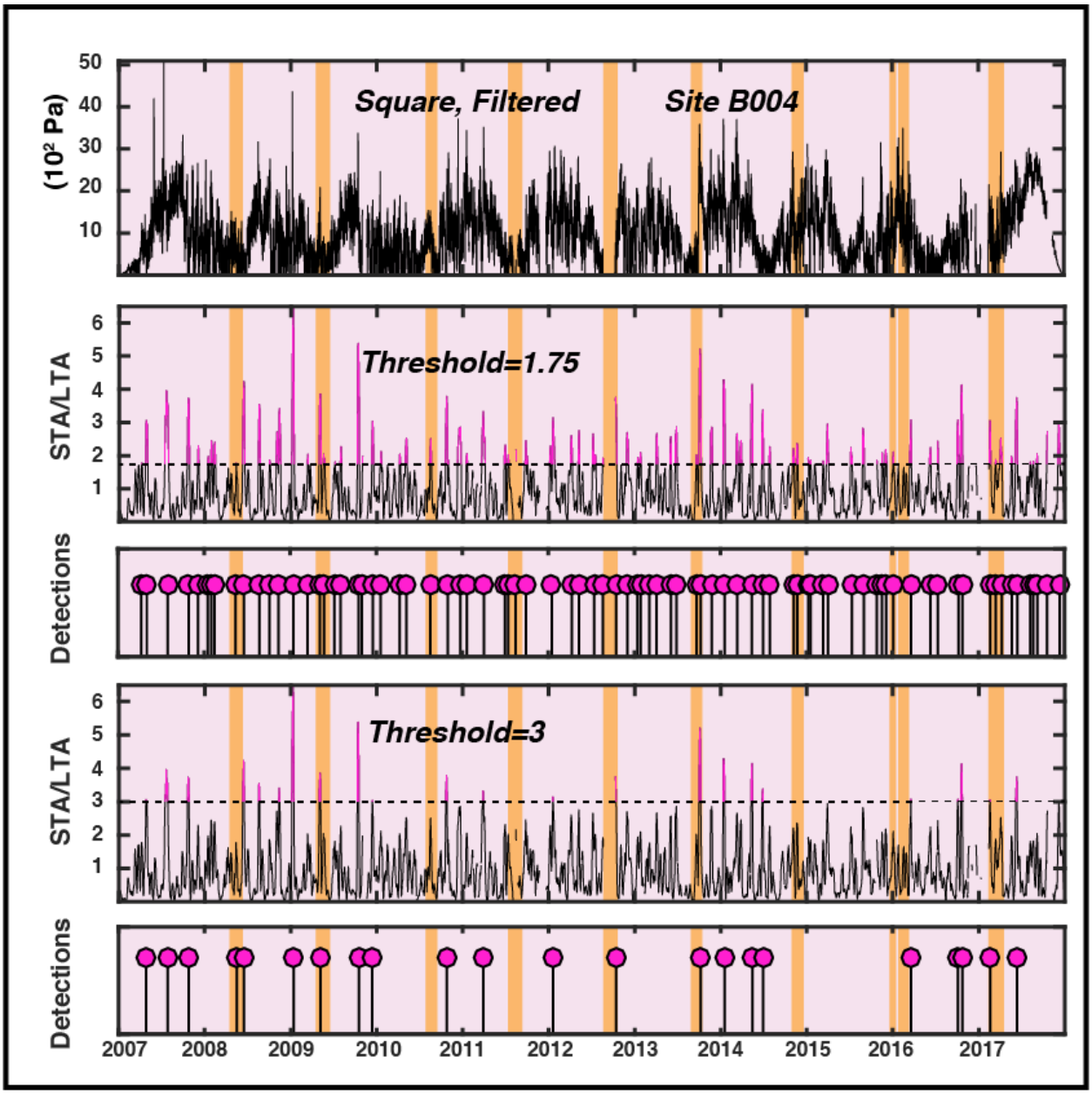

Figure 4D. STA/LTA Results, Site B004, Square Value of Filtered Data- This figure is identical to figure 4C, except the processed data in the top plot are now the absolute value of the filtered data. The higher threshold returns some detections during 5 SSEs, but note that many detections occur outside of these events.

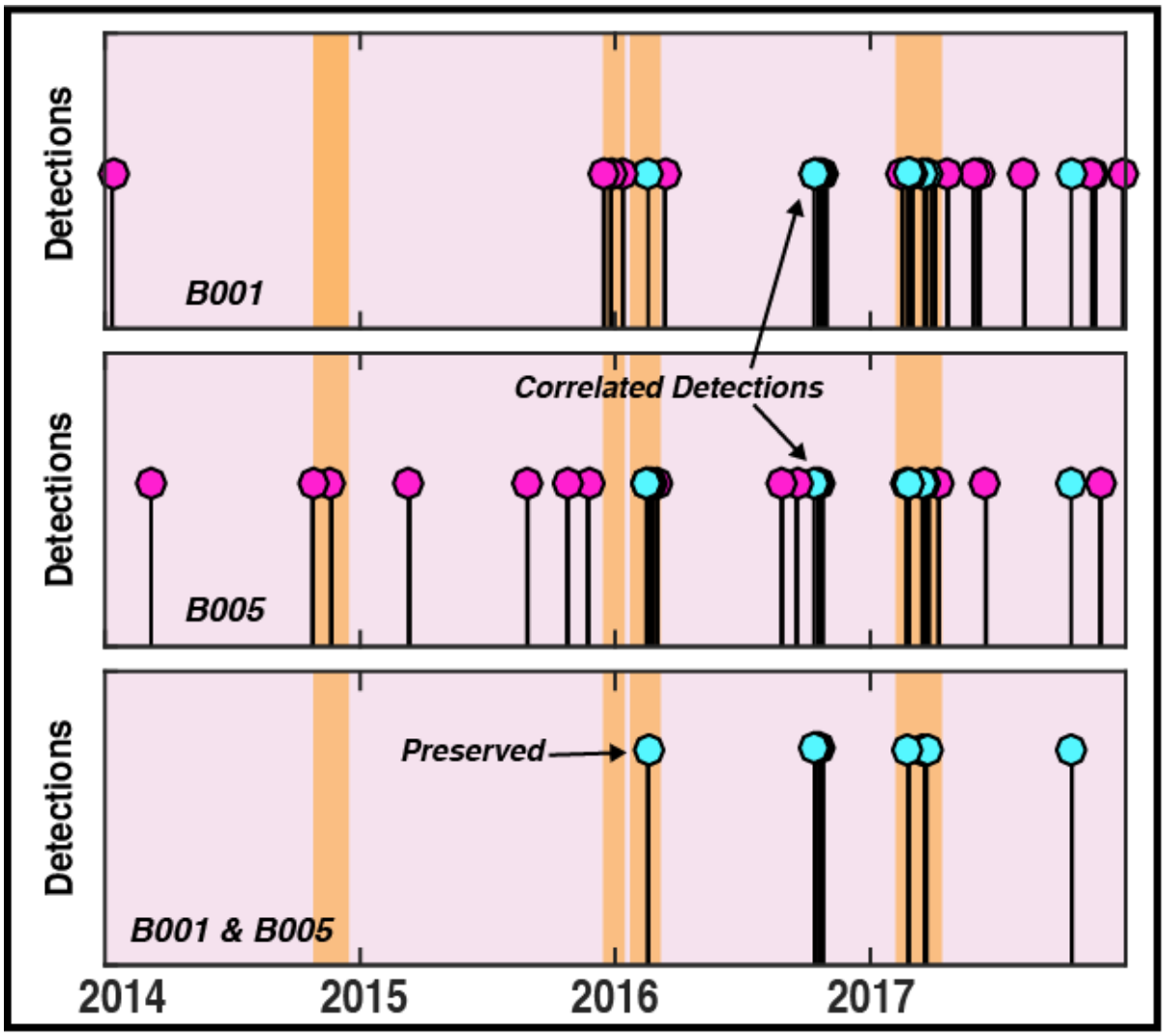

Figure 5. Example of Joint Detection Procedure, Sites B004 and B005- The top two plots show the detections found for sites B004 and B005. The lowermost plot shows the detections that are temporally correlated. The correlated detections are shown by the blue dots, and the uncorrelated detections are show by the purple dots. A four-day average window is used for these detections. Note that the correlation removes most of the detections that occur outside of the SSEs.

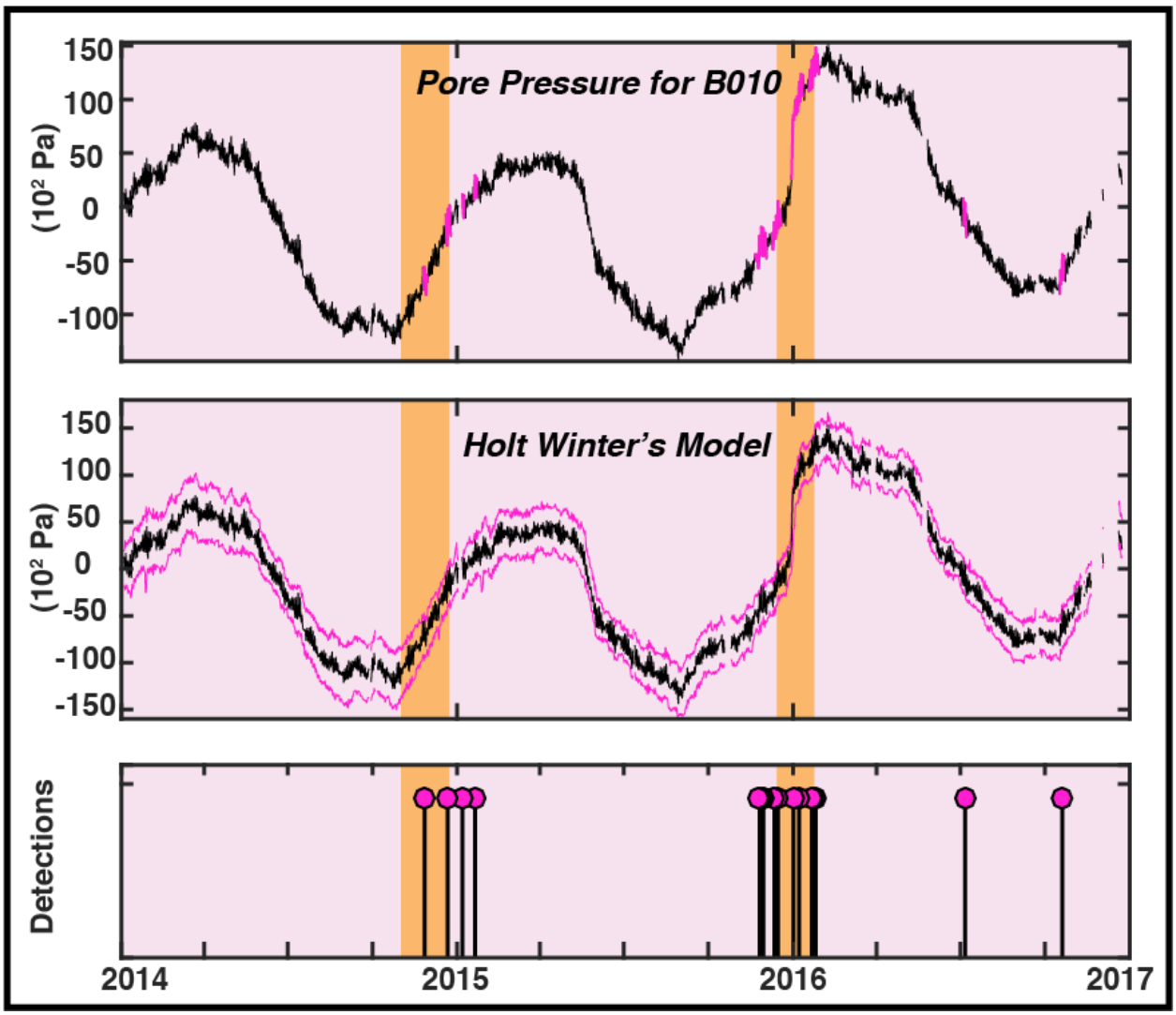

Figure 6. Holt-Winter's Model for Site B010- The top plot shows the raw pore pressure data with anomalous data marked in purple. The second plot shows these data with the Brutlag confidence bands (in purple) calculated from the predictive model. The lowermost plot shows the data that surpass the confidence bands as detections. All SSEs are marked in orange. Data gaps during the SSE of 2017 omit any possible detections for the 2017 event. No temporal windows are used in the detections.

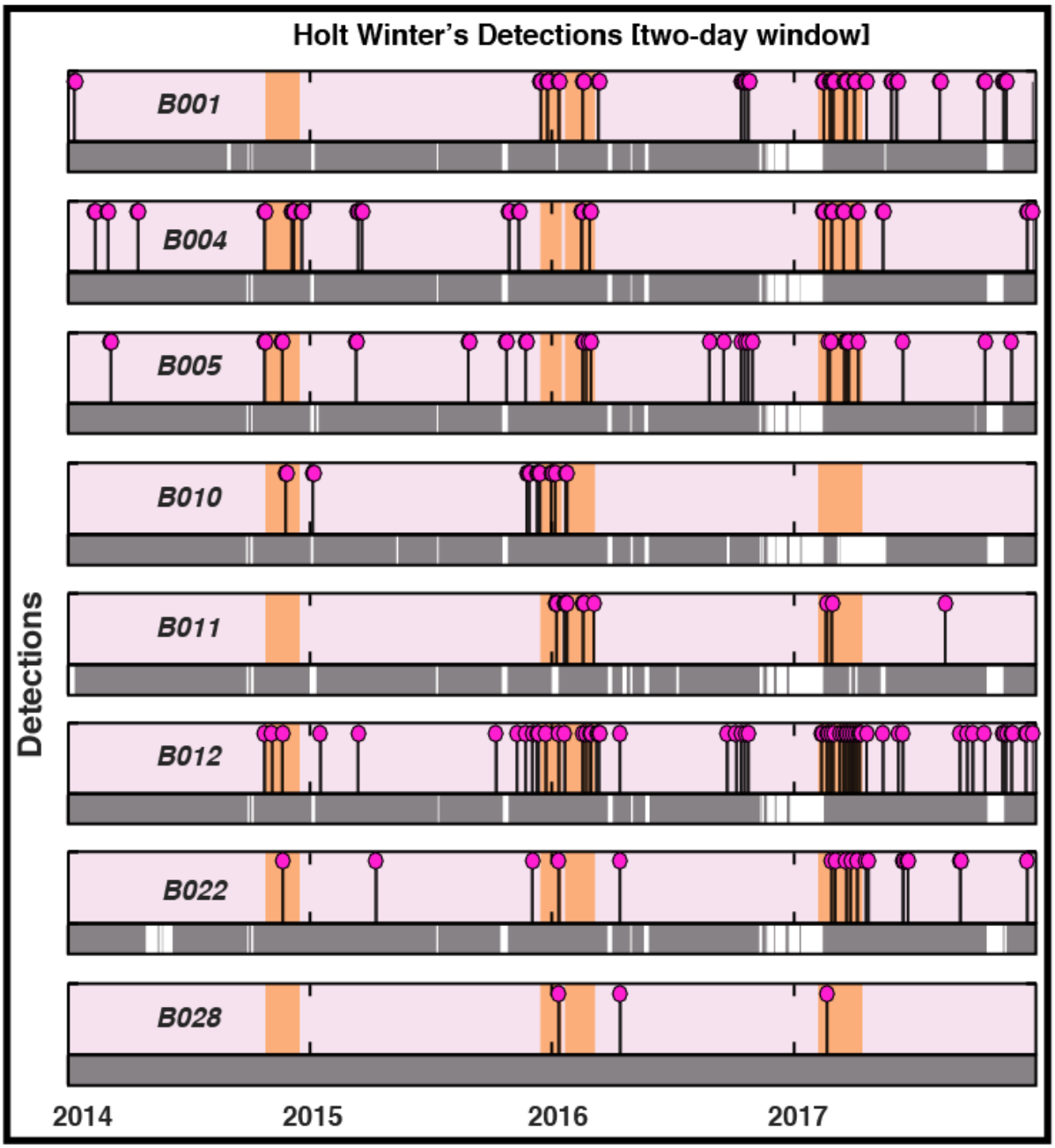

Figure 7. Holt-Winter's Model Detections- Each plot shows the pore pressure detections found for all borehole sites from 2014 forward. Known times of slow slip are marked by the orange rectangles. Purple dots mark the detections. Grey color bars indicate when the borehole station is online, white marks when the station is offline. Two-day windows are used in detections for this plot. Note that very few of these detections outside of SSEs are correlated between wells.

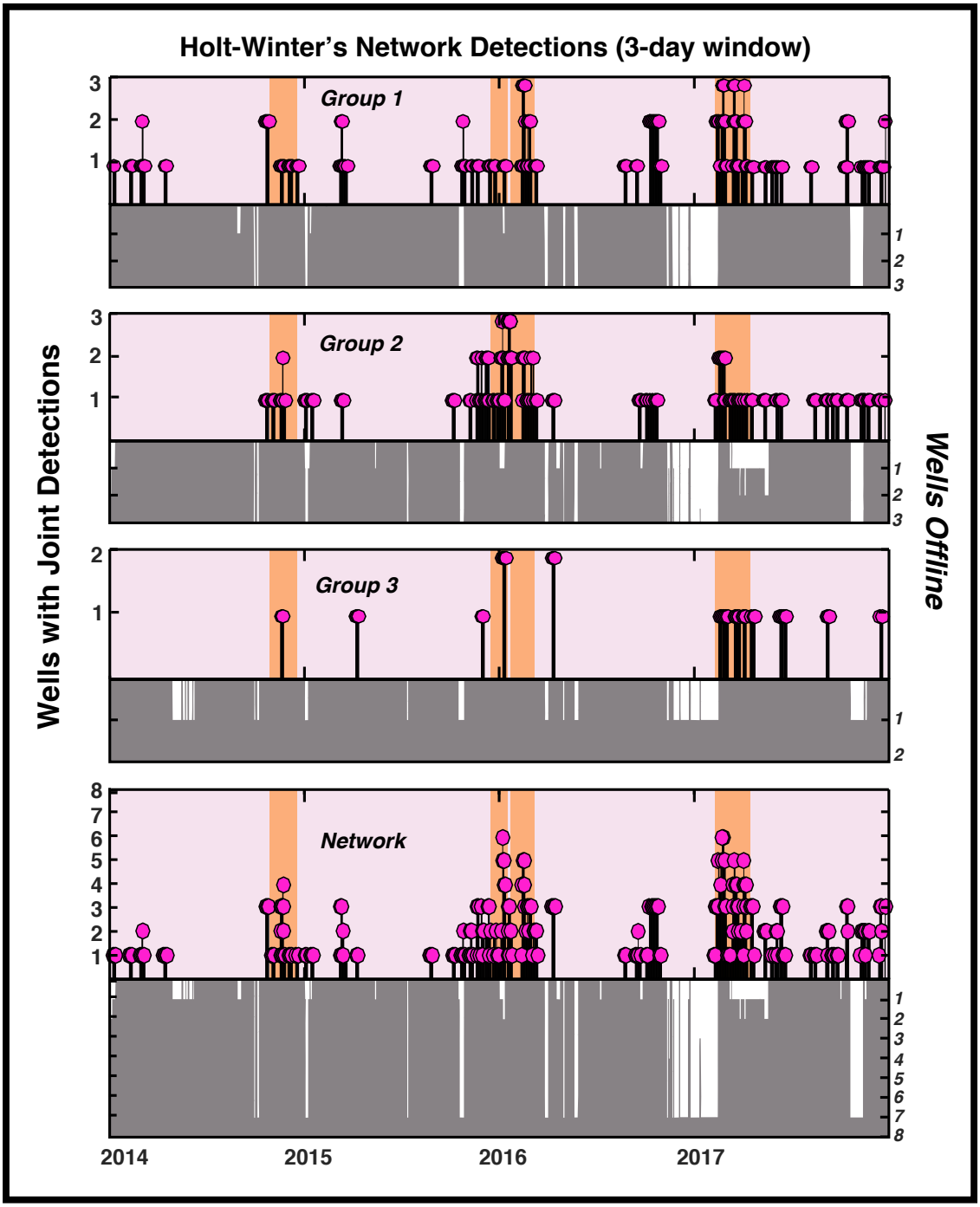

Figure 8. Holt-Winter's Model Group Detections- The first three stem plots show the correlated detections for Group 1, 2, and 3 respectively. The lowermost plot shows correlated detections across the entire network. The height of the stems shows the number of stations that share that specific detection. The grey color bars indicate how many wells are online. White means offline, increasing downwards. Known SSEs are marked by orange rectangles. A three-day moving window is used for cross correlating detections. A four-day moving window returns identical results.

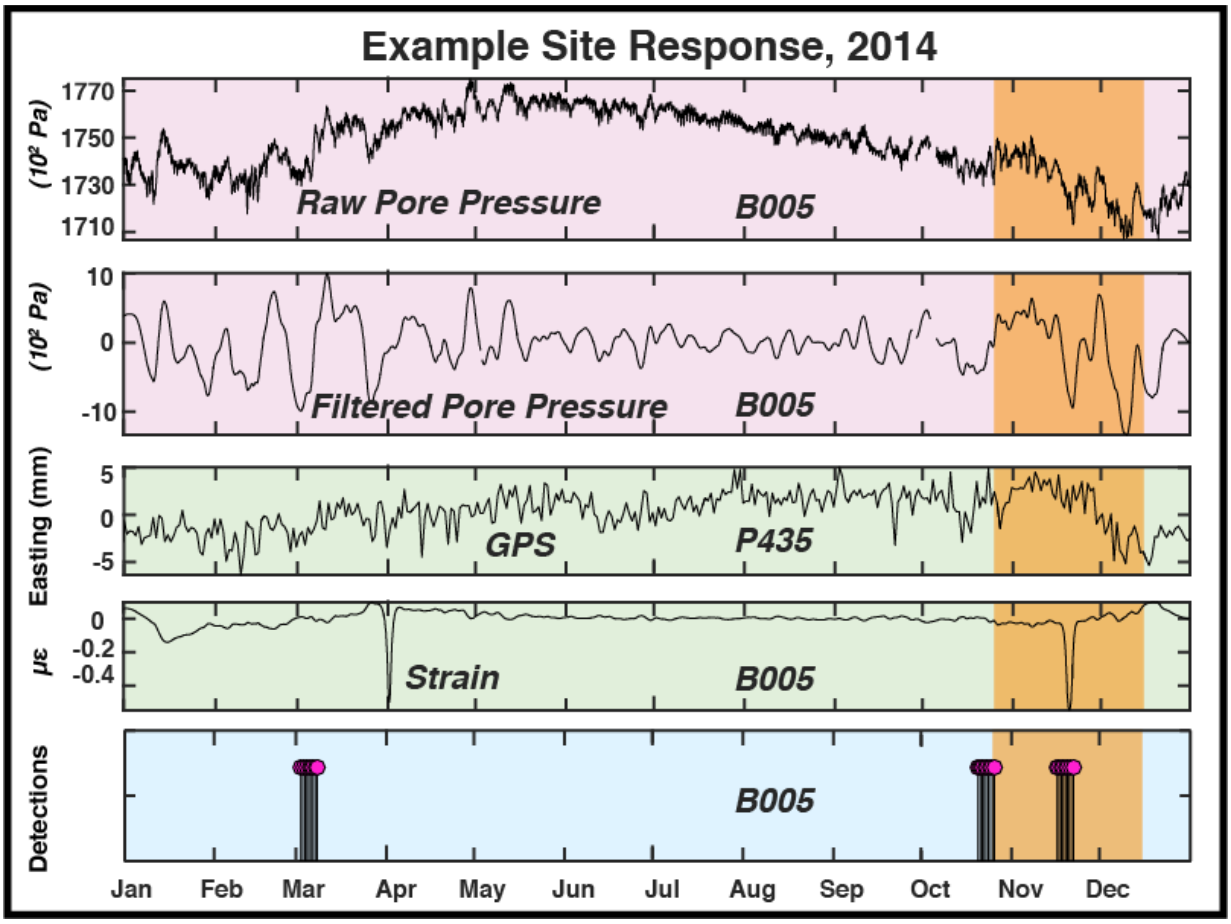

Figure 9. Example Site Response, SSE of 2014- The first two plots show the raw and filtered pore pressure data, respectively, from site B005. The third and fourth plots show the GPS data from station P435 and strainmeter data from B005. The lowermost plot shows the site detections from the Holt-Winter's model. The SSE for this year, 2014, is marked by the orange rectangle. Note that the detections coincide with the strainmeter, GPS, and pore pressure transients.

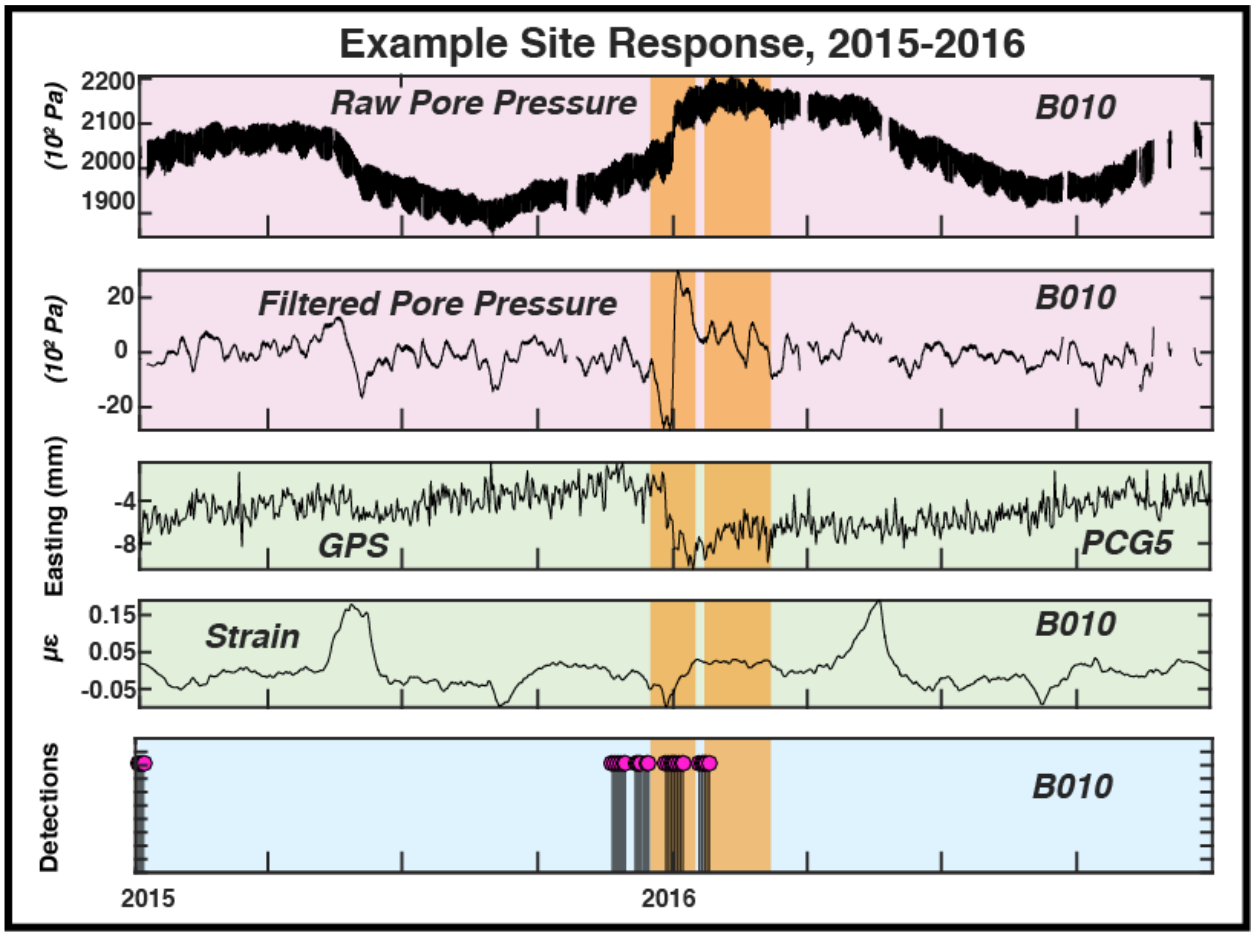

Figure 10. Example Site Response, SSE of 2015-2016- This figure is identical to Figure 9, except these data are from 2015-2016. Station data is from site B010. GPS data are from station PCG5. Note the step-like transient in pore pressure that coincides with the GPS and strainmeter transients, as well as the detections made within the network.

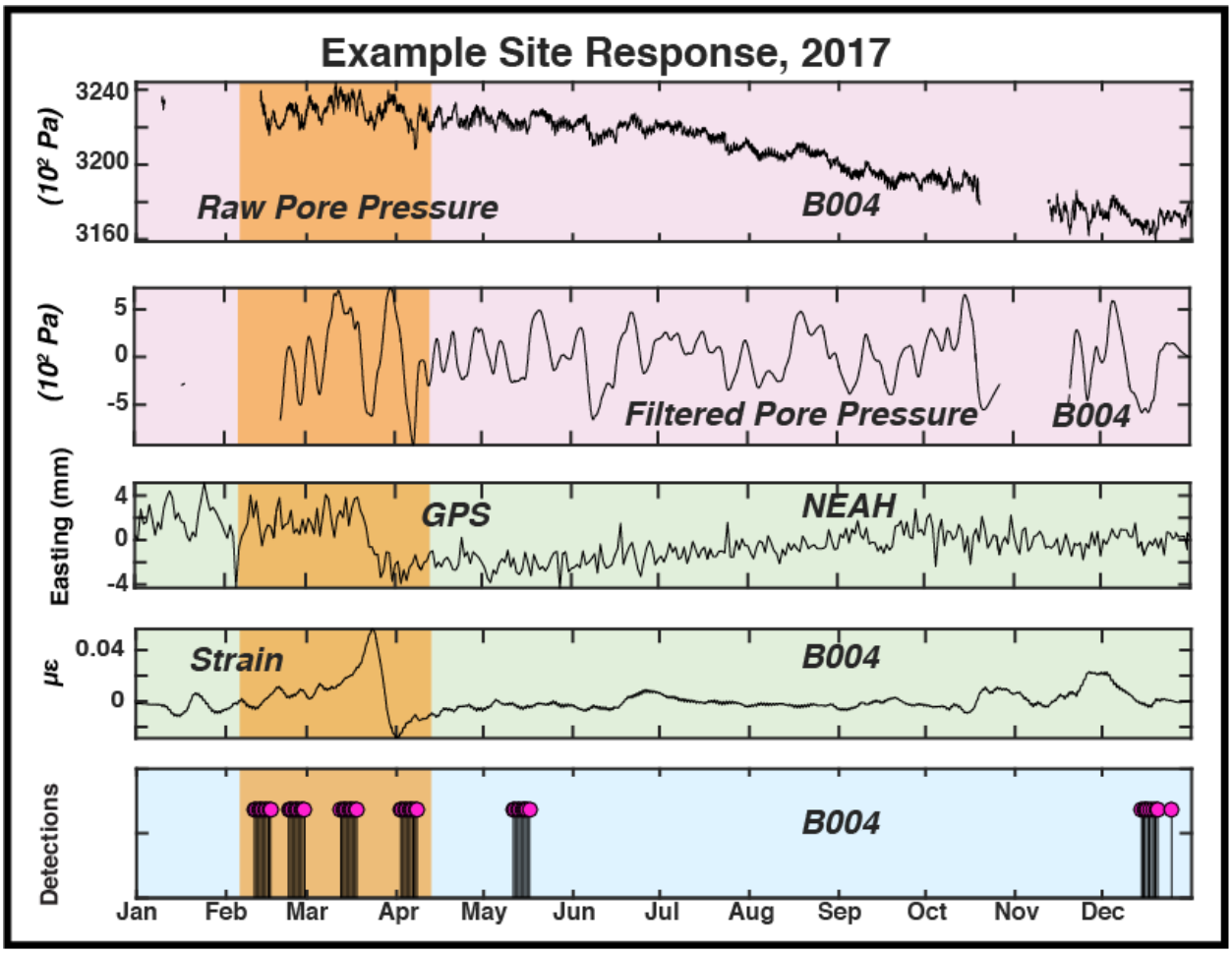

Figure 11. Example Site Response, SSE of 2017- This figure is identical to Figures 9 and 10, except these data are from 2017. Station data is from site B004. GPS data are from station NEAH. No readily discernable transient is within the pore pressure data, however detections are still made within the network (and at this location) that are correlated with the GPS and strainmeter transients during the SSE.

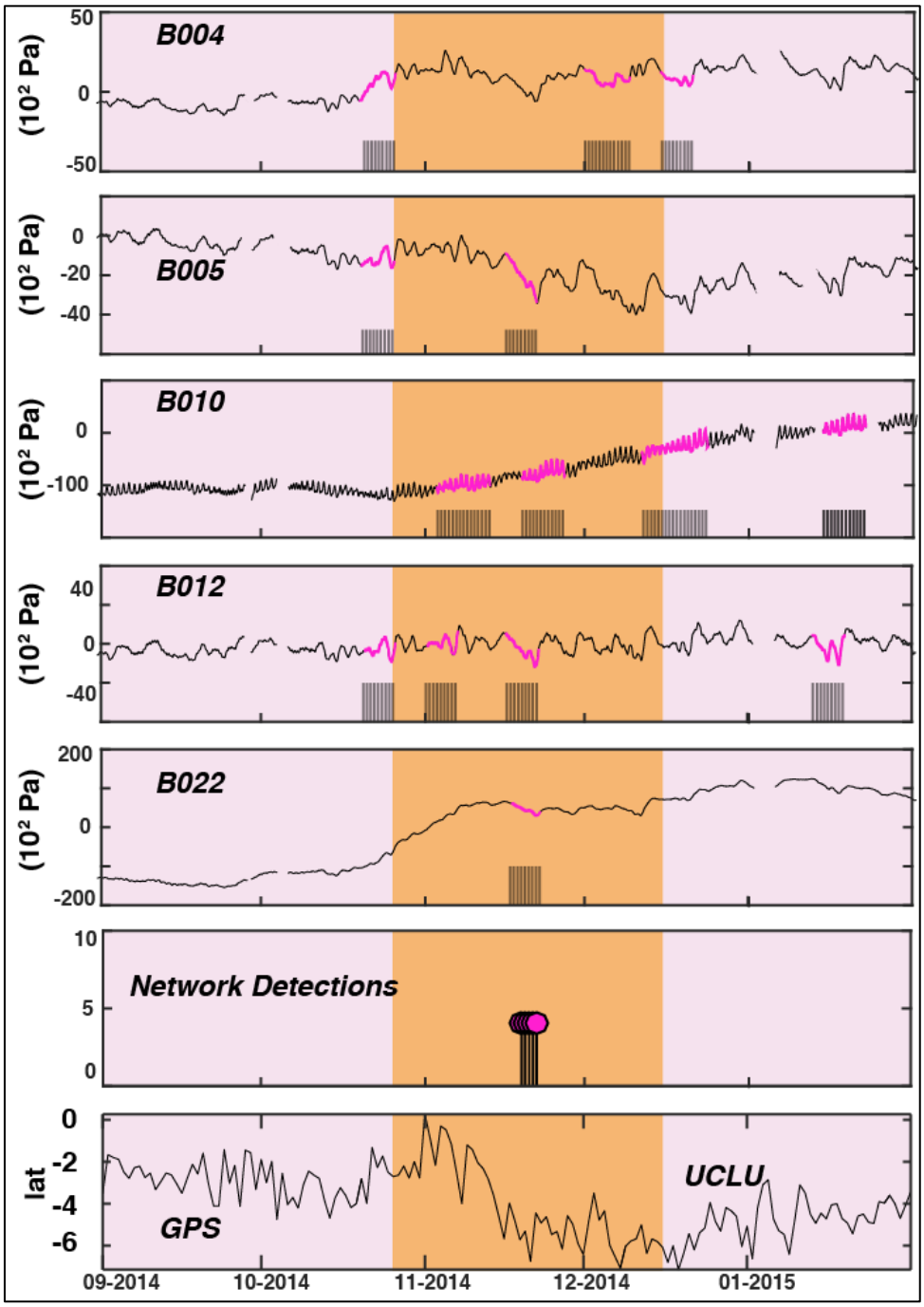

Figure 12. Pore Pressure Data with Detections, SSE of 2014- The top five plots show the raw pore pressure data (downsampled to 1/300 Hz) with anomalous data from the Holt-Winter's model marked in purple. Each plot has black stems that indicate the individual site detections found from the Holt-Winters model. The last stem plot contains the joint detections that were found to be correlated across at least 4 stations. Only stations containing detections are shown. The lowermost plot contains the strongest GPS signal for this SSE, at site UCLU. The joint detections are found using a four-day window average. The SSE duration for 2014 is marked in orange. Note the concurrence of the detections, marked data, and the GPS transient.

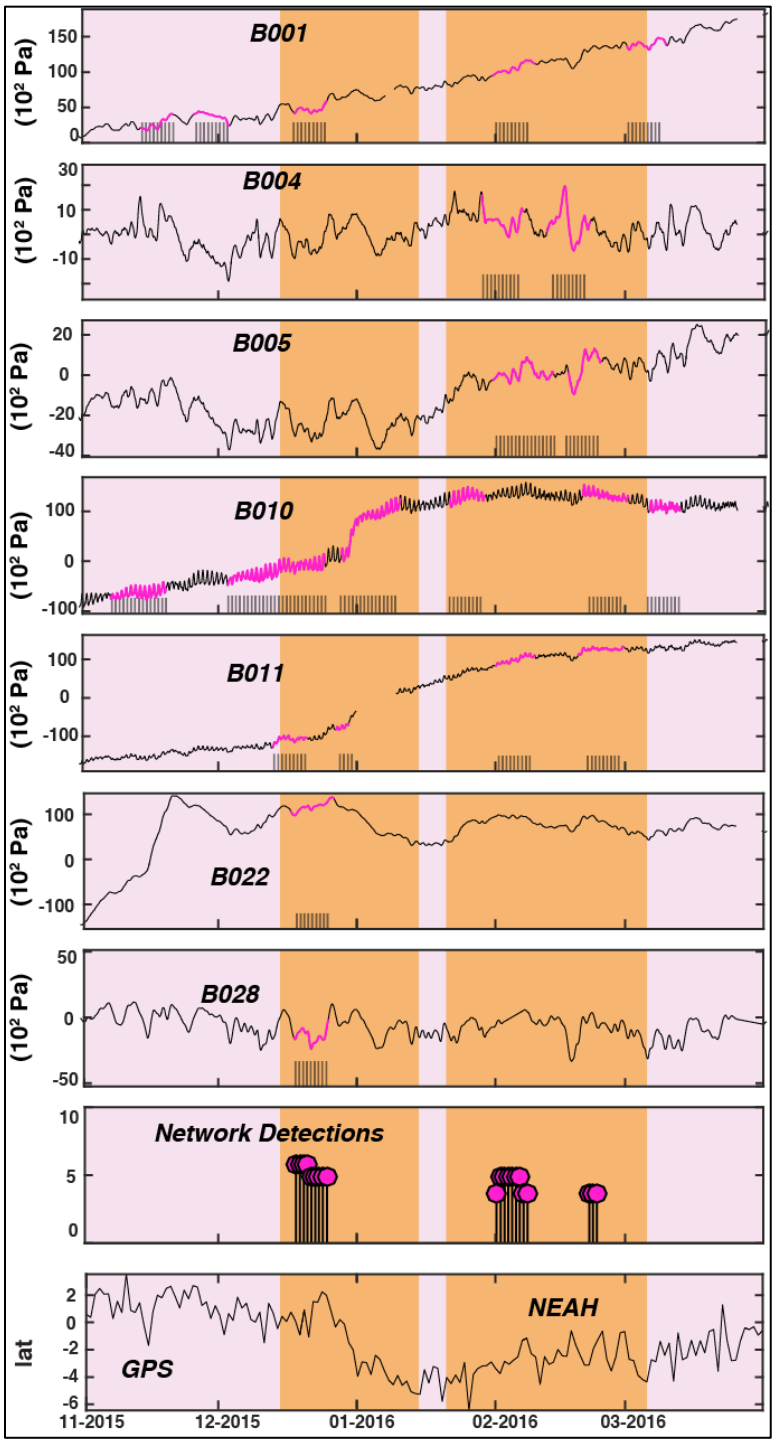

Figure 13. Pore Pressure Data with Detections, SSE of 2015-2016- This figure is identical to Figure 12, here the top seven plots show the raw pore pressure data for each site containing detections. GPS data are from site NEAH, exhibiting the strongest response to the SSE. Note the two groups of detections, which correlate with the event pausing in late 2015 and beginning again in early 2016.

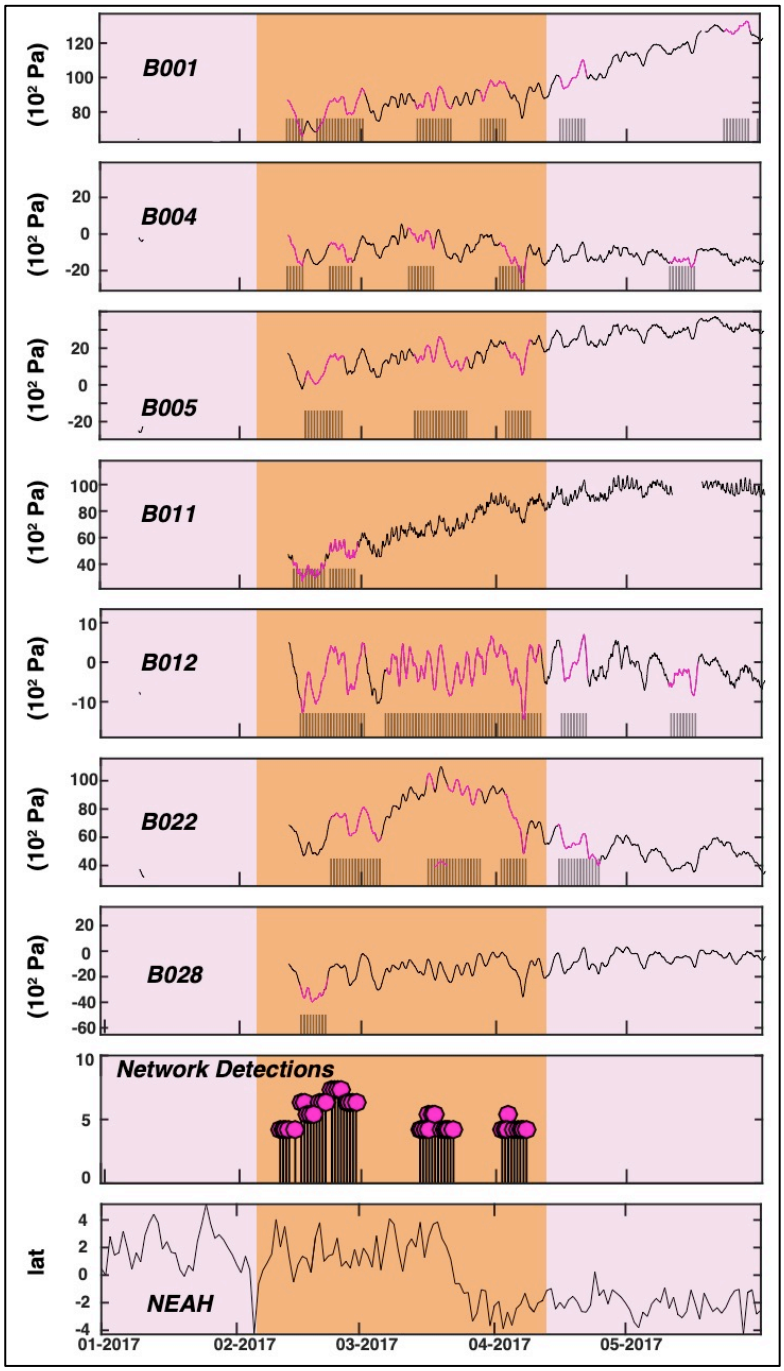

Figure 14. Pore Pressure Data with Detections, SSE of 2017- This figure is identical to Figures 12 and 13, here the top seven plots show the raw pore pressure data for each site containing detections. GPS data are from site NEAH, which exhibits the strongest GPS response to the SSE. Note the data gaps, which prevent full correlation between all sites, and the strong correlation of detections during the GPS transient.

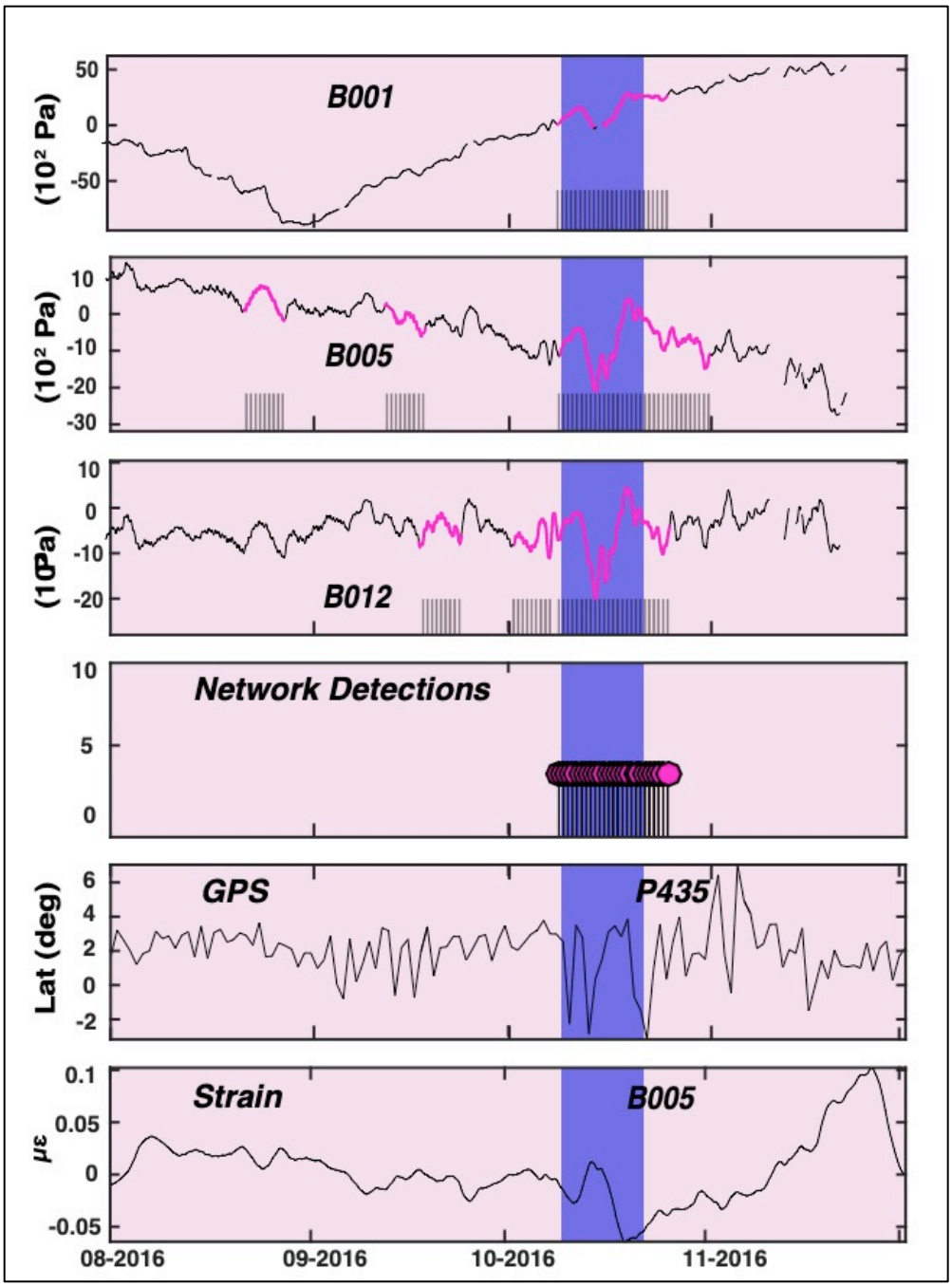

Figure 15. Pore Pressure Data with Detections, Uncatalogued Event of Fall 2016- This figure is identical to Figure 12, 13, and 14, here the top three plots show the raw pore pressure data for each site containing detections. The dark purple bars mark the time of interest in which detections occur at sites B001, B005, and B012 alongside an anomalous step in pore pressure, here marked in purple. Strainmeter data are included in the lowermost plot. Note the strain transient that coincides with the detections in pore pressure data.

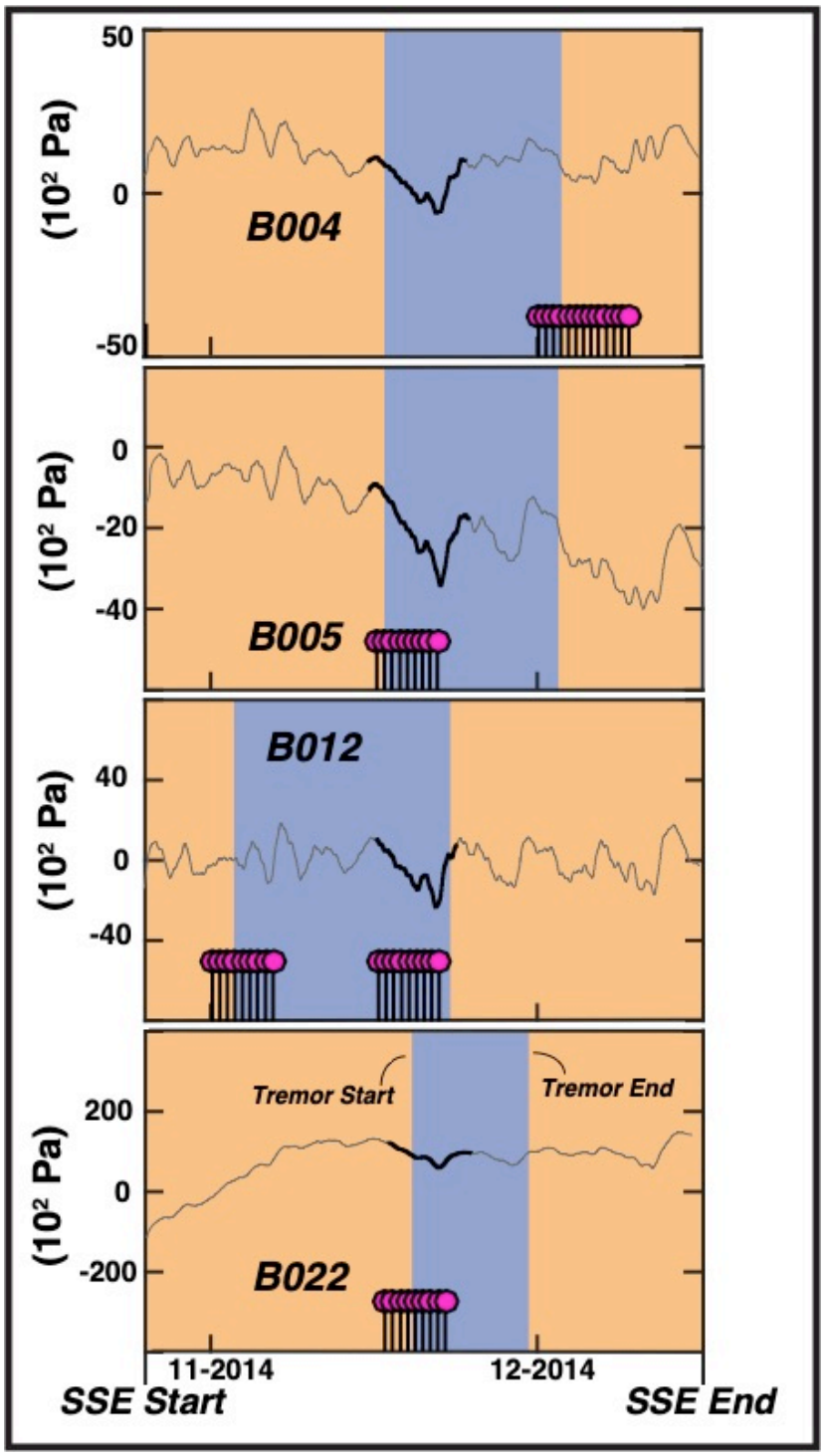

Figure 16. Speculated Pore Pressure Responses to SSEs, SSE of 2014- Data are shown for the entire SSE of 2014. The blue rectangles mark when tremor occurs within the vicinity of each site. The black data show the indicative pore pressure signal speculated to be related to the SSE, which is also found at other sites for other SSEs. Individual site detections are shown by the purple stem plots.

Detection Method	Data Treatment	Detection Qualifier	Details
STA/LTA		Must Surpass:	
8- day STA, 80- day LTA	Demeaned, Abs-Value	STA/LTA Ratio Threshold	Threshold Range: 1.25-2.25*
8- day STA, 80- day LTA	Demeaned, Squared	STA/LTA Ratio Threshold	Threshold Range: 1.25-2.25*
8- day STA, 80- day LTA	Bandpass Filter, Abs-Value	STA/LTA Ratio Threshold	Threshold Range: 2-3.5*
8- day STA, 80- day LTA	Bandpass Filter, Squared	STA/LTA Ratio Threshold	Threshold Range: 2-3.5*
		**Widens or narrows confidence bands	*Thresholds are incremented by 0.25

Table 1. List of Applied STA/LTA Parameters

Borehole	p(SS)	p(Pd)	p(Pd|SS)	***p(SS|Pd)***	Threshold	Value
B004	11.75%	23.20%	30.51%	***15.45%***	1.25	Absolute
B005	11.75%	12.20%	9.53%	***9.18%***	1.25	Absolute
B012	11.75%	16.26%	15.68%	***11.33%***	1.25	Absolute
B022	11.75%	12.72%	19.70%	***18.20%***	1.25	Absolute
B004	11.75%	2.49%	8.26%	***39.00%***	1.75	Absolute
B005	11.75%	0.57%	0.00%	***0.00%***	1.75	Absolute
B012	11.75%	1.24%	1.48%	***14.00%***	1.75	Absolute
B022	11.75%	0.37%	0.00%	***0.00%***	1.75	Absolute
B004	11.75%	28.33%	32.84%	***13.62%***	1.25	Squared
B005	11.75%	17.77%	12.08%	***7.98%***	1.25	Squared
B012	11.75%	26.06%	25.00%	***11.27%***	1.25	Squared
B022	11.75%	19.64%	28.39%	***16.98%***	1.25	Squared
B004	11.75%	4.03%	8.69%	***25.31%***	2.25	Squared
B005	11.75%	0.87%	0.00%	***0.00%***	2.25	Squared
B012	11.75%	1.94%	2.33%	***14.10%***	2.25	Squared
B022	11.75%	0.95%	0.00%	***0.00%***	2.25	Squared

Table 2. Posterior Probabilities for Absolute Valued and Squared-Unfiltered Data- Lower STA/LTA threshold values are marked in grey, higher threshold values are marked in blue.

Borehole	p(SS)	p(Pd)	p(Pd|SS)	***p(SS|Pd)***	Threshold	Value
B004	11.75%	7.42%	7.63%	***12.08%***	1.75	Absolute
B005	11.75%	7.64%	6.99%	***10.75%***	1.75	Absolute
B012	11.75%	6.82%	11.44%	***19.71%***	1.75	Absolute
B022	11.75%	10.06%	6.99%	***8.17%***	1.75	Absolute
B004	11.75%	0.35%	0.42%	***14.29%***	2.75	Absolute
B005	11.75%	0.17%	0.85%	***57.14%***	2.75	Absolute
B012	11.75%	0.37%	1.27%	***40.00%***	2.75	Absolute
B022	11.75%	0.95%	0.42%	***5.26%***	2.75	Absolute
B004	11.75%	15.83%	17.80%	***13.21%***	1.75	Squared
B005	11.75%	16.06%	15.89%	***11.63%***	1.75	Squared
B012	11.75%	16.80%	23.09%	***16.15%***	1.75	Squared
B022	11.75%	14.74%	12.29%	***9.80%***	1.75	Squared
B004	11.75%	3.39%	3.81%	***13.24%***	3	Squared
B005	11.75%	3.49%	4.03%	***13.57%***	3	Squared
B012	11.75%	3.34%	5.72%	***20.15%***	3	Squared
B022	11.75%	3.96%	2.75%	***8.18%***	3	Squared

Table 3. Posterior probabilities for Absolute Valued and Squared-Filtered Data- Lower STA/LTA threshold values are marked in grey, higher threshold values are marked in blue.

Well-Pair	p(SS)	p(Pd)	p(Pd|SS)	***p(SS|Pd)***	Detections
B001-B010	14.41%	0.87%	2.07%	***34.29%***	35
B001-B011	14.41%	0.77%	1.38%	***25.81%***	31
B001-B012	14.41%	0.60%	0.69%	***16.67%***	24
B003-B004	14.41%	0.67%	1.21%	***25.93%***	27
B003-B005	14.41%	0.87%	1.04%	***17.14%***	35
B004-B011	14.41%	0.45%	0.69%	***22.22%***	18
B004-B012	14.41%	0.77%	1.90%	***35.48%***	31
B005-B011	14.41%	0.55%	0.86%	***22.73%***	22
B005-B012	14.41%	1.19%	1.55%	***18.75%***	48
B010-B011	14.41%	1.37%	1.73%	***18.18%***	55
B010-B012	14.41%	0.55%	0.52%	***13.64%***	22
B010-B022	14.41%	0.22%	1.21%	***77.78%***	9

Table 4. Joint Probabilities, Square Value of the Filtered Data- Joint detections are found using a four-day temporal window, from which these probabilities are calculated. The STA/LTA threshold used for detecting anomalies is set to 3.25

Well	p(ss)	p(Pd)	p(Pd|SS)	***p(SS|Pd)***	Detections
B001	14.10%	11.38%	34.24%	***42.44%***	25
B004	14.10%	10.47%	32.20%	***43.38%***	29
B005	14.10%	12.43%	31.19%	***35.38%***	27
B010	14.10%	4.59%	20.34%	***62.50%***	11
B011	14.10%	4.30%	30.17%	***98.89%***	9
B012	14.10%	23.80%	67.46%	***39.96%***	55
B022	14.10%	8.46%	26.44%	***44.07%***	17
B028	14.10%	1.72%	8.14%	***66.67%***	6

Table 5. Holt-Winter's Probabilities, Single Station- The probabilities are calculated using the four-day averages of the individual site detections.

Responsive Wells	Group	p(ss)	p(Pd)	p(Pd|SS)	***p(SS|Pd)***	Detections
1	*B001-B004-B005*	14.06%	14.87%	37.97%	***35.90%***	312
2	*B001-B004-B005*	14.06%	3.38%	13.56%	***56.34%***	71
3	*B001-B004-B005*	14.06%	0.43%	3.05%	***100.00%***	9
1	*B010-B011-B012*	14.06%	16.83%	56.27%	***47.03%***	353
2	*B010-B011-B012*	14.06%	2.14%	12.54%	***82.22%***	45
3	*B010-B011-B012*	14.06%	0.19%	2.37%	***100.00%***	4
1	*B022-B028*	14.06%	4.86%	16.27%	***47.06%***	102
2	*B022-B028*	14.06%	0.57%	2.03%	***50.00%***	12

Table 6. Holt-Winter's Joint Probabilities - "Responsive wells" indicates the number of wells in which detections are correlated across within the group. Detections: how many detections are found to be correlated between the sites based on the responsive well limit. Joint detections are found using a four-day window averages.

Responsive Wells	p(ss)	p(Pd)	p(Pd|SS)	***p(SS|Pd)***	Detections
1	14.10%	37.33%	88.14%	***33.29%***	781
2	14.10%	20.27%	64.07%	***44.58%***	424
3	14.10%	12.52%	48.14%	***54.20%***	262
4	14.10%	3.97%	28.14%	***100.00%***	83
5	14.10%	2.25%	15.93%	***100.00%***	47
6	14.10%	0.72%	5.08%	***100.00%***	15
7	14.10%	0.10%	0.68%	***100.00%***	2
8	0.00%	0.00%	0.00%	***0.00%***	0

Table 7. Holt-Winter's Network Probabilities- Responsive wells indicate only correlated detections found on this number of sites within the full network of eight wells. These are used in the posterior probability calculation. Detections define how many detections are found to be correlated between the sites based on the responsive well limit. Joint detections are found using a four-day window averages.

Well	α	β	γ
B001	0.2	0.001	0.4
B004	0.001	0.001	0.35
B005	0.3	0.001	0.25
B010	0.3	0.001	0.24
B011	0.19	0.01	0.3
B012	0.0012	0.001	0.5
B022	0.2	0.00001	0.4
B028	0.001	0.001	0.3

Table 8. Predictive Model Smoothing Parameters

APPENDIX B

SUPPLEMENTAL TABLES

This appendix contains supplemental data tables for all applied detections methods. Tables Supp. 1 through Supp. 5 show single and joint-station posterior probabilities for all applied STA/LTA parameters. Tables Supp. 6 through Supp. 16 show all posterior single sand joint station probabilities for all applied Holt-Winter's predictive model parameters.

Table Supp. 1. Posterior Probabilities, STA/LTA, Absolute Value of the Unfiltered Data

Borehole	p(SS)	p(Pd)	p(Pd|SS)	***p(SS|Pd)***	Threshold
B001	11.75	37.94	36.65	***11.35***	1
B003	11.75	44.49	49.58	***13.09***	1
B004	11.75	46.88	43.22	***10.83***	1
B005	11.75	47.92	37.29	***9.14***	1
B010	11.75	51.23	61.02	***13.99***	1
B011	11.75	58.08	57.84	***11.70***	1
B012	11.75	49.91	44.92	***10.57***	1
B022	11.75	45.33	57.20	***14.83***	1
B028	11.75	51.74	54.68	***12.08***	1

Borehole	p(SS)	p(Pd)	p(Pd|SS)	***p(SS|Pd)***	Threshold
B001	11.75%	6.45%	6.57%	***11.97%***	1.25
B003	11.75%	278.82%	2.97%	***12.50%***	1.25
B004	11.75%	23.20%	30.51%	***15.45%***	1.25
B005	11.75%	12.20%	9.53%	***9.18%***	1.25
B010	11.75%	5.73%	5.51%	***11.30%***	1.25
B011	11.75%	3.44%	0.85%	***2.90%***	1.25
B012	11.75%	16.26%	15.68%	***11.33%***	1.25
B022	11.75%	12.72%	19.70%	***18.20%***	1.25
B028	11.75%	15.37%	14.33%	***10.65%***	1.25

Borehole	p(SS)	p(Pd)	p(Pd|SS)	***p(SS|Pd)***	Threshold
B001	11.75%	1.22%	1.27%	***12.24%***	1.5
B003	11.75%	0.77%	1.48%	***22.58%***	1.5
B004	11.75%	7.57%	14.83%	***23.03%***	1.5
B005	11.75%	1.94%	2.12%	***12.82%***	1.5
B010	11.75%	1.15%	0.00%	***0.00%***	1.5
B011	11.75%	0.22%	0.00%	***0.00%***	1.5
B012	11.75%	2.76%	2.97%	***12.61%***	1.5
B022	11.75%	2.04%	2.12%	***12.20%***	1.5
B028	11.43%	4.75%	1.17%	***2.82%***	1.5

Table Supp. 1 Continued

Borehole	p(SS)	p(Pd)	p(Pd|SS)	***p(SS|Pd)***	Threshold
B001	11.75%	0.67%	0.00%	***0.00%***	1.75
B003	11.75%	0.37%	1.27%	***40.00%***	1.75
B004	11.75%	2.49%	8.26%	***39.00%***	1.75
B005	11.75%	0.57%	0.00%	***0.00%***	1.75
B010	11.75%	0.40%	0.00%	***0.00%***	1.75
B011	11.75%	0.15%	0.00%	***0.00%***	1.75
B012	11.75%	1.24%	1.48%	***14.00%***	1.75
B022	11.75%	0.37%	0.00%	***0.00%***	1.75
B028	11.43%	2.27%	0.00%	***0.00%***	1.75

Borehole	p(SS)	p(Pd)	p(Pd|SS)	***p(SS|Pd)***	Threshold
B001	11.75%	0.27%	0.00%	***0.00%***	2
B003	11.75%	0.17%	0.85%	***57.14%***	2
B004	11.75%	0.80%	2.97%	***43.75%***	2
B005	11.75%	0.15%	0.00%	***0.00%***	2
B010	11.75%	0.00%	0.00%	***0.00%***	2
B011	11.75%	0.10%	0.00%	***0.00%***	2
B012	11.75%	0.30%	0.85%	***33.33%***	2
B022	11.75%	0.00%	0.00%	***0.00%***	2
B028	11.43%	1.07%	0.00%	***0.00%***	2

Table Supp. 2. Posterior Probabilities, STA/LTA, Square Value of the Unfiltered Data

Borehole	p(SS)	p(Pd)	p(Pd|SS)	***p(SS|Pd)***	Threshold
B001	11.75%	10.13%	12.08%	***14.00%***	1.25
B003	11.75%	5.50%	5.08%	***10.86%***	1.25
B004	11.75%	28.33%	32.84%	***13.62%***	1.25
B005	11.75%	17.77%	12.08%	***7.98%***	1.25
B010	11.75%	15.09%	22.03%	***17.16%***	1.25
B011	11.75%	7.69%	5.51%	***8.41%***	1.25
B012	11.75%	26.06%	25.00%	***11.27%***	1.25
B022	11.75%	19.64%	28.39%	***16.98%***	1.25
B028	11.75%	21.99%	21.35%	***11.09%***	1.25

Borehole	p(SS)	p(Pd)	p(Pd|SS)	***p(SS|Pd)***	Threshold
B001	11.75%	3.76%	4.87%	***15.23%***	1.5
B003	11.75%	2.54%	2.97%	***13.73%***	1.5
B004	11.75%	17.67%	23.73%	***15.77%***	1.5
B005	11.75%	8.51%	5.08%	***7.02%***	1.5
B010	11.75%	3.09%	1.91%	***7.26%***	1.5
B011	11.75%	1.99%	0.00%	***0.00%***	1.5
B012	11.75%	13.57%	14.19%	***12.29%***	1.5
B022	11.75%	9.19%	14.41%	***18.43%***	1.5
B028	11.75%	11.16%	11.70%	***11.27%***	1.5

Borehole	p(SS)	p(Pd)	p(Pd|SS)	***p(SS|Pd)***	Threshold
B001	11.75%	2.46%	2.12%	***10.10%***	1.75
B003	11.75%	1.44%	2.12%	***17.24%***	1.75
B004	11.75%	10.95%	18.22%	***19.55%***	1.75
B005	11.75%	3.66%	3.18%	***10.20%***	1.75
B010	11.75%	1.67%	0.00%	***0.00%***	1.75
B011	11.75%	0.67%	0.00%	***0.00%***	1.75
B012	11.75%	6.62%	6.99%	***12.41%***	1.75
B022	11.75%	3.96%	5.30%	***15.72%***	1.75
B028	11.43%	7.85%	7.02%	***10.21%***	1.75

Table Supp. 2 Continued

Borehole	p(SS)	p(Pd)	p(Pd|SS)	***p(SS|Pd)***	Threshold
B001	11.75%	1.24%	0.85%	***8.00%***	2
B003	11.75%	0.80%	1.91%	***28.13%***	2
B004	11.75%	6.97%	13.77%	***23.21%***	2
B005	11.75%	1.82%	1.69%	***10.96%***	2
B010	11.75%	0.87%	0.00%	***0.00%***	2
B011	11.75%	0.22%	0.00%	***0.00%***	2
B012	11.75%	3.53%	4.03%	***13.38%***	2
B022	11.75%	2.12%	1.48%	***8.24%***	2
B028	11.43%	4.58%	0.88%	***2.19%***	2

Borehole	p(SS)	p(Pd)	p(Pd|SS)	***p(SS|Pd)***	Threshold
B001	11.75%	0.62%	0.00%	***0.00%***	2.25
B003	11.75%	0.47%	1.91%	***47.37%***	2.25
B004	11.75%	4.03%	8.69%	***25.31%***	2.25
B005	11.75%	0.87%	0.00%	***0.00%***	2.25
B010	11.75%	0.52%	0.00%	***0.00%***	2.25
B011	11.75%	0.17%	0.00%	***0.00%***	2.25
B012	11.75%	1.94%	2.33%	***14.10%***	2.25
B022	11.75%	0.95%	0.00%	***0.00%***	2.25
B028	11.43%	2.97%	0.00%	***0.00%***	2.25

Borehole	p(SS)	p(Pd)	p(Pd|SS)	***p(SS|Pd)***	Threshold
B001	11.75%	0.47%	0.00%	***0.00%***	2.5
B003	11.75%	0.42%	1.91%	***52.94%***	2.5
B004	11.75%	2.07%	6.99%	***39.76%***	2.5
B005	11.75%	0.55%	0.00%	***0.00%***	2.5
B010	11.75%	0.05%	0.00%	***0.00%***	2.5
B011	11.75%	0.15%	0.00%	***0.00%***	2.5
B012	11.75%	1.27%	1.48%	***13.73%***	2.5
B022	11.75%	0.40%	0.00%	***0.00%***	2.5
B028	11.43%	2.14%	0.00%	***0.00%***	2.5

Table Supp. 3. Posterior Probabilities, STA/LTA, Absolute Value of the Filtered Data- Filtering parameters follow those described in the main text.

Borehole	p(SS)	p(Pd)	p(Pd|SS)	***p(SS|Pd)***	Threshold
B001	11.75%	8.07%	8.05%	***11.73%***	1.75
B003	11.75%	6.10%	5.72%	***11.02%***	1.75
B004	11.75%	7.42%	7.63%	***12.08%***	1.75
B005	11.75%	7.64%	6.99%	***10.75%***	1.75
B010	11.75%	10.43%	13.56%	***15.27%***	1.75
B011	11.75%	8.99%	11.02%	***14.40%***	1.75
B012	11.75%	6.82%	11.44%	***19.71%***	1.75
B022	11.75%	10.06%	6.99%	***8.17%***	1.75
B028	11.43%	6.72%	7.02%	***11.94%***	1.75

Borehole	p(SS)	p(Pd)	p(Pd|SS)	***p(SS|Pd)***	Threshold
B001	11.75%	5.18%	5.08%	***11.54%***	2
B003	11.75%	2.71%	2.12%	***9.17%***	2
B004	11.75%	3.68%	3.60%	***11.49%***	2
B005	11.75%	3.16%	3.60%	***13.39%***	2
B010	11.75%	6.00%	8.26%	***16.18%***	2
B011	11.75%	4.73%	6.78%	***16.84%***	2
B012	11.75%	3.19%	5.72%	***21.09%***	2
B022	11.75%	5.50%	4.66%	***9.95%***	2
B028	11.43%	3.51%	4.09%	***13.33%***	2

Borehole	p(SS)	p(Pd)	p(Pd|SS)	***p(SS|Pd)***	Threshold
B001	11.75%	3.04%	3.39%	***13.11%***	2.25
B003	11.75%	1.32%	1.27%	***11.32%***	2.25
B004	11.75%	1.72%	1.48%	***10.14%***	2.25
B005	11.75%	1.29%	1.48%	***13.46%***	2.25
B010	11.75%	2.79%	3.81%	***16.07%***	2.25
B011	11.75%	2.54%	4.66%	***21.57%***	2.25
B012	11.75%	1.44%	2.12%	***17.24%***	2.25
B022	11.75%	2.89%	2.75%	***11.21%***	2.25
B028	11.43%	1.84%	2.63%	***16.36%***	2.25

Table Supp. 3 Continued

Borehole	p(SS)	p(Pd)	p(Pd|SS)	***p(SS|Pd)***	Threshold
B001	11.75%	1.77%	2.54%	***16.90%***	2.5
B003	11.75%	0.42%	0.85%	***23.53%***	2.5
B004	11.75%	0.65%	1.27%	***23.08%***	2.5
B005	11.75%	0.50%	1.27%	***30.00%***	2.5
B010	11.75%	1.52%	0.85%	***6.56%***	2.5
B011	11.75%	1.17%	1.69%	***17.02%***	2.5
B012	11.75%	0.70%	1.91%	***32.14%***	2.5
B022	11.75%	1.64%	0.85%	***6.06%***	2.5
B028	11.43%	0.74%	0.00%	***0.00%***	2.5

Borehole	p(SS)	p(Pd)	p(Pd|SS)	***p(SS|Pd)***	Threshold
B001	11.75%	0.75%	0.85%	***13.33%***	2.75
B003	11.75%	0.07%	0.64%	***100.00%***	2.75
B004	11.75%	0.35%	0.42%	***14.29%***	2.75
B005	11.75%	0.17%	0.85%	***57.14%***	2.75
B010	11.75%	0.72%	0.00%	***0.00%***	2.75
B011	11.75%	0.60%	0.00%	***0.00%***	2.75
B012	11.75%	0.37%	1.27%	***40.00%***	2.75
B022	11.75%	0.95%	0.42%	***5.26%***	2.75
B028	11.43%	0.33%	0.00%	***0.00%***	2.75

Table Supp. 4. Posterior Probabilities, STA/LTA, Square Value of the Filtered Data

Borehole	p(SS)	p(Pd)	p(Pd|SS)	***p(SS|Pd)***	Threshold
B001	11.75%	12.50%	12.08%	***11.35%***	1.75
B003	11.75%	13.59%	14.19%	***12.27%***	1.75
B004	11.75%	15.83%	17.80%	***13.21%***	1.75
B005	11.75%	16.06%	15.89%	***11.63%***	1.75
B010	11.75%	16.83%	18.43%	***12.87%***	1.75
B011	11.75%	17.25%	16.53%	***11.26%***	1.75
B012	11.75%	16.80%	23.09%	***16.15%***	1.75
B022	11.75%	14.74%	12.29%	***9.80%***	1.75
B028	11.43%	16.31%	17.84%	***12.50%***	1.75

Borehole	p(SS)	p(Pd)	p(Pd|SS)	***p(SS|Pd)***	Threshold
B001	11.75%	9.58%	9.75%	***11.95%***	2
B003	11.75%	10.11%	10.81%	***12.56%***	2
B004	11.75%	11.55%	12.08%	***12.28%***	2
B005	11.75%	12.80%	12.92%	***11.87%***	2
B010	11.75%	13.57%	15.89%	***13.76%***	2
B011	11.75%	12.70%	14.19%	***13.14%***	2
B012	11.75%	12.27%	17.80%	***17.04%***	2
B022	11.75%	11.75%	9.11%	***9.11%***	2
B028	11.43%	12.10%	12.87%	***12.15%***	2

Borehole	p(SS)	p(Pd)	p(Pd|SS)	***p(SS|Pd)***	Threshold
B001	11.75%	8.07%	8.47%	***12.35%***	2.25
B003	11.75%	7.62%	7.42%	***11.44%***	2.25
B004	11.75%	8.86%	8.05%	***10.67%***	2.25
B005	11.75%	9.41%	9.11%	***11.38%***	2.25
B010	11.75%	10.90%	14.19%	***15.30%***	2.25
B011	11.75%	10.08%	11.44%	***13.33%***	2.25
B012	11.75%	8.61%	12.71%	***17.34%***	2.25
B022	11.75%	9.71%	7.42%	***8.97%***	2.25
B028	11.43%	8.89%	10.53%	***13.53%***	2.25

Table Supp. 4 Continued

Borehole	p(SS)	p(Pd)	p(Pd|SS)	***p(SS|Pd)***	Threshold
B001	11.75%	6.72%	7.42%	***12.96%***	2.5
B003	11.75%	5.58%	5.08%	***10.71%***	2.5
B004	11.75%	6.62%	5.30%	***9.40%***	2.5
B005	11.75%	6.85%	7.20%	***12.36%***	2.5
B010	11.75%	8.81%	11.44%	***15.25%***	2.5
B011	11.75%	7.89%	10.38%	***15.46%***	2.5
B012	11.75%	6.25%	11.02%	***20.72%***	2.5
B022	11.75%	7.39%	5.30%	***8.42%***	2.5
B028	11.43%	6.55%	8.48%	***14.80%***	2.5

Borehole	p(SS)	p(Pd)	p(Pd|SS)	***p(SS|Pd)***	Threshold
B001	11.75%	5.78%	6.14%	***12.50%***	2.75
B003	11.75%	4.08%	4.03%	***11.59%***	2.75
B004	11.75%	4.73%	4.24%	***10.53%***	2.75
B005	11.75%	4.75%	5.51%	***13.61%***	2.75
B010	11.75%	6.82%	9.11%	***15.69%***	2.75
B011	11.75%	6.27%	9.53%	***17.86%***	2.75
B012	11.75%	4.43%	7.20%	***19.10%***	2.75
B022	11.75%	5.63%	4.24%	***8.85%***	2.75
B028	11.43%	4.85%	6.14%	***14.48%***	2.75

Borehole	p(SS)	p(Pd)	p(Pd|SS)	***p(SS|Pd)***	Threshold
B001	11.75%	4.80%	5.51%	***13.47%***	3
B003	11.75%	2.96%	2.97%	***11.76%***	3
B004	11.75%	3.39%	3.81%	***13.24%***	3
B005	11.75%	3.49%	4.03%	***13.57%***	3
B010	11.75%	4.90%	6.36%	***15.23%***	3
B011	11.75%	4.41%	7.63%	***20.34%***	3
B012	11.75%	3.34%	5.72%	***20.15%***	3
B022	11.75%	3.96%	2.75%	***8.18%***	3
B028	11.43%	3.54%	4.68%	***15.09%***	3

Table Supp. 4 Continued

Borehole	p(SS)	p(Pd)	p(Pd|SS)	***p(SS|Pd)***	Threshold
B001	11.75%	3.98%	4.24%	***12.50%***	3.25
B003	11.75%	2.27%	2.54%	***13.19%***	3.25
B004	11.75%	2.59%	2.97%	***13.46%***	3.25
B005	11.75%	2.36%	2.97%	***14.74%***	3.25
B010	11.75%	3.81%	4.66%	***14.38%***	3.25
B011	11.75%	3.34%	6.57%	***23.13%***	3.25
B012	11.75%	2.61%	4.24%	***19.05%***	3.25
B022	11.75%	3.04%	2.33%	***9.02%***	3.25
B028	11.43%	2.37%	3.51%	***16.90%***	3.25

Borehole	p(SS)	p(Pd)	p(Pd|SS)	***p(SS|Pd)***	Threshold
B001	11.75%	3.21%	3.81%	***13.95%***	3.5
B003	11.75%	1.77%	2.12%	***14.08%***	3.5
B004	11.75%	1.97%	2.75%	***16.46%***	3.5
B005	11.75%	1.67%	2.97%	***20.90%***	3.5
B010	11.75%	2.69%	2.75%	***12.04%***	3.5
B011	11.75%	2.61%	4.87%	***21.90%***	3.5
B012	11.75%	2.04%	2.33%	***13.41%***	3.5
B022	11.75%	2.36%	1.69%	***8.42%***	3.5
B028	11.43%	1.70%	3.22%	***21.57%***	3.5

Table Supp. 5. Joint-Station Probabilities, STA/LTA, Square of the Filtered Data- Shading separates well pairs by the first well used in the correlation. The number of shared detections is shown in the 5th column.

Well Pair	p(SS)	p(Pd)	p(Pd|SS)	***p(SS|Pd)***	Detections	Threshold
B001-B003	14.41%	3.06%	3.28%	***15.45%***	123	1.75
B001-B004	14.41%	2.96%	6.22%	***30.25%***	119	1.75
B001-B005	14.41%	3.19%	3.80%	***17.19%***	128	1.75
B001-B010	14.41%	4.41%	5.01%	***16.38%***	177	1.75
B001-B011	14.41%	4.16%	5.01%	***17.37%***	167	1.75
B001-B012	14.41%	3.93%	6.56%	***24.05%***	158	1.75
B001-B022	14.41%	2.19%	2.76%	***18.18%***	88	1.75
B001-B028	14.04%	2.04%	2.86%	***19.67%***	61	1.75
B003-B004	14.41%	5.75%	4.66%	***11.69%***	231	1.75
B003-B005	14.41%	8.02%	5.18%	***9.32%***	322	1.75
B003-B010	14.41%	4.66%	5.70%	***17.65%***	187	1.75
B003-B011	14.41%	5.95%	3.11%	***7.53%***	239	1.75
B003-B012	14.41%	9.21%	9.15%	***14.32%***	370	1.75
B003-B022	14.41%	3.16%	2.76%	***12.60%***	127	1.75
B003-B028	14.04%	1.67%	1.67%	***14.00%***	50	1.75
B004-B005	14.41%	7.62%	7.43%	***14.05%***	306	1.75
B004-B010	14.41%	4.95%	7.43%	***21.61%***	199	1.75
B004-B011	14.41%	4.93%	6.04%	***17.68%***	198	1.75
B004-B012	14.41%	7.32%	10.54%	***20.75%***	294	1.75
B004-B022	14.41%	5.23%	5.35%	***14.76%***	210	1.75
B004-B028	14.04%	1.54%	2.62%	***23.91%***	46	1.75
B005-B010	14.41%	5.00%	5.01%	***14.43%***	201	1.75
B005-B011	14.41%	5.55%	3.80%	***9.87%***	223	1.75
B005-B012	14.41%	8.86%	7.25%	***11.80%***	356	1.75
B005-B022	14.41%	4.41%	2.76%	***9.04%***	177	1.75
B005-B028	14.04%	1.44%	2.38%	***23.26%***	43	1.75
B010-B011	14.41%	9.41%	8.29%	***12.70%***	378	1.75
B010-B012	14.41%	5.43%	9.84%	***26.15%***	218	1.75
B010-B022	14.41%	3.86%	4.15%	***15.48%***	155	1.75
B010-B028	14.04%	2.84%	1.67%	***8.24%***	85	1.75
B011-B012	14.41%	7.42%	8.64%	***16.78%***	298	1.75
B011-B022	14.41%	3.09%	3.63%	***16.94%***	124	1.75
B011-B028	14.04%	2.97%	2.62%	***12.36%***	89	1.75
B012-B022	14.41%	3.73%	4.32%	***16.67%***	150	1.75
B012-B028	14.04%	2.54%	3.57%	***19.74%***	76	1.75
B022-B028	14.04%	1.87%	0.71%	***5.36%***	56	1.75

Table Supp. 5 Continued

Well	p(SS)	p(Pd)	p(Pd|SS)	***p(SS|Pd)***	Detections	Threshold
B001-B003	14.41%	1.99%	1.38%	***10.00%***	80	2
B001-B004	14.41%	1.92%	3.45%	***25.97%***	77	2
B001-B005	14.41%	1.94%	1.38%	***10.26%***	78	2
B001-B010	14.41%	3.26%	4.32%	***19.08%***	131	2
B001-B011	14.41%	3.19%	4.32%	***19.53%***	128	2
B001-B012	14.41%	2.96%	5.18%	***25.21%***	119	2
B001-B022	14.41%	1.34%	1.04%	***11.11%***	54	2
B001-B028	14.04%	0.90%	1.90%	***29.63%***	27	2
B003-B004	14.41%	3.78%	3.28%	***12.50%***	152	2
B003-B005	14.41%	6.20%	4.32%	***10.04%***	249	2
B003-B010	14.41%	3.19%	3.63%	***16.41%***	128	2
B003-B011	14.41%	4.08%	2.07%	***7.32%***	164	2
B003-B012	14.41%	6.60%	6.22%	***13.58%***	265	2
B003-B022	14.41%	2.22%	2.07%	***13.48%***	89	2
B003-B028	14.04%	0.60%	0.71%	***16.67%***	18	2
B004-B005	14.41%	5.20%	5.18%	***14.35%***	209	2
B004-B010	14.41%	2.96%	4.66%	***22.69%***	119	2
B004-B011	14.41%	3.09%	3.97%	***18.55%***	124	2
B004-B012	14.41%	4.75%	7.77%	***23.56%***	191	2
B004-B022	14.41%	2.96%	1.73%	***8.40%***	119	2
B004-B028	14.04%	0.74%	2.14%	***40.91%***	22	2
B005-B010	14.41%	3.46%	3.63%	***15.11%***	139	2
B005-B011	14.41%	3.83%	2.76%	***10.39%***	154	2
B005-B012	14.41%	6.22%	5.01%	***11.60%***	250	2
B005-B022	14.41%	2.99%	1.21%	***5.83%***	120	2
B005-B028	14.04%	0.84%	1.43%	***24.00%***	25	2
B010-B011	14.41%	6.77%	6.39%	***13.60%***	272	2
B010-B012	14.41%	4.08%	7.25%	***25.61%***	164	2
B010-B022	14.41%	2.49%	1.73%	***10.00%***	100	2
B010-B028	14.04%	1.80%	1.19%	***9.26%***	54	2
B011-B012	14.41%	5.50%	6.74%	***17.65%***	221	2
B011-B022	14.41%	1.87%	1.38%	***10.67%***	75	2
B011-B028	14.04%	1.24%	1.67%	***18.92%***	37	2
B012-B022	14.41%	2.07%	1.04%	***7.23%***	83	2
B012-B028	14.04%	1.27%	1.67%	***18.42%***	38	2
B022-B028	14.04%	1.00%	0.00%	***0.00%***	30	2

Table Supp. 5 Continued

Well	p(SS)	p(Pd)	p(Pd|SS)	***p(SS|Pd)***	Detections	Threshold
B001-B003	14.41%	1.67%	0.86%	***7.46%***	67	2.25
B001-B004	14.41%	1.57%	2.25%	***20.63%***	63	2.25
B001-B005	14.41%	1.42%	0.86%	***8.77%***	57	2.25
B001-B010	14.41%	2.49%	3.11%	***18.00%***	100	2.25
B001-B011	14.41%	2.56%	3.80%	***21.36%***	103	2.25
B001-B012	14.41%	2.14%	3.63%	***24.42%***	86	2.25
B001-B022	14.41%	1.00%	0.69%	***10.00%***	40	2.25
B001-B028	14.04%	0.33%	1.43%	***60.00%***	10	2.25
B003-B004	14.41%	2.79%	2.42%	***12.50%***	112	2.25
B003-B005	14.41%	4.28%	2.76%	***9.30%***	172	2.25
B003-B010	14.41%	2.17%	2.07%	***13.79%***	87	2.25
B003-B011	14.41%	3.14%	1.55%	***7.14%***	126	2.25
B003-B012	14.41%	4.61%	3.97%	***12.43%***	185	2.25
B003-B022	14.41%	1.54%	1.73%	***16.13%***	62	2.25
B003-B028	14.04%	0.33%	0.24%	***10.00%***	10	2.25
B004-B005	14.41%	3.86%	3.63%	***13.55%***	155	2.25
B004-B010	14.41%	1.84%	2.59%	***20.27%***	74	2.25
B004-B011	14.41%	2.27%	3.63%	***23.08%***	91	2.25
B004-B012	14.41%	2.94%	5.35%	***26.27%***	118	2.25
B004-B022	14.41%	1.62%	0.00%	***0.00%***	65	2.25
B004-B028	14.04%	0.57%	1.90%	***47.06%***	17	2.25
B005-B010	14.41%	2.46%	2.59%	***15.15%***	99	2.25
B005-B011	14.41%	2.61%	1.90%	***10.48%***	105	2.25
B005-B012	14.41%	4.36%	3.80%	***12.57%***	175	2.25
B005-B022	14.41%	1.89%	0.17%	***1.32%***	76	2.25
B005-B028	14.04%	0.30%	0.24%	***11.11%***	9	2.25
B010-B011	14.41%	5.13%	4.84%	***13.59%***	206	2.25
B010-B012	14.41%	2.51%	3.97%	***22.77%***	101	2.25
B010-B022	14.41%	1.57%	1.55%	***14.29%***	63	2.25
B010-B028	14.04%	1.27%	0.95%	***10.53%***	38	2.25
B011-B012	14.41%	3.53%	4.15%	***16.90%***	142	2.25
B011-B022	14.41%	1.17%	0.86%	***10.64%***	47	2.25
B011-B028	14.04%	0.64%	0.95%	***21.05%***	19	2.25
B012-B022	14.41%	1.12%	0.17%	***2.22%***	45	2.25
B012-B028	14.04%	0.64%	0.24%	***5.26%***	19	2.25
B022-B028	0.00%	0.00%	0.00%	***0.00%***	0	2.25

Table Supp. 5 Continued

Well	p(SS)	p(Pd)	p(Pd|SS)	***p(SS|Pd)***	Detections	Threshold
B001-B003	14.41%	1.12%	0.69%	***8.89%***	45	2.5
B001-B004	14.41%	1.22%	1.21%	***14.29%***	49	2.5
B001-B005	14.41%	0.95%	0.35%	***5.26%***	38	2.5
B001-B010	14.41%	1.82%	2.76%	***21.92%***	73	2.5
B001-B011	14.41%	1.99%	3.28%	***23.75%***	80	2.5
B001-B012	14.41%	1.49%	3.28%	***31.67%***	60	2.5
B001-B022	14.41%	0.60%	0.35%	***8.33%***	24	2.5
B001-B028	14.04%	0.13%	0.48%	***50.00%***	4	2.5
B003-B004	14.41%	1.94%	2.07%	***15.38%***	78	2.5
B003-B005	14.41%	2.74%	2.42%	***12.73%***	110	2.5
B003-B010	14.41%	1.62%	0.86%	***7.69%***	65	2.5
B003-B011	14.41%	2.54%	1.55%	***8.82%***	102	2.5
B003-B012	14.41%	2.86%	3.11%	***15.65%***	115	2.5
B003-B022	14.41%	0.77%	0.86%	***16.13%***	31	2.5
B003-B028	0.00%	0.00%	0.00%	***0.00%***	0	2.5
B004-B005	14.41%	2.74%	2.25%	***11.82%***	110	2.5
B004-B010	14.41%	1.39%	1.73%	***17.86%***	56	2.5
B004-B011	14.41%	1.64%	2.07%	***18.18%***	66	2.5
B004-B012	14.41%	1.92%	3.97%	***29.87%***	77	2.5
B004-B022	0.00%	0.00%	0.00%	***0.00%***	0	2.5
B004-B028	14.04%	0.27%	0.71%	***37.50%***	8	2.5
B005-B010	14.41%	1.72%	2.07%	***17.39%***	69	2.5
B005-B011	14.41%	1.69%	1.38%	***11.76%***	68	2.5
B005-B012	14.41%	2.84%	2.94%	***14.91%***	114	2.5
B005-B022	0.00%	0.00%	0.00%	***0.00%***	0	2.5
B005-B028	0.00%	0.00%	0.00%	***0.00%***	0	2.5
B010-B011	14.41%	3.68%	4.32%	***16.89%***	148	2.5
B010-B012	14.41%	1.62%	2.94%	***26.15%***	65	2.5
B010-B022	14.41%	1.10%	1.55%	***20.45%***	44	2.5
B010-B028	0.00%	0.00%	0.00%	***0.00%***	0	2.5
B011-B012	14.41%	2.39%	3.63%	***21.88%***	96	2.5
B011-B022	14.41%	0.60%	0.69%	***16.67%***	24	2.5
B011-B028	14.04%	0.33%	0.95%	***40.00%***	10	2.5
B012-B022	0.00%	0.00%	0.00%	***0.00%***	0	2.5
B012-B028	0.00%	0.00%	0.00%	***0.00%***	0	2.5
B022-B028	0.00%	0.00%	0.00%	***0.00%***	0	2.5

Table Supp. 5 Continued

Well	p(SS)	p(Pd)	p(Pd|SS)	***p(SS|Pd)***	Detections	Threshold
B001-B003	14.41%	0.80%	0.52%	***9.38%***	32	2.75
B001-B004	14.41%	0.97%	0.86%	***12.82%***	39	2.75
B001-B005	14.41%	0.75%	0.17%	***3.33%***	30	2.75
B001-B010	14.41%	1.32%	2.76%	***30.19%***	53	2.75
B001-B011	14.41%	1.47%	2.42%	***23.73%***	59	2.75
B001-B012	14.41%	1.15%	2.25%	***28.26%***	46	2.75
B001-B022	14.41%	0.40%	0.17%	***6.25%***	16	2.75
B001-B028	14.04%	0.07%	0.48%	***100.00%***	2	2.75
B003-B004	14.41%	1.32%	1.73%	***18.87%***	53	2.75
B003-B005	14.41%	1.39%	1.38%	***14.29%***	56	2.75
B003-B010	14.41%	0.97%	0.35%	***5.13%***	39	2.75
B003-B011	14.41%	1.74%	1.55%	***12.86%***	70	2.75
B003-B012	14.41%	1.99%	2.59%	***18.75%***	80	2.75
B003-B022	14.41%	0.35%	0.52%	***21.43%***	14	2.75
B003-B028	0.00%	0.00%	0.00%	***0.00%***	0	2.75
B004-B005	14.41%	1.69%	1.90%	***16.18%***	68	2.75
B004-B010	14.41%	0.95%	1.21%	***18.42%***	38	2.75
B004-B011	14.41%	1.15%	1.55%	***19.57%***	46	2.75
B004-B012	14.41%	1.42%	3.11%	***31.58%***	57	2.75
B004-B022	0.00%	0.00%	0.00%	***0.00%***	0	2.75
B004-B028	0.00%	0.00%	0.00%	***0.00%***	0	2.75
B005-B010	14.41%	0.92%	1.04%	***16.22%***	37	2.75
B005-B011	14.41%	1.02%	1.04%	***14.63%***	41	2.75
B005-B012	14.41%	2.07%	2.07%	***14.46%***	83	2.75
B005-B022	0.00%	0.00%	0.00%	***0.00%***	0	2.75
B005-B028	0.00%	0.00%	0.00%	***0.00%***	0	2.75
B010-B011	14.41%	2.79%	3.63%	***18.75%***	112	2.75
B010-B012	14.41%	0.92%	1.73%	***27.03%***	237	2.75
B010-B022	14.41%	0.77%	1.21%	***22.58%***	31	2.75
B010-B028	0.00%	0.00%	0.00%	***0.00%***	0	2.75
B011-B012	14.41%	1.64%	2.94%	***25.76%***	66	2.75
B011-B022	14.41%	0.45%	0.69%	***22.22%***	18	2.75
B011-B028	14.04%	0.20%	0.95%	***66.67%***	6	2.75
B012-B022	0.00%	0.00%	0.00%	***0.00%***	0	2.75
B012-B028	0.00%	0.00%	0.00%	***0.00%***	0	2.75
B022-B028	0.00%	0.00%	0.00%	***0.00%***	0	2.75

Table Supp. 5 Continued

Well	p(SS)	p(Pd)	p(Pd|SS)	***p(SS|Pd)***	Detections	Threshold
B001-B003	0.00%	0.00%	0.00%	***0.00%***	0	3
B001-B004	14.41%	0.57%	0.52%	***13.04%***	23	3
B001-B005	0.00%	0.00%	0.00%	***0.00%***	0	3
B001-B010	14.41%	1.02%	2.42%	***34.15%***	41	3
B001-B011	14.41%	1.05%	2.07%	***28.57%***	42	3
B001-B012	14.41%	0.87%	1.73%	***28.57%***	35	3
B001-B022	0.00%	0.00%	0.00%	***0.00%***	0	3
B001-B028	0.00%	0.00%	0.00%	***0.00%***	0	3
B003-B004	14.41%	0.92%	1.55%	***24.32%***	37	3
B003-B005	14.41%	1.10%	1.04%	***13.64%***	44	3
B003-B010	0.00%	0.00%	0.00%	***0.00%***	0	3
B003-B011	14.41%	1.19%	1.38%	***16.67%***	48	3
B003-B012	14.41%	1.34%	1.90%	***20.37%***	54	3
B003-B022	0.00%	0.00%	0.00%	***0.00%***	0	3
B003-B028	0.00%	0.00%	0.00%	***0.00%***	0	3
B004-B005	14.41%	1.12%	1.38%	***17.78%***	45	3
B004-B010	14.41%	0.60%	0.52%	***12.50%***	24	3
B004-B011	14.41%	0.72%	1.21%	***24.14%***	29	3
B004-B012	14.41%	1.12%	2.59%	***33.33%***	45	3
B004-B022	0.00%	0.00%	0.00%	***0.00%***	0	3
B004-B028	0.00%	0.00%	0.00%	***0.00%***	0	3
B005-B010	0.00%	0.00%	0.00%	***0.00%***	0	3
B005-B011	14.41%	0.60%	0.86%	***20.83%***	24	3
B005-B012	14.41%	1.59%	1.55%	***14.06%***	64	3
B005-B022	0.00%	0.00%	0.00%	***0.00%***	0	3
B005-B028	0.00%	0.00%	0.00%	***0.00%***	0	3
B010-B011	14.41%	1.74%	2.42%	***20.00%***	70	3
B010-B012	14.41%	0.70%	1.21%	***25.00%***	28	3
B010-B022	14.41%	0.45%	1.21%	***38.89%***	18	3
B010-B028	0.00%	0.00%	0.00%	***0.00%***	0	3
B011-B012	14.41%	0.95%	2.07%	***31.58%***	38	3
B011-B022	0.00%	0.00%	0.00%	***0.00%***	0	3
B011-B028	0.00%	0.00%	0.00%	***0.00%***	0	3
B012-B022	0.00%	0.00%	0.00%	***0.00%***	0	3
B012-B028	0.00%	0.00%	0.00%	***0.00%***	0	3
B022-B028	0.00%	0.00%	0.00%	***0.00%***	0	3

Table Supp. 5 Continued

Well	p(SS)	p(Pd)	p(Pd|SS)	***p(SS|Pd)***	Detections	Threshold
B001-B003	0.00%	0.00%	0.00%	***0.00%***	0	3.25
B001-B004	0.00%	0.00%	0.00%	***0.00%***	0	3.25
B001-B005	0.00%	0.00%	0.00%	***0.00%***	0	3.25
B001-B010	14.41%	0.87%	2.07%	***34.29%***	35	3.25
B001-B011	14.41%	0.77%	1.38%	***25.81%***	31	3.25
B001-B012	14.41%	0.60%	0.69%	***16.67%***	24	3.25
B001-B022	0.00%	0.00%	0.00%	***0.00%***	0	3.25
B001-B028	0.00%	0.00%	0.00%	***0.00%***	0	3.25
B003-B004	14.41%	0.67%	1.21%	***25.93%***	27	3.25
B003-B005	14.41%	0.87%	1.04%	***17.14%***	35	3.25
B003-B010	0.00%	0.00%	0.00%	***0.00%***	0	3.25
B003-B011	14.41%	1.05%	1.38%	***19.05%***	42	3.25
B003-B012	14.41%	1.12%	1.55%	***20.00%***	45	3.25
B003-B022	0.00%	0.00%	0.00%	***0.00%***	0	3.25
B003-B028	0.00%	0.00%	0.00%	***0.00%***	0	3.25
B004-B005	14.41%	0.82%	1.38%	***24.24%***	33	3.25
B004-B010	0.00%	0.00%	0.00%	***0.00%***	0	3.25
B004-B011	14.41%	0.45%	0.69%	***22.22%***	18	3.25
B004-B012	14.41%	0.77%	1.90%	***35.48%***	31	3.25
B004-B022	0.00%	0.00%	0.00%	***0.00%***	0	3.25
B004-B028	0.00%	0.00%	0.00%	***0.00%***	0	3.25
B005-B010	0.00%	0.00%	0.00%	***0.00%***	0	3.25
B005-B011	14.41%	0.55%	0.86%	***22.73%***	22	3.25
B005-B012	14.41%	1.19%	1.55%	***18.75%***	48	3.25
B005-B022	0.00%	0.00%	0.00%	***0.00%***	0	3.25
B005-B028	0.00%	0.00%	0.00%	***0.00%***	0	3.25
B010-B011	14.41%	1.37%	1.73%	***18.18%***	55	3.25
B010-B012	14.41%	0.55%	0.52%	***13.64%***	22	3.25
B010-B022	14.41%	0.22%	1.21%	***77.78%***	9	3.25
B010-B028	0.00%	0.00%	0.00%	***0.00%***	0	3.25
B011-B012	14.41%	0.75%	1.55%	***30.00%***	30	3.25
B011-B022	0.00%	0.00%	0.00%	***0.00%***	0	3.25
B011-B028	0.00%	0.00%	0.00%	***0.00%***	0	3.25
B012-B022	0.00%	0.00%	0.00%	***0.00%***	0	3.25
B012-B028	0.00%	0.00%	0.00%	***0.00%***	0	3.25
B022-B028	0.00%	0.00%	0.00%	***0.00%***	0	3.25

Table Supp. 6: Single Station Posterior Probabilities, Holt-Winter's Model- A temporal window one day in length is used for these detections.

Well	p(SS)	p(Pd)	p(Pd|SS)	***p(SS|Pd)***
B001	14.04%	3.33%	10.51%	***44.29%***
B004	14.04%	2.81%	8.81%	***44.07%***
B005	14.04%	3.62%	10.85%	***42.11%***
B010	14.04%	1.57%	6.10%	***54.55%***
B011	14.04%	1.24%	8.81%	***100.00%***
B012	14.04%	7.62%	24.07%	***44.38%***
B022	14.06%	4.58%	14.24%	***43.75%***
B028	14.04%	0.43%	2.03%	***66.67%***

Table Supp. 7. Single Station Posterior Probabilities, Holt-Winter's Model- A temporal window two days in length is used for these detections.

Well	p(SS)	p(Pd)	p(Pd|SS)	***p(SS|Pd)***
B001	14.06%	6.34%	19.32%	***42.86%***
B004	14.06%	5.43%	16.27%	***42.11%***
B005	14.06%	6.91%	18.98%	***38.62%***
B010	14.06%	2.72%	11.19%	***57.89%***
B011	14.06%	2.38%	16.95%	***100.00%***
B012	14.06%	14.06%	43.05%	***43.05%***
B022	14.06%	4.58%	14.24%	***43.75%***
B028	14.06%	0.86%	4.07%	***66.67%***

Table Supp. 8. Single Station Posterior Probabilities, Holt-Winter's Model- A temporal window three days in length is used for these detections.

Well	p(SS)	p(Pd)	p(Pd|SS)	***p(SS|Pd)***
B001	14.08%	8.97%	26.44%	***41.49%***
B004	14.08%	8.02%	24.07%	***42.26%***
B005	14.06%	6.91%	18.98%	***38.62%***
B010	14.08%	3.72%	16.27%	***61.54%***
B011	14.08%	3.39%	24.07%	***100.00%***
B012	14.08%	19.33%	56.61%	***41.23%***
B022	14.08%	6.68%	21.02%	***44.29%***
B028	14.08%	1.29%	6.10%	***66.67%***

Table Supp. 9. Single Station Posterior Probabilities, Holt-Winter's Model- A temporal window three days in length is used for these detections.

Well	p(SS)	p(Pd)	p(Pd|SS)	***p(SS|Pd)***
B001	14.10%	11.38%	34.24%	***42.44%***
B004	14.10%	10.47%	32.20%	***43.38%***
B005	14.10%	12.43%	31.19%	***35.38%***
B010	14.10%	4.59%	20.34%	***62.50%***
B011	14.10%	4.30%	30.17%	***98.89%***
B012	14.10%	23.80%	67.46%	***39.96%***
B022	14.10%	8.46%	26.44%	***44.07%***
B028	14.10%	1.72%	8.14%	***66.67%***

Table Supp. 10. Joint Station Probabilities, Holt-Winter's Model, Well Group 1, consisting of sites B001, B004, and B005- Colors indicate the size of temporal window used for the cross correlation of detections, noted in column 7. "Responsive wells" indicates the number of wells in which detections are correlated across within the group.

Responsive Wells	p(SS)	p(Pd)	p(Pd|SS)	***p(SS|Pd)***	Detections	Window
1	14.10%	25.33%	58.98%	***32.83%***	530	four days
2	14.10%	7.31%	27.80%	***53.59%***	153	four days
3	14.10%	1.63%	11.53%	***100.00%***	34	four days
1	14.08%	20.53%	48.81%	***33.49%***	430	three days
2	14.08%	5.44%	20.68%	***53.51%***	114	three days
3	14.08%	0.91%	6.44%	***100.00%***	19	three days
1	14.06%	14.87%	37.97%	***35.90%***	312	two days
2	14.06%	3.38%	13.56%	***56.34%***	71	two days
3	14.06%	0.43%	3.05%	***100.00%***	9	two days
1	14.04%	8.19%	23.73%	***40.70%***	172	one day
2	14.04%	1.52%	6.10%	***56.25%***	32	one day
3	14.04%	0.05%	0.34%	***100.00%***	1	one day

Table Supp. 11. Joint Station Probabilities, Holt-Winter's Model, Well Group 2, consisting of sites B010, B011, and B012-This table is similar to Table Supp. 10.

Responsive Wells	p(SS)	p(Pd)	p(Pd|SS)	***p(SS|Pd)***	Detections	Window
1	14.10%	26.58%	78.64%	***41.73%***	556	four days
2	14.10%	5.45%	31.53%	***81.58%***	114	four days
3	14.10%	0.67%	7.46%	***100.00%***	14	four days
1	14.08%	22.24%	69.83%	***44.21%***	466	three days
2	14.08%	3.82%	22.37%	***82.50%***	80	three days
3	14.08%	0.38%	4.75%	***100.00%***	8	three days
1	14.06%	16.83%	56.27%	***47.03%***	353	two days
2	14.06%	2.14%	12.54%	***82.22%***	45	two days
3	14.06%	0.19%	2.37%	***100.00%***	4	two days
1	14.04%	9.57%	33.56%	***49.25%***	201	one day
2	14.04%	0.86%	5.42%	***88.89%***	18	one day
3	14.04%	0.00%	0.00%	***0.00%***	0	one day

Table Supp. 12. Joint Station Probabilities, Holt-Winter's Model, Well Group 3, consisting of sites B022 and B028- This table is similar to Table Supp. 10.

Responsive Wells	p(SS)	p(Pd)	p(Pd|SS)	***p(SS|Pd)***	Detections	Xcorr win
1	14.10%	8.94%	29.49%	***46.52%***	187	four days
2	14.10%	1.24%	4.75%	***53.85%***	26	four days
1	14.08%	7.11%	24.07%	***47.65%***	149	three days
2	14.08%	0.86%	3.05%	***50.00%***	18	three days
1	14.06%	4.86%	16.27%	***47.06%***	102	two days
2	14.06%	0.57%	2.03%	***50.00%***	12	two days
1	14.04%	2.48%	8.14%	***46.15%***	52	one day
2	14.04%	0.29%	1.02%	***50.00%***	6	one day

Table Supp. 13. Network-Wide Joint Probabilities, Holt-Winter's Model, Four Day Temporal Window- "Responsive wells" indicates the number of wells in which detections are correlated across within the group.

Responsive Wells	p(SS)	p(Pd)	p(Pd|SS)	***p(SS|Pd)***	Detections
1	14.10%	37.33%	88.14%	***33.29%***	781
2	14.10%	20.27%	64.07%	***44.58%***	424
3	14.10%	12.52%	48.14%	***54.20%***	262
4	14.10%	3.97%	28.14%	***100.00%***	83
5	14.10%	2.25%	15.93%	***100.00%***	47
6	14.10%	0.72%	5.08%	***100.00%***	15
7	14.10%	0.10%	0.68%	***100.00%***	2
8	0.00%	0.00%	0.00%	***0.00%***	0

Table Supp. 14. Network-Wide Joint Probabilities, Holt-Winter's Model, Three Day Temporal Window- This table is similar to Table Supp. 13.

Responsive Wells	p(SS)	p(Pd)	p(Pd|SS)	***p(SS|Pd)***	Detections
1	14.08%	31.60%	79.32%	***35.35%***	662
2	14.08%	15.99%	53.22%	***46.87%***	335
3	14.08%	9.26%	35.93%	***54.64%***	194
4	14.08%	2.82%	20.00%	***100.00%***	59
5	14.08%	1.34%	9.49%	***100.00%***	28
6	14.08%	0.29%	2.03%	***100.00%***	6
7	0.00%	0.00%	0.00%	***0.00%***	0
8	0.00%	0.00%	0.00%	***0.00%***	0

Table Supp. 15. Network-Wide Joint Probabilities, Holt-Winter's Model, Two Day Temporal Window- This table is similar to Table. Supp. 13

Responsive Wells	p(SS)	p(Pd)	p(Pd|SS)	***p(SS|Pd)***	Detections
1	14.06%	24.26%	66.44%	***38.51%***	509
2	14.06%	11.11%	39.66%	***50.21%***	233
3	14.06%	5.67%	22.03%	***54.62%***	119
4	14.06%	1.67%	11.86%	***100.00%***	35
5	14.06%	0.48%	3.39%	***100.00%***	10
6	14.06%	0.10%	0.68%	***100.00%***	2
7	0.00%	0.00%	0.00%	***0.00%***	0
8	0.00%	0.00%	0.00%	***0.00%***	0

Table Supp. 16. Network-Wide Joint Probabilities, Holt-Winter's Model, One Day Temporal Window-This table is similar to Table Supp.13.

Responsive Wells	p(ss)	p(Pd)	p(Pd|SS)	***p(SS|Pd)***	Detections
1	14.04%	14.61%	44.07%	***42.35%***	307
2	14.04%	5.24%	20.00%	***53.64%***	110
3	14.04%	2.43%	9.49%	***54.90%***	51
4	14.04%	0.67%	4.75%	***100.00%***	14
5	0.00%	0.00%	0.00%	***0.00%***	0
6	0.00%	0.00%	0.00%	***0.00%***	0
7	0.00%	0.00%	0.00%	***0.00%***	0
8	0.00%	0.00%	0.00%	***0.00%***	0

APPENDIX C

SUPPLEMENTAL FIGURES

This appendix contains supplemental figures that depict the results from the Holt-Winter's predictive model. Figures Supp. 1-Supp. 8 depict the individual site data and detections. Figures Supp. 9- Supp. 10 depict joint-detections for varying temporal windows. Figures Supp. 11-Supp. 12 depict single site detections for varying temporal windows. Figures Supp. 13- Supp. 16 are similar to Figures 12-15 in the main text but include the data from the borehole sites that contain no anomalous activity found by the Holt-Winter's model. Figures Supp. 17 and Supp. 18 show the amount of correlated data points between pairs of stations for the Holt-Winter's model.

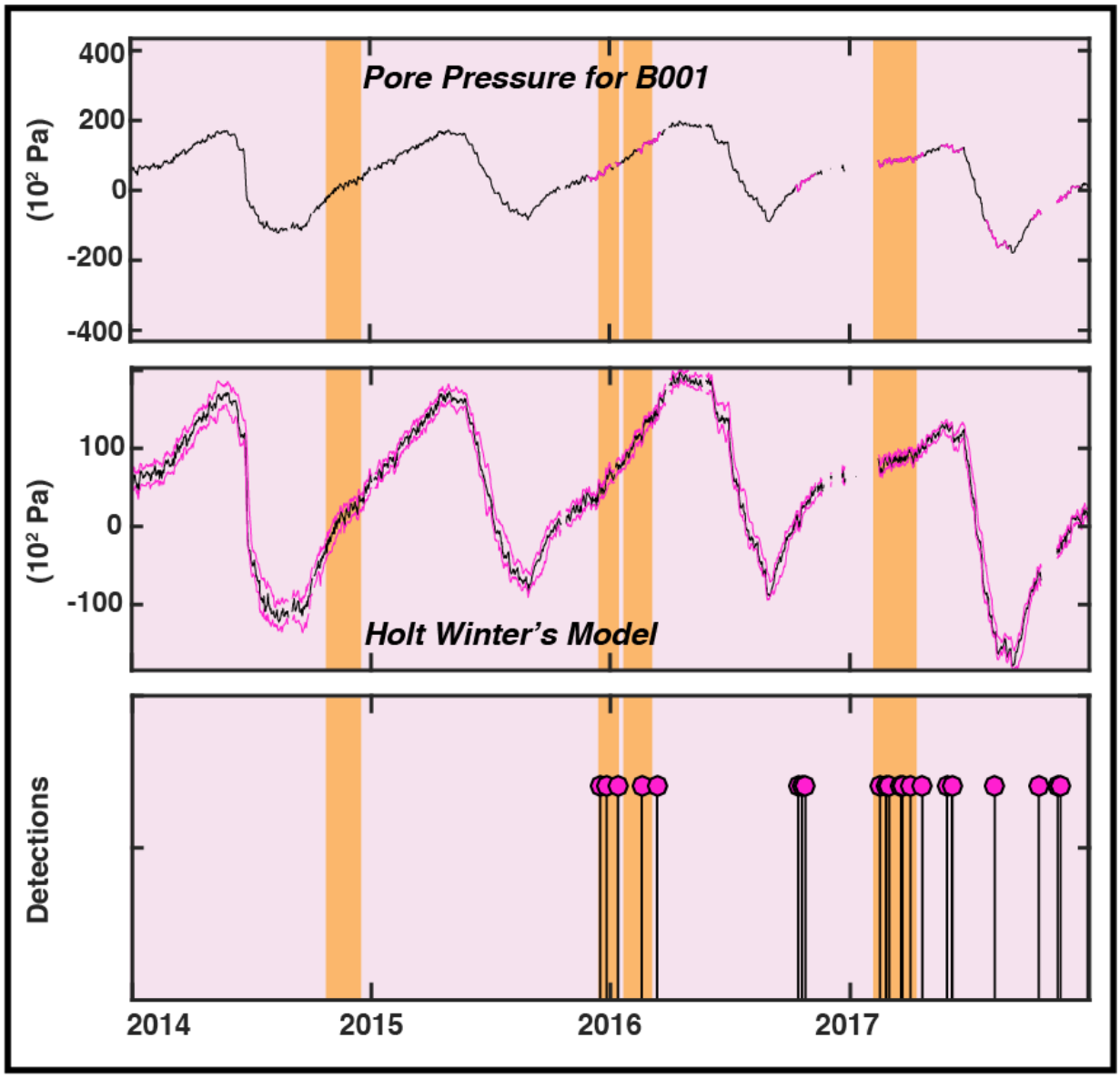

Figure Supp. 1. Holt-Winter's Predictive Model for Site B001- The top panel shows the raw pore pressure data downsampled to 1/300 Hz, with anomalous data marked in purple. The second panel shows these data again plotted with the Brutlag confidence bands from the predictive model. The third panel shows the detections from the predictive model as a stem plot. Known times of SSEs are marked with orange rectangles. Data gaps are not interpolated.

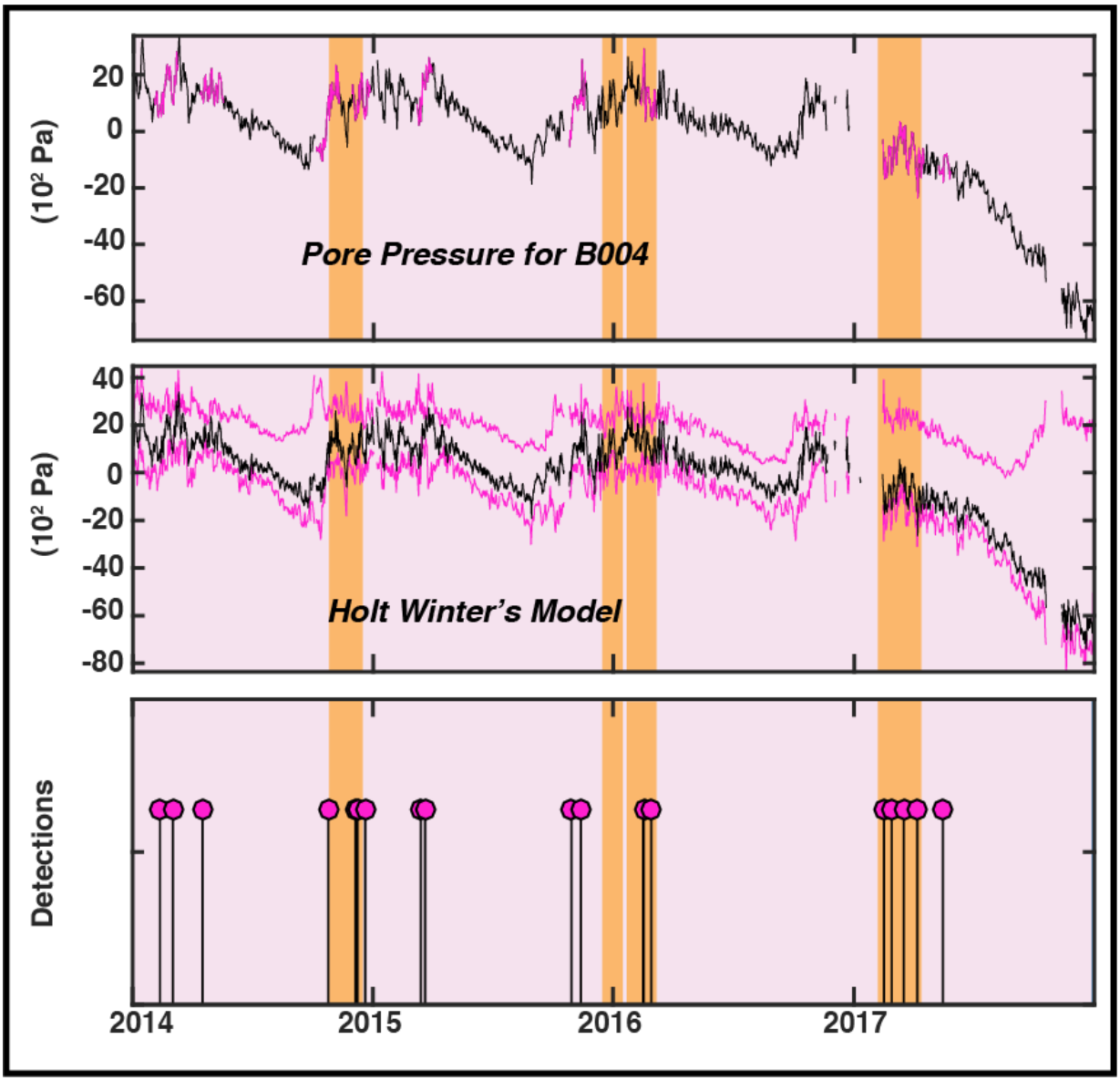

Figure Supp. 2. Holt-Winter's Predictive Model for Site B004- The top panel shows the raw pore pressure data downsampled to 1/300 Hz, with anomalous data marked in purple. The second panel shows these data again plotted with the Brutlag confidence bands from the predictive model. The third panel shows the detections from the predictive model as a stem plot. Known times of SSEs are marked with orange rectangles. Data gaps are not interpolated.

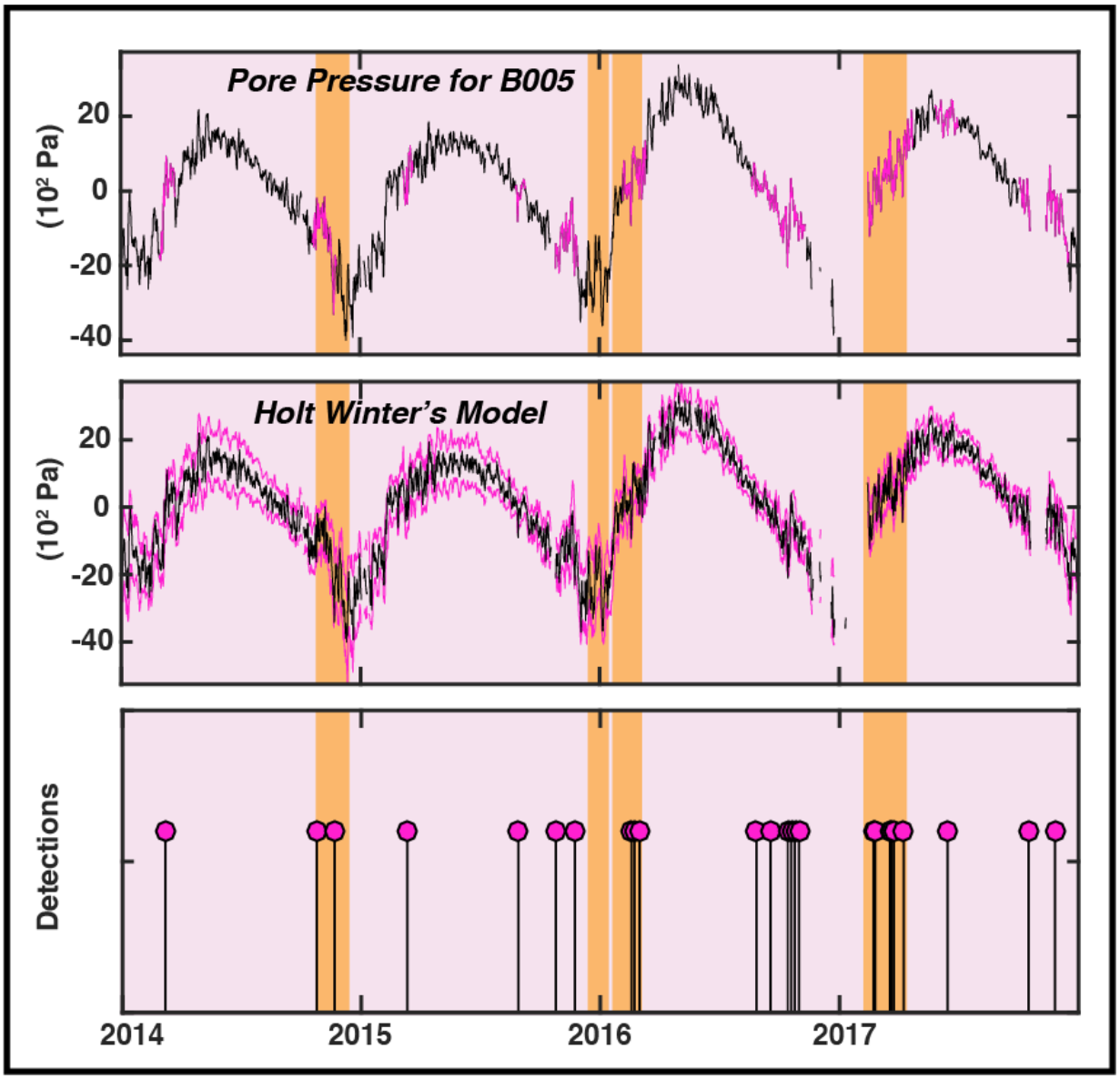

Figure Supp. 3. Holt-Winter's Predictive Model for Site B005- The top panel shows the raw pore pressure data downsampled to 1/300 Hz, with anomalous data marked in purple. The second panel shows these data again plotted with the Brutlag confidence bands from the predictive model. The third panel shows the detections from the predictive model as a stem plot. Known times of SSEs are marked with orange rectangles. Data gaps are not interpolated.

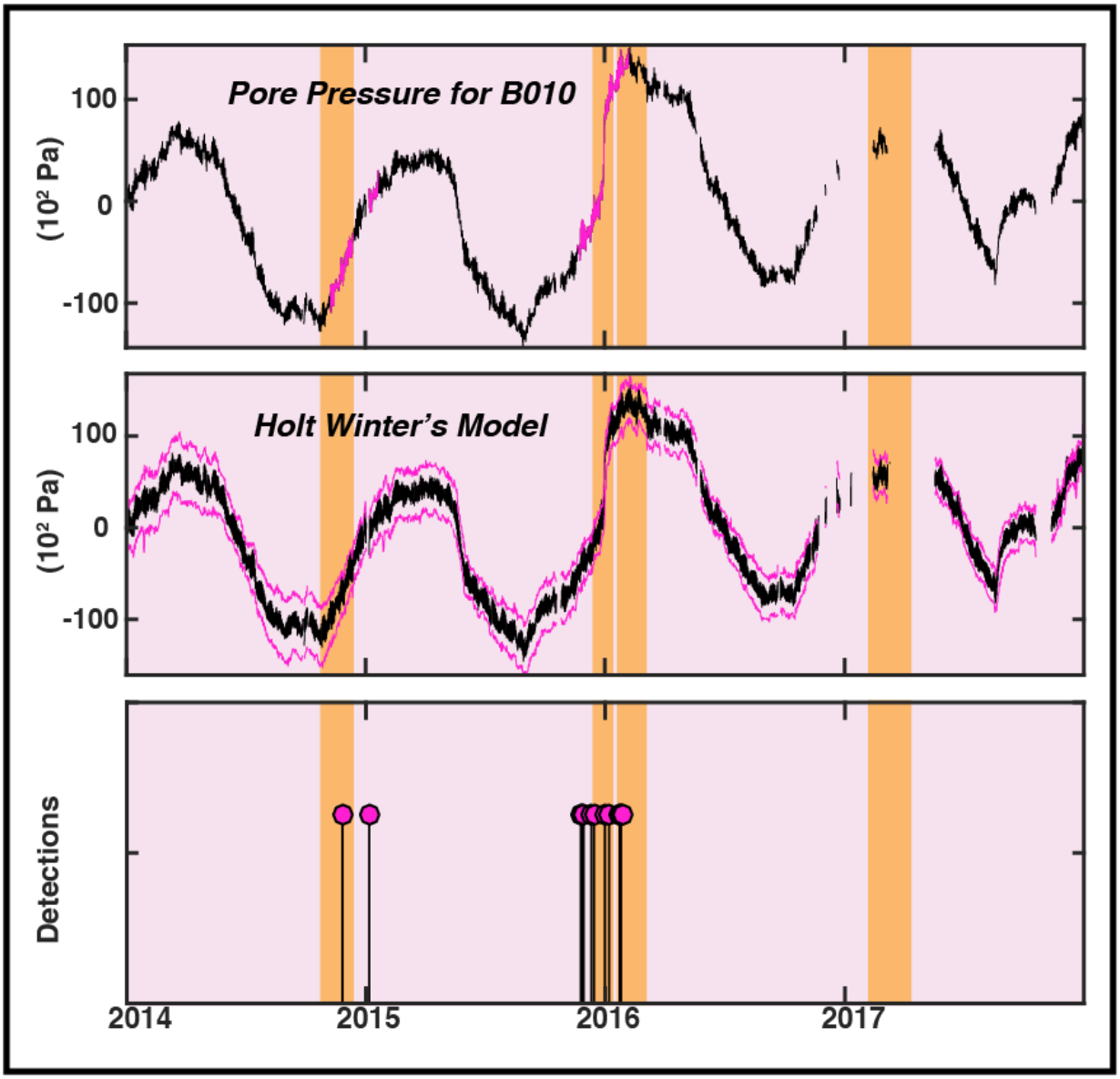

Figure Supp. 4. Holt-Winter's Predictive Model for Site B010- The top panel shows the raw pore pressure data downsampled to 1/300 Hz, with anomalous data marked in purple. The second panel shows these data again plotted with the Brutlag confidence bands from the predictive model. The third panel shows the detections from the predictive model as a stem plot. Known times of SSEs are marked with orange rectangles. Data gaps are not interpolated.

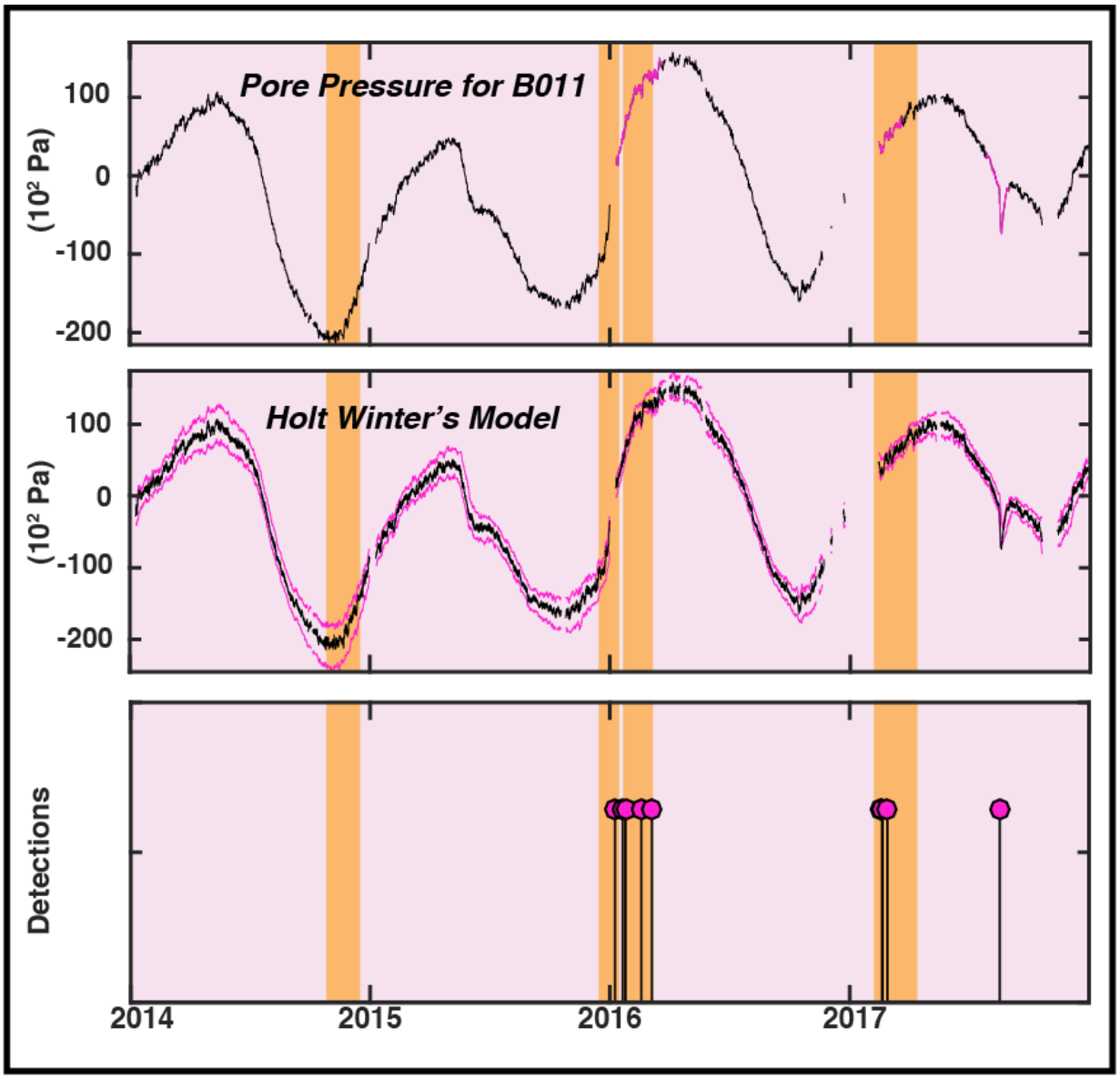

Figure Supp. 5. Holt-Winter's Predictive Model for Site B011- The top panel shows the raw pore pressure data downsampled to 1/300 Hz, with anomalous data marked in purple. The second panel shows these data again plotted with the Brutlag confidence bands from the predictive model. The third panel shows the detections from the predictive model as a stem plot. Known times of SSEs are marked with orange rectangles. Data gaps are not interpolated.

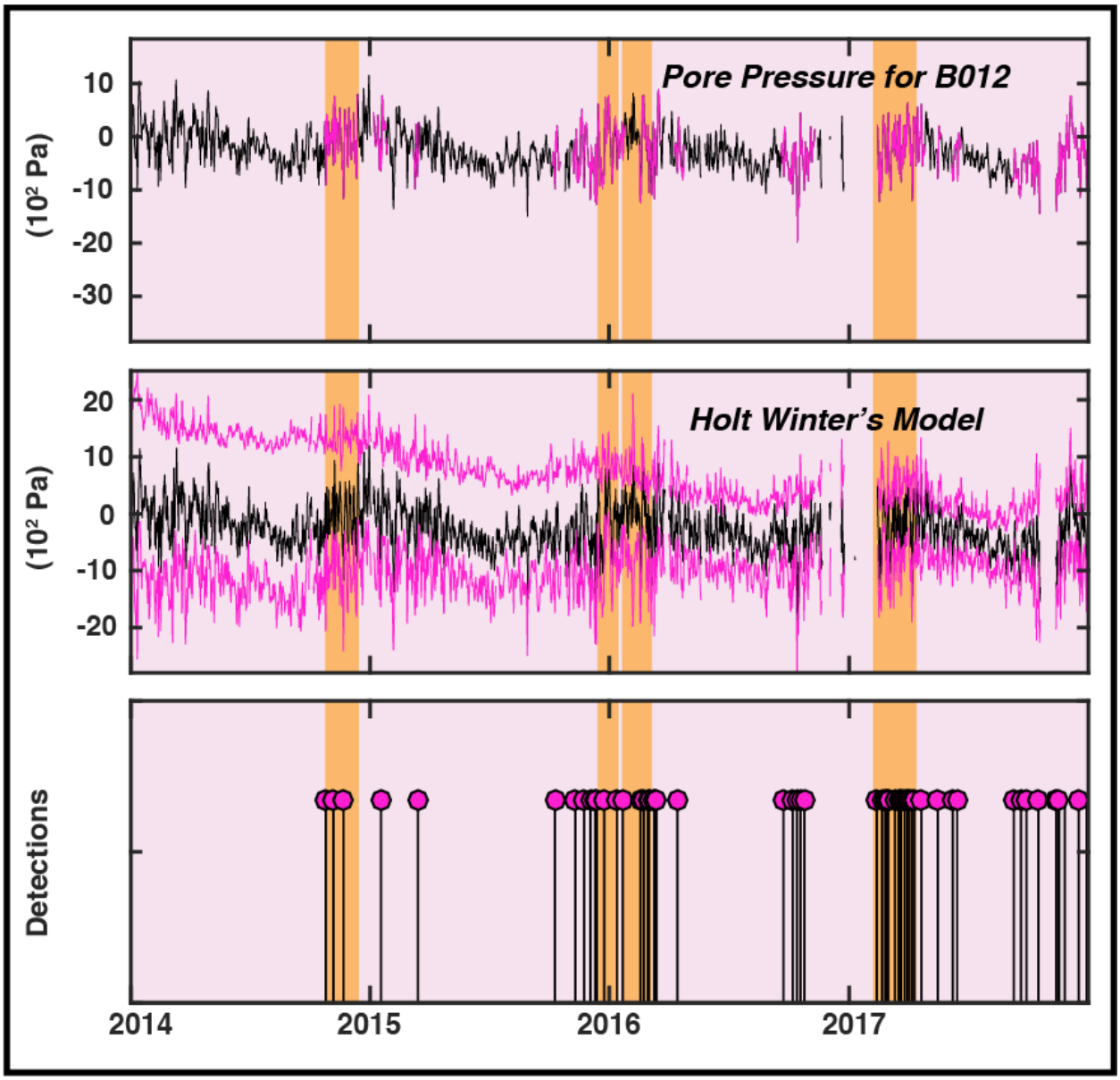

Figure Supp. 6. Holt-Winter's Predictive Model for Site B012- The top panel shows the raw pore pressure data downsampled to 1/300 Hz, with anomalous data marked in purple. The second panel shows these data again plotted with the Brutlag confidence bands from the predictive model. The third panel shows the detections from the predictive model as a stem plot. Known times of SSEs are marked with orange rectangles. Data gaps are not interpolated.

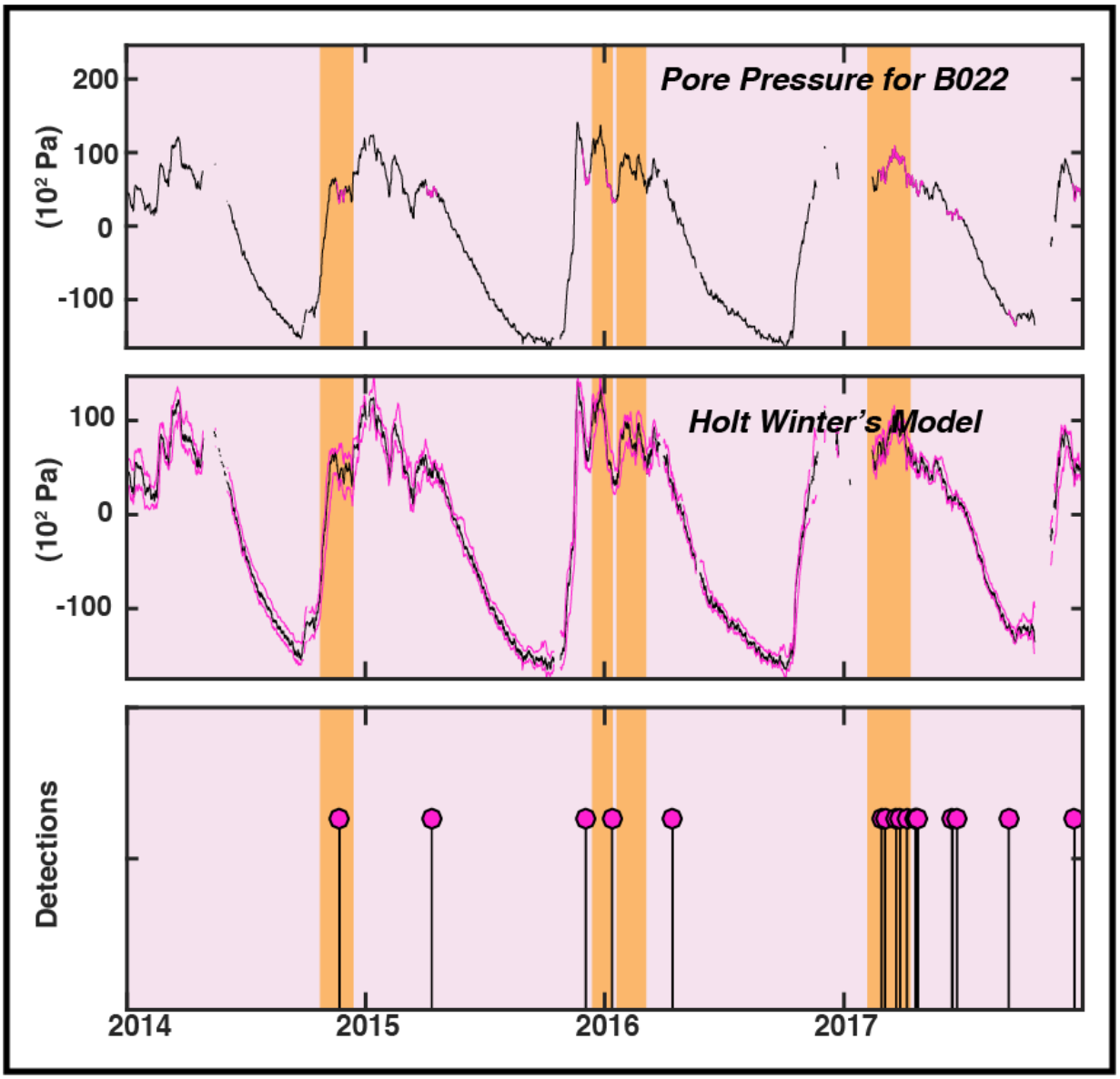

Figure Supp. 7. Holt-Winter's Predictive Model for Site B022- The top panel shows the raw pore pressure data downsampled to 1/300 Hz, with anomalous data marked in purple. The second panel shows these data again plotted with the Brutlag confidence bands from the predictive model. The third panel shows the detections from the predictive model as a stem plot. Known times of SSEs are marked with orange rectangles. Data gaps are not interpolated.

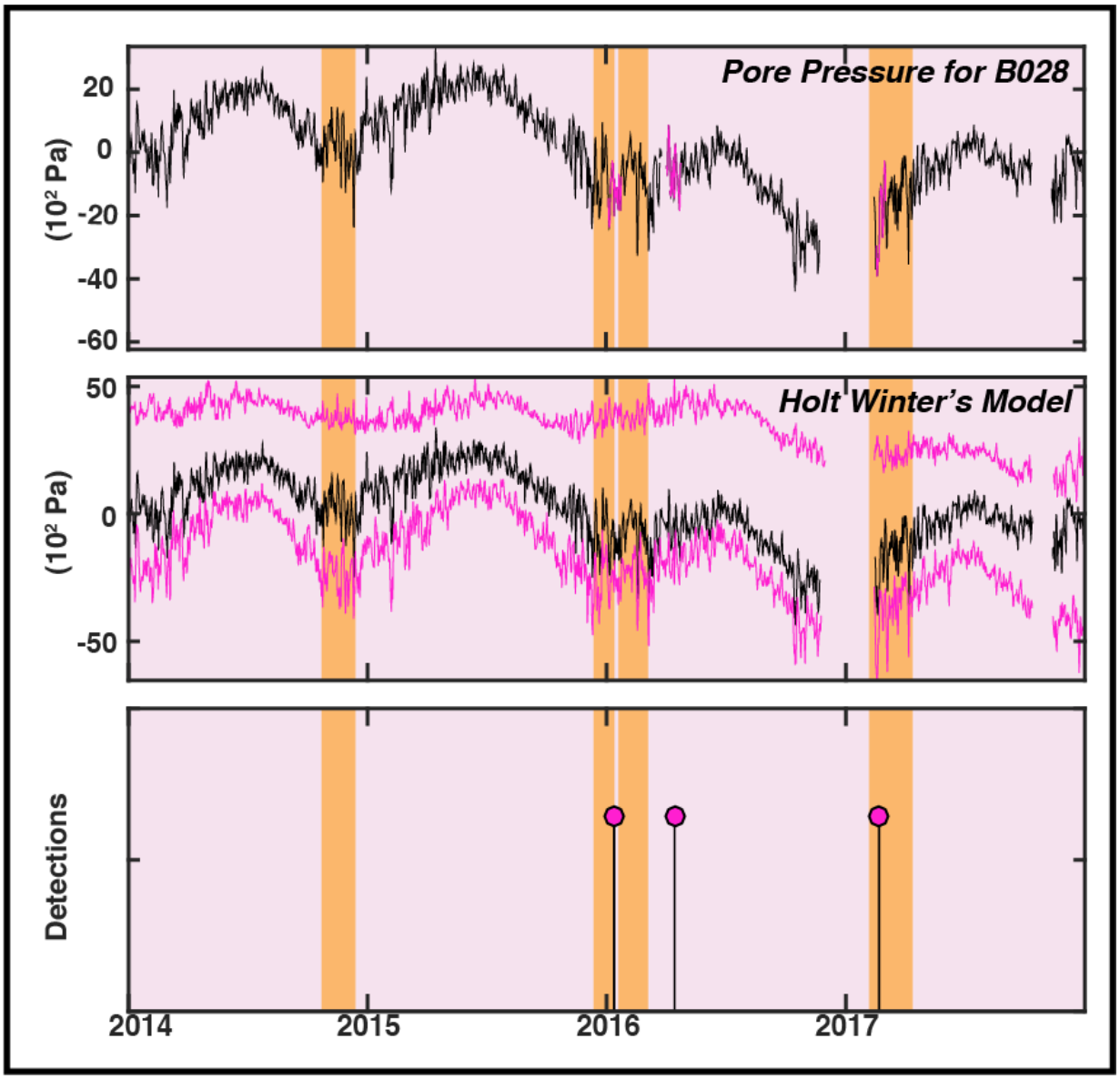

Figure Supp. 8. Holt-Winter's Predictive Model for Site B028- The top panel shows the raw pore pressure data downsampled to 1/300 Hz, with anomalous data marked in purple. The second panel shows these data again plotted with the Brutlag confidence bands from the predictive model. The third panel shows the detections from the predictive model as a stem plot. Known times of SSEs are marked with orange rectangles. Data gaps are not interpolated.

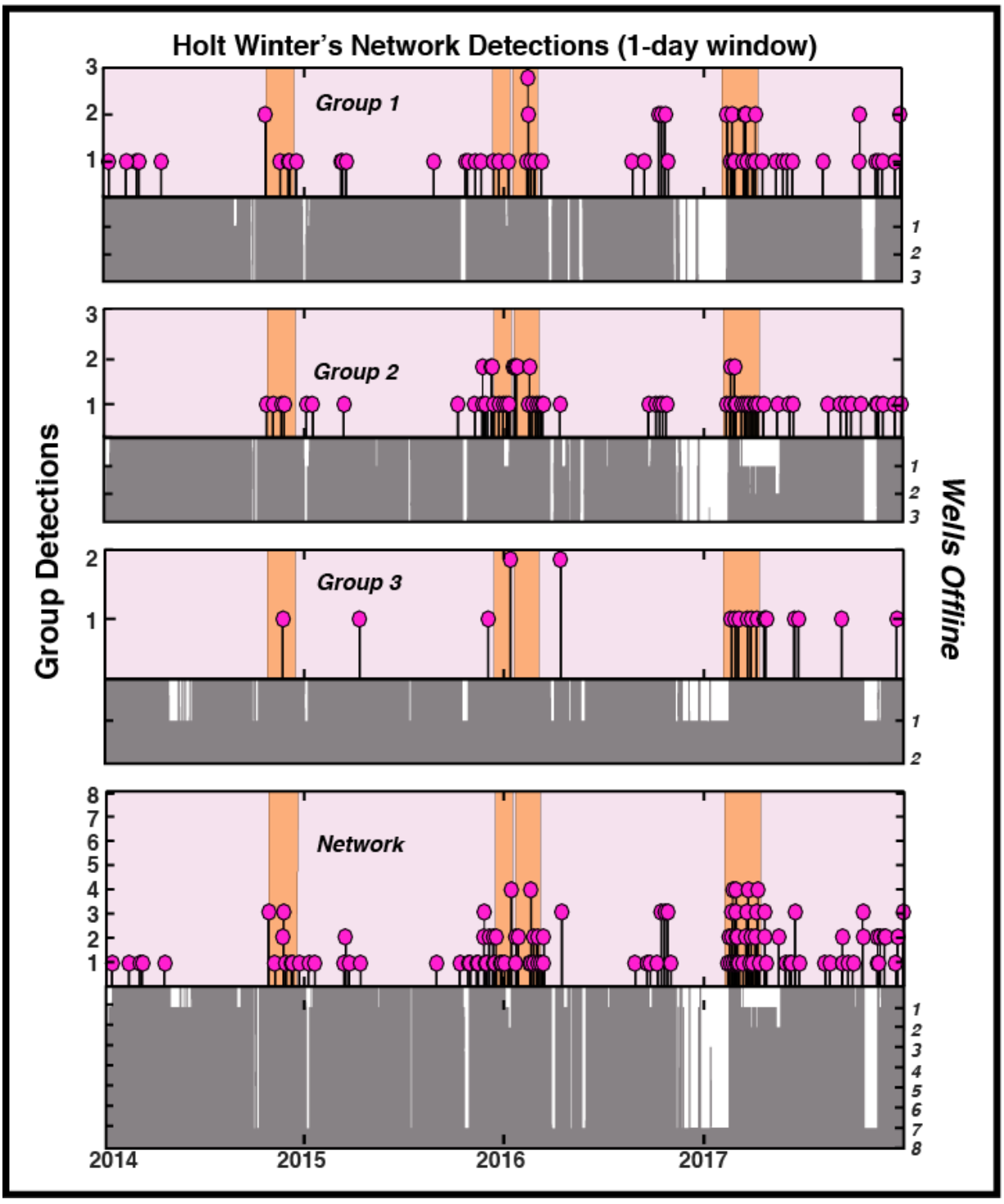

Figure Supp. 9. Holt-Winter's Model Group Detections, One Day Window- The first three stem plots show the correlated detections for Group 1, 2, and 3 respectively. The lowermost plot shows correlated detections across the entire network. The height of the stems shows the number of stations that share that specific detection. The grey color bars indicate how many wells are online. White means offline, increasing downwards. Known SSEs are marked by orange rectangles. A one-day moving window is used for cross correlating detections.

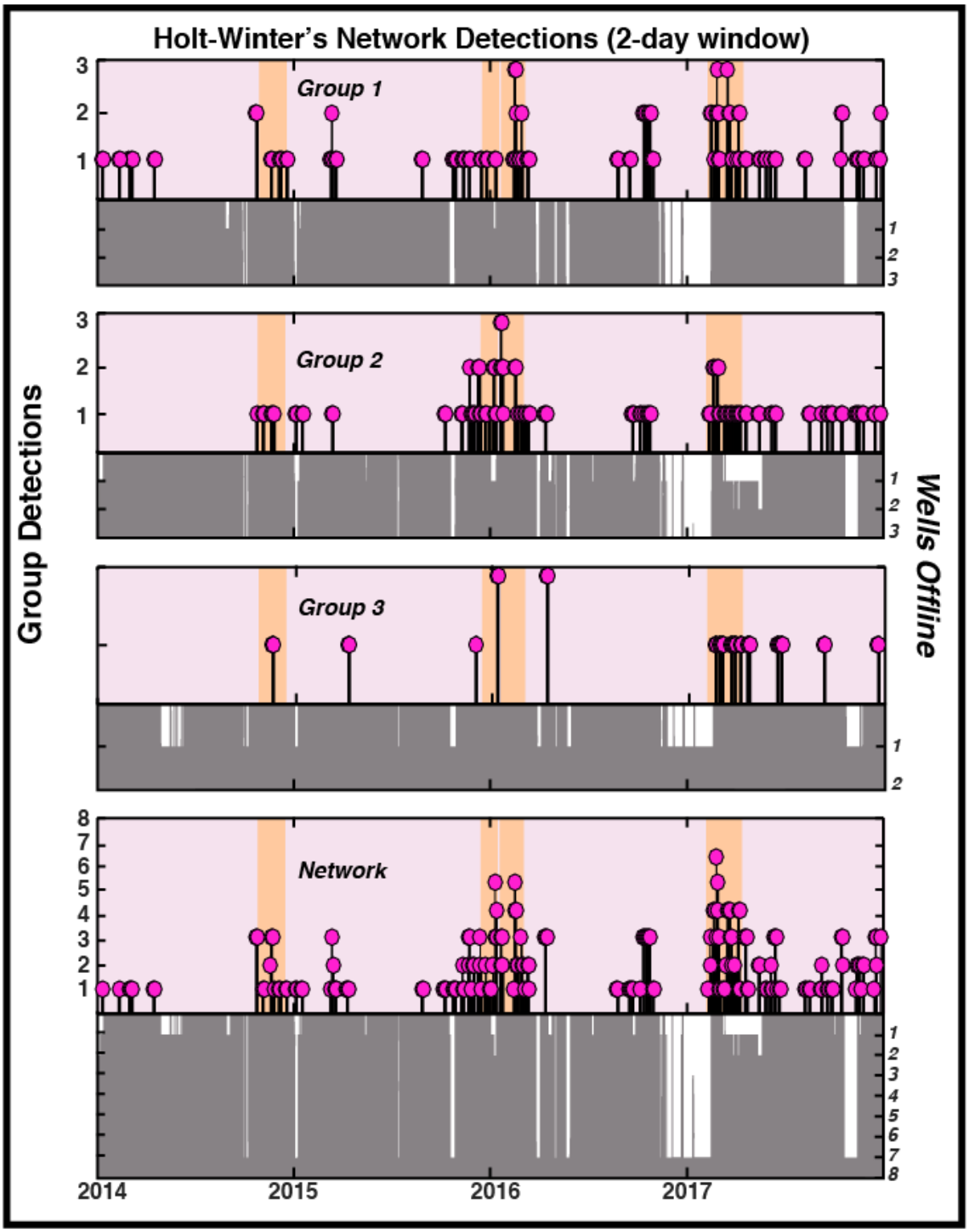

Figure Supp. 10. Holt-Winter's Model Group Detections, Two Day Window- The first three stem plots show the correlated detections for Group 1, 2, and 3 respectively. The lowermost plot shows correlated detections across the entire network. The height of the stems shows the number of stations that share that specific detection. The grey color bars indicate how many wells are online. White means offline, increasing downwards. Known SSEs are marked by orange rectangles. A two-day moving window is used for cross correlating detections. Note the increase in the number of detections and wells in which they are correlated across.

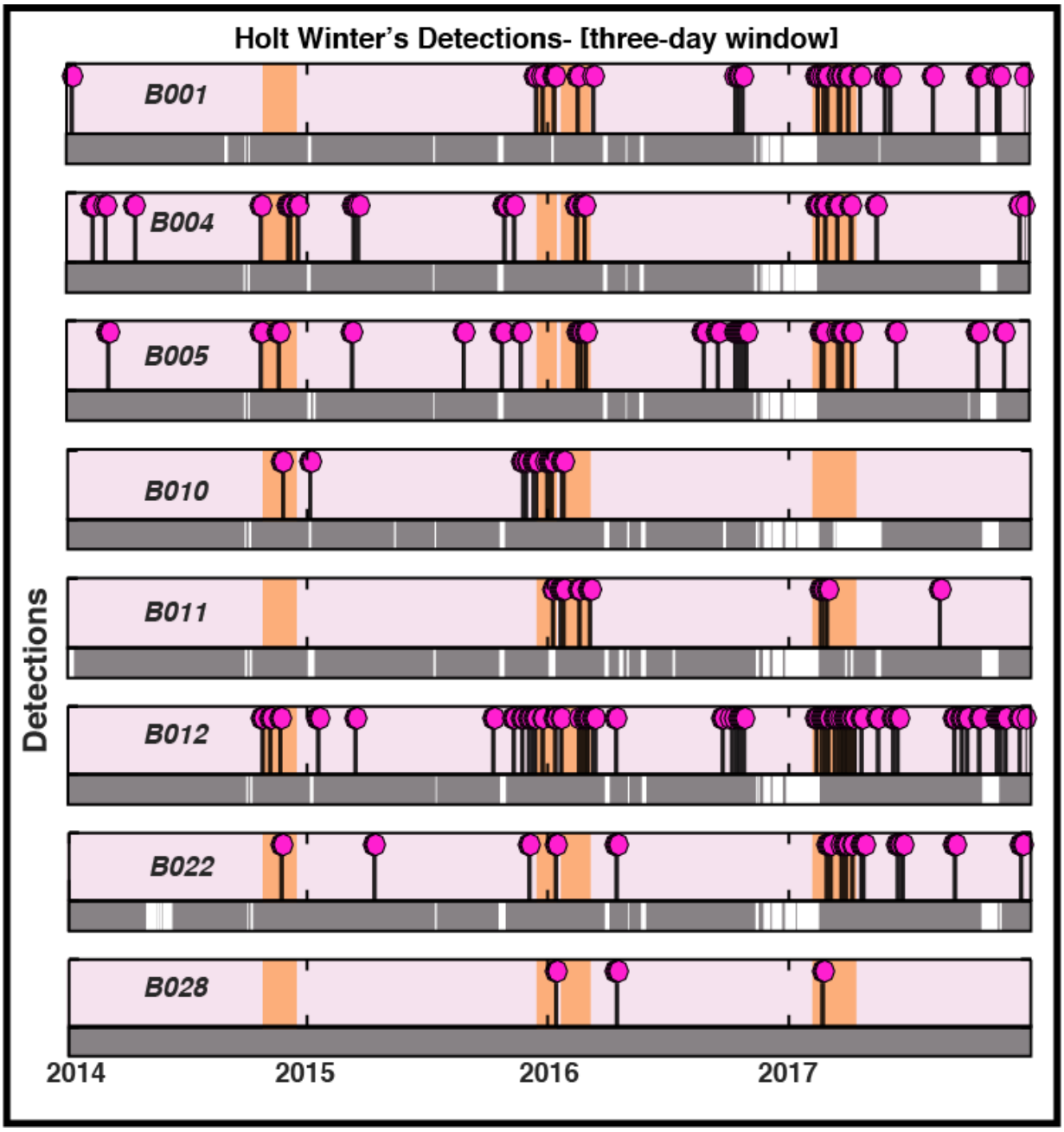

Figure Supp. 11. Holt-Winter's Model Detections, Three-Day Window- Each plot shows the pore pressure detections found for all borehole sites from 2014 forward. Known times of slow slip are marked by the orange rectangles. Purple dots mark the detections. Grey color bars indicate when the borehole station is online, white marks when the station is offline. Three-day moving windows are used in detections for this plot.

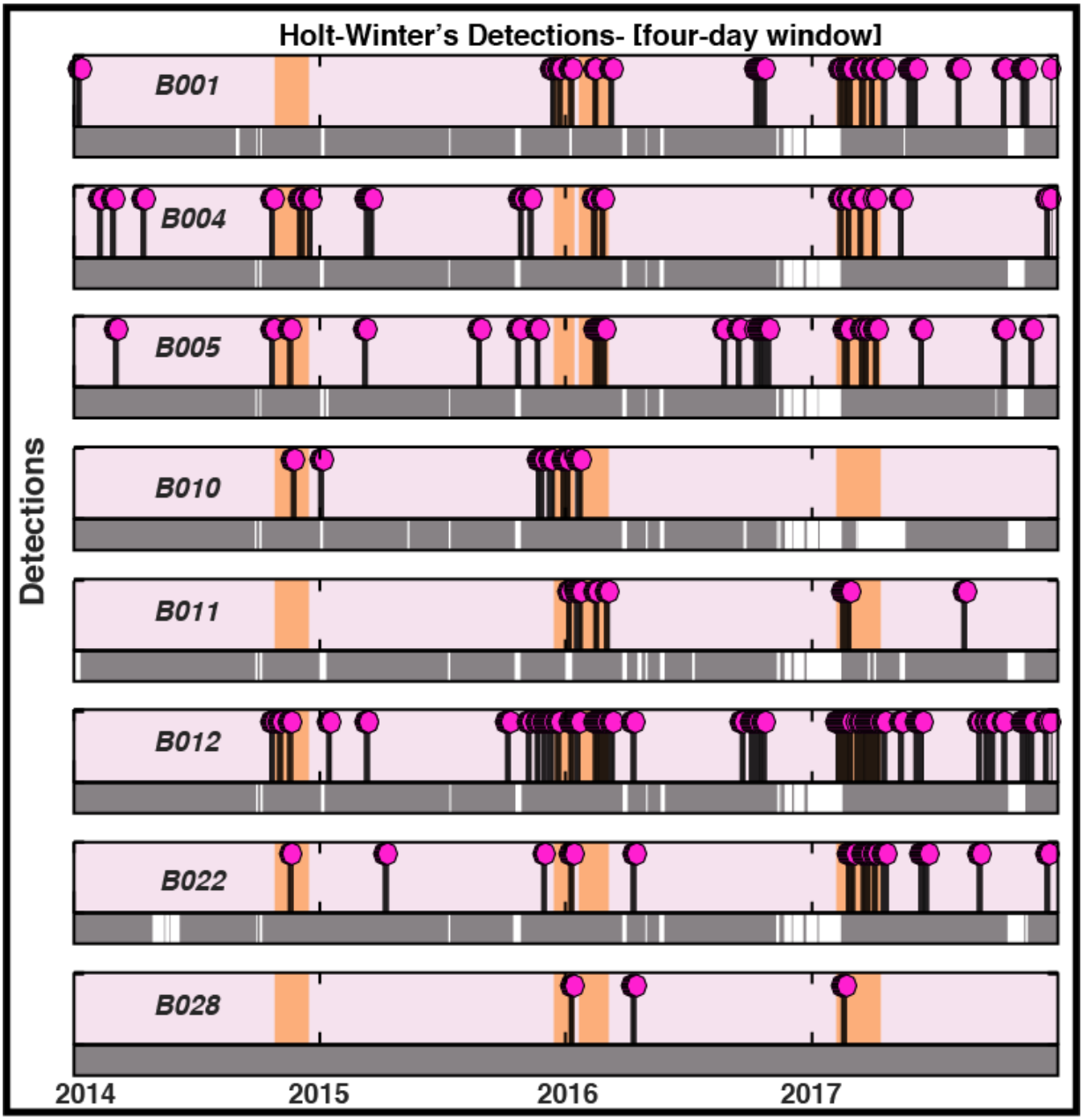

Figure Supp. 12. Holt-Winter's Model Detections, Four-Day Window- Each plot shows the pore pressure detections found for all borehole sites from 2014 forward. Known times of slow slip are marked by the orange rectangles. Purple dots mark the detections. Grey color bars indicate when the borehole station is online, white marks when the station is offline. Four-day moving windows are used in detections for this plot.

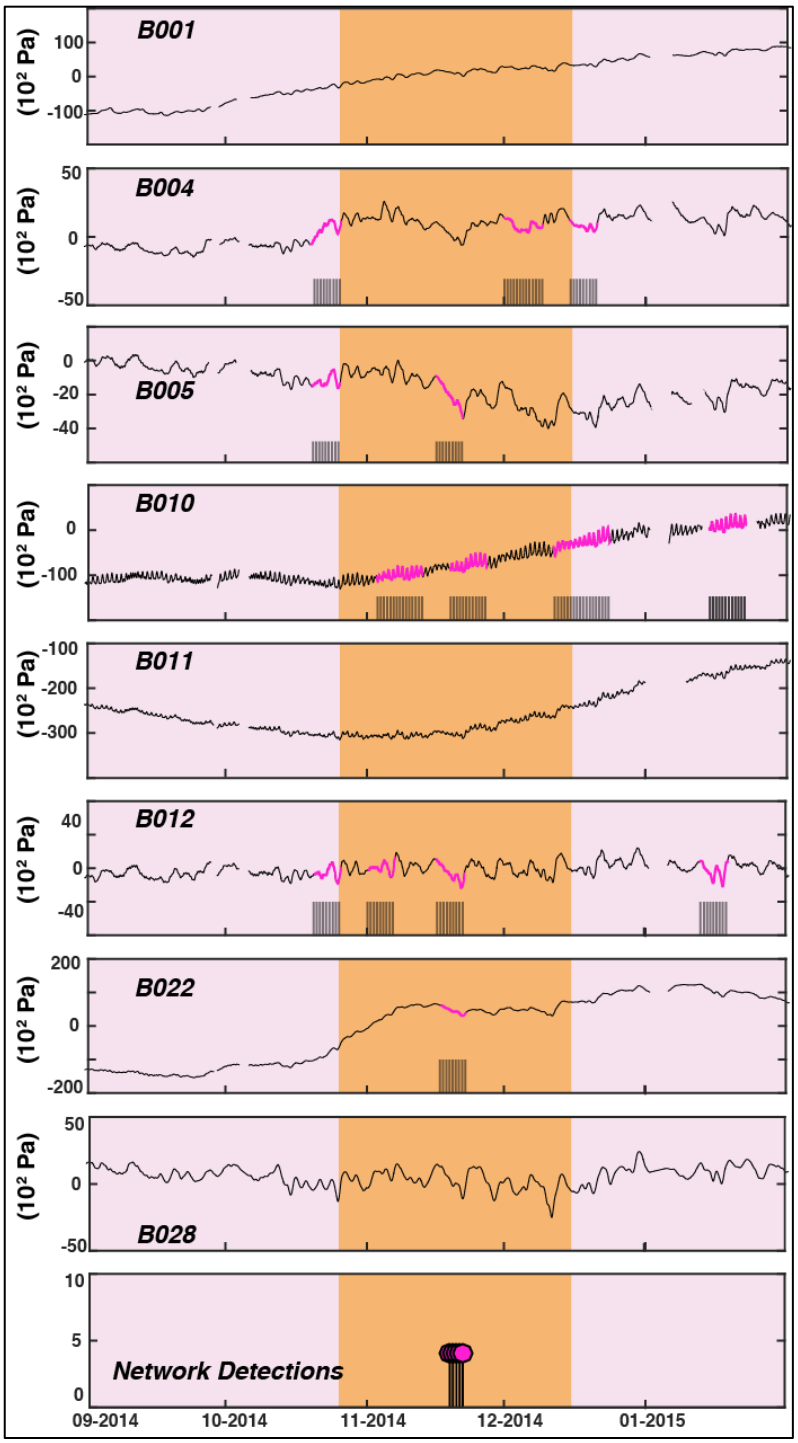

Figure Supp. 13. Pore Pressure Data with Detections, All Sites, SSE of 2014- The top eight plots show the raw pore pressure data (downsampled to 1/300 Hz) with anomalous data from the Holt-Winter's model marked in purple. Each plot has black stems that indicate the individual site detections found from the Holt-Winters model. The last stem plot contains the joint detections that were found to be correlated across at least 4 stations. Only stations containing detections are shown. The joint detections are found using a four-day window average. The SSE duration for 2014 is marked in orange.

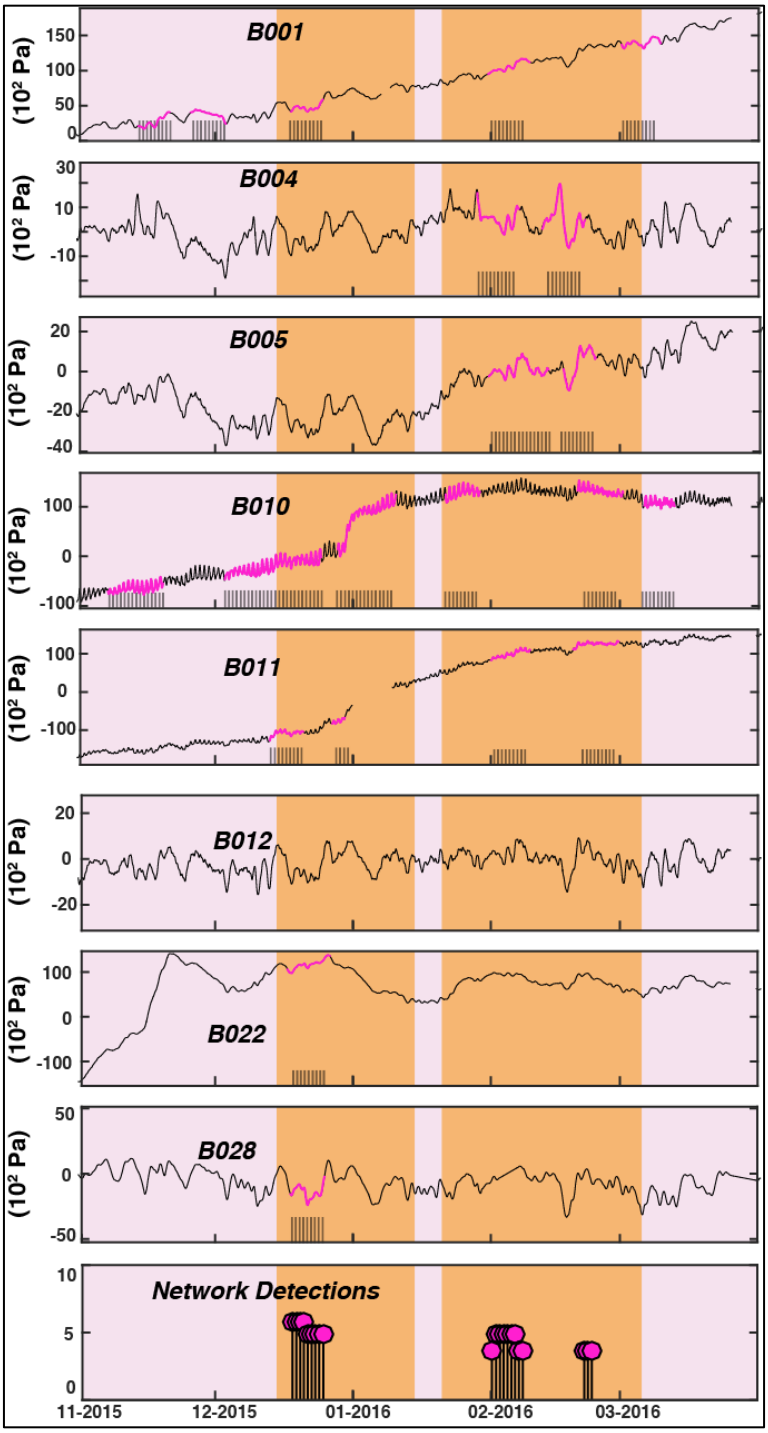

Figure Supp. 14. Pore Pressure Data with Detections, All Sites, SSE of 2015-2016- The top eight plots show the raw pore pressure data (downsampled to 1/300 Hz) with anomalous data from the Holt-Winter's model marked in purple. Each plot has black stems that indicate the individual site detections found from the Holt-Winters model. The last stem plot contains the joint detections that were found to be correlated across at least 4 stations. Only stations containing detections are shown. The joint detections are found using a four-day window average. The SSE duration for 2015-2016 is marked in orange.

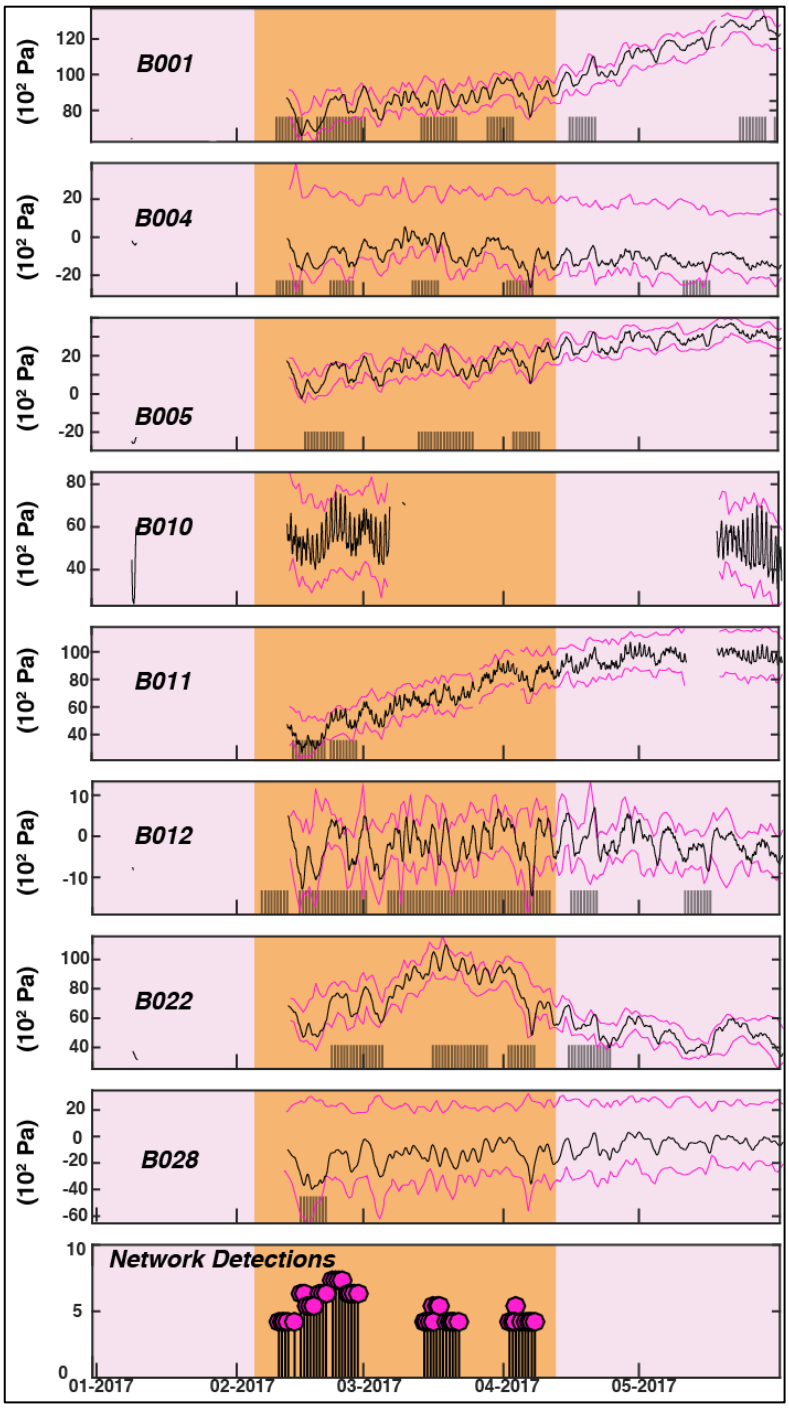

Figure Supp. 15. Pore Pressure Data with Detections, All Sites, SSE of 2017- The top eight plots show the raw pore pressure data (downsampled to 1/300 Hz with anomalous data from the Holt-Winter's model marked in purple. Each plot has black stems that indicate the individual site detections found from the Holt-Winters model. The last stem plot contains the joint detections that were found to be correlated across at least 4 stations. Only stations containing detections are shown. The joint detections are found using a four-day window average. The SSE duration for 2017 is marked in orange.

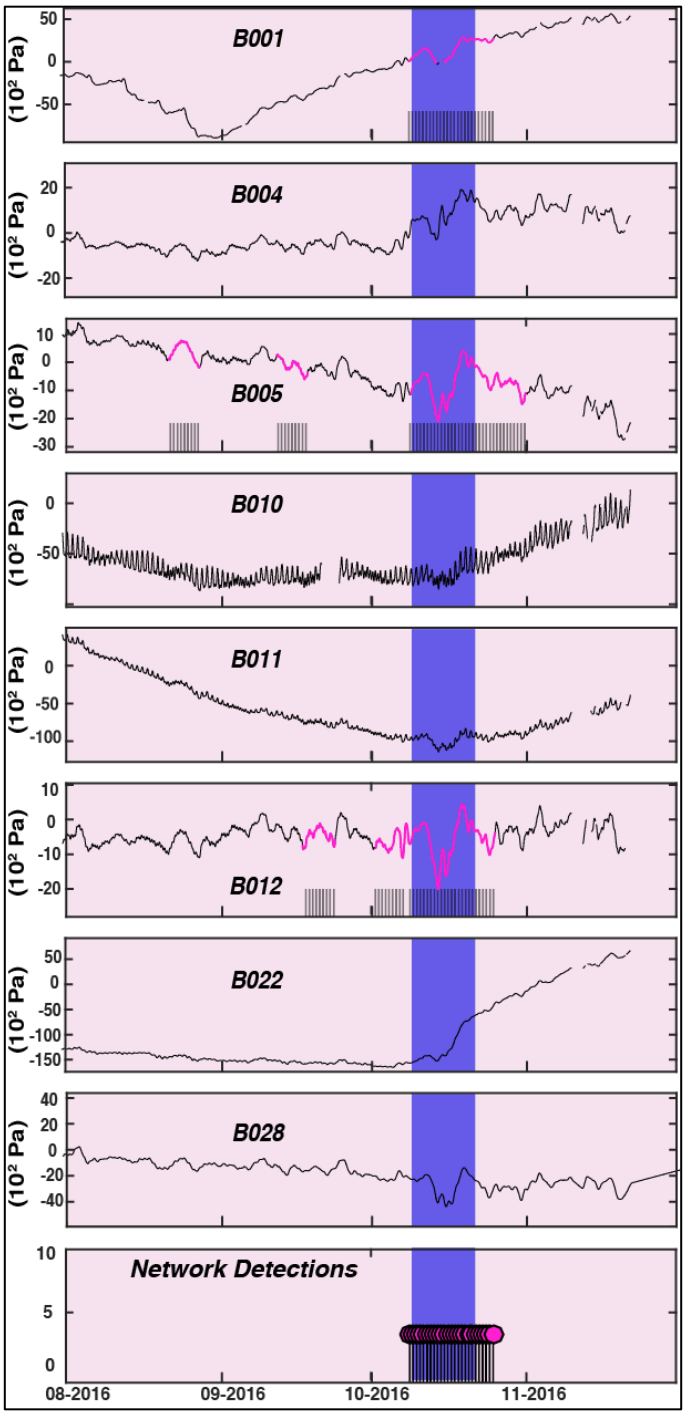

Figure Supp. 16. Pore Pressure Data with Detections, All Sites, Uncatalogued even of Fall 2016- Here, the top eight plots show the raw pore pressure data for each site containing detections. The dark purple bars mark the time of interest in which detections occur at sites B001, B005, and B012 alongside an anomalous step in pore pressure, here marked in purple.

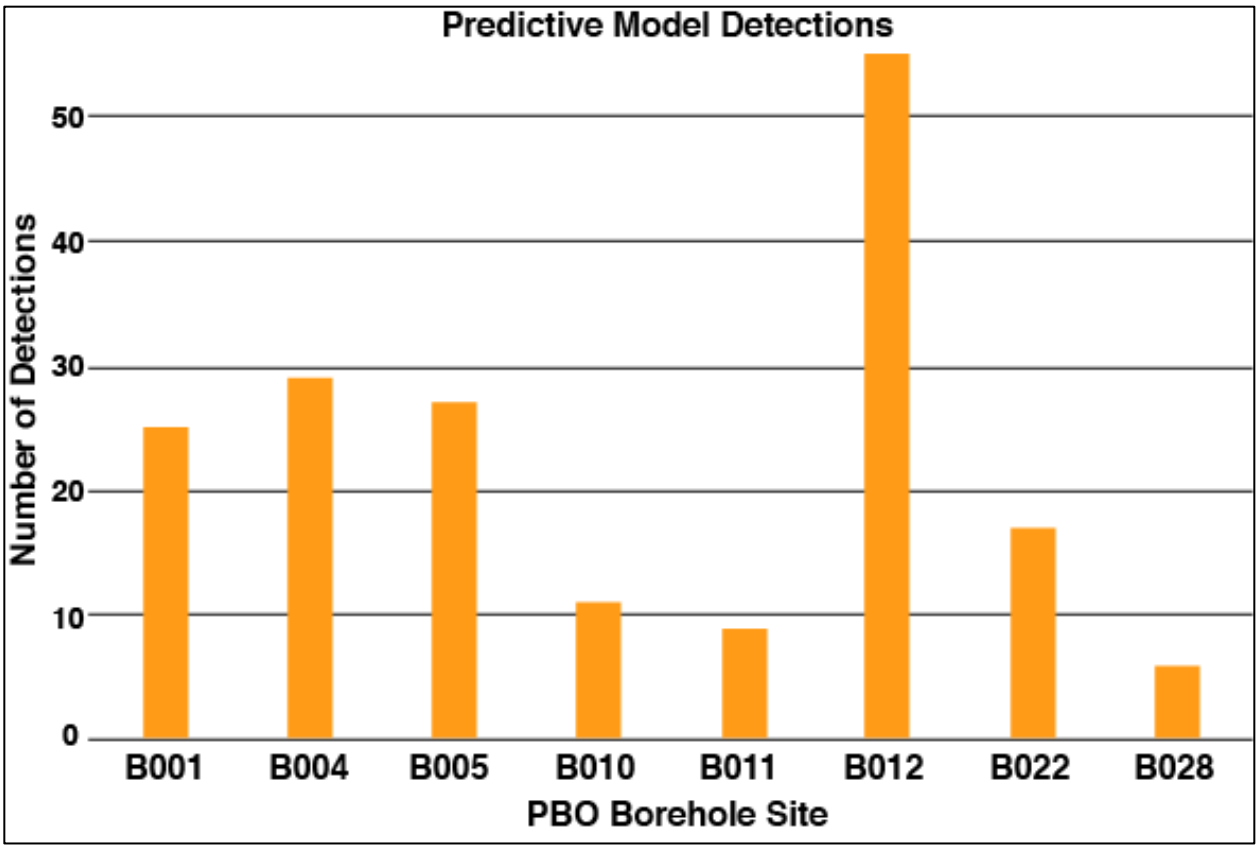

Figure Supp. 17. Number of Holt-Winter's Model Detections- The chart shows the number of anomalous pore pressure detections found with the Holt-Winter's predictive model for each individual site. No moving window is used for these detections.

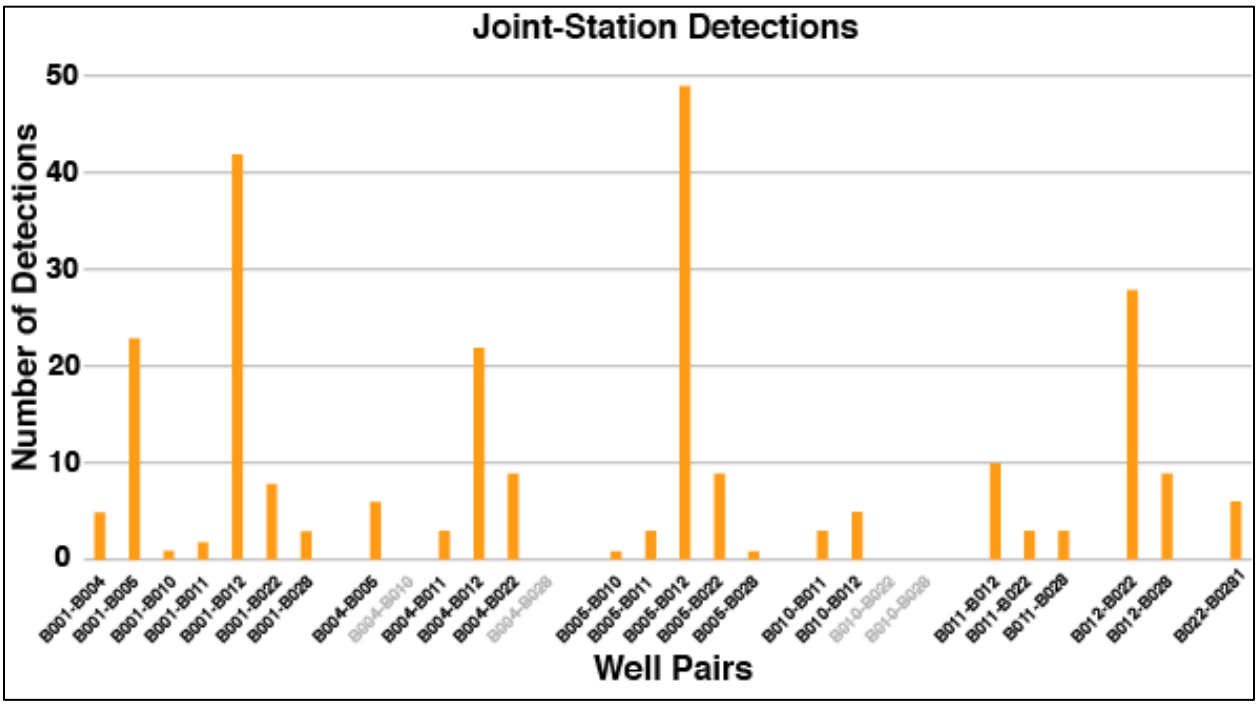

Figure Supp. 18. Number of Joint Station Holt-Winter's Model Detections- The chart shows the number of correlated anomalous pore pressure detections found with the Holt-Winter's predictive model for each pair of borehole sites. Grayed out pairs contain no correlated detections. No moving window is used for these detections.